Dysregulated Calcium Signaling in Cardiomyocytes from Diabetic Atrial Fibrillation to Chemotherapy-Induced Cardiac Hypertrophy

By

XIAN LIU

DISSERTATION

Submitted in partial fulfillment of the requirements for the degree of

DOCTOR OF PHILOSOPHY IN KINESIOLOGY

University of Texas at Arlington

August 2020

Supervising Committee:

Dr. Zui Pan, Supervising Advisor

Dr. Marco Brotto, Committee Member

Dr. Paul Fadel, Committee Member

Dr. Yi Hong, Committee Member

Copyright © by
Xian Liu
2020
All Rights Reserved

ABSTRACT

Ca^{2+} is a vital second messenger in cardiomyocytes and controls excitation-contraction coupling. It also regulates cell cycle, apoptosis, hypertrophy and downstream gene transcription in the heart remodeling. Calcium homeostasis is a complicated network and the intracellular Ca^{2+} signaling is composed of different Ca^{2+} movements like Ca^{2+} spikes [1], waves and oscillations [2-4].

The spatially-temporally regulated Ca^{2+} signaling is orchestrated with the Ca^{2+} release through ryanodine receptor (RyR) or IP_3 receptor (IP_3R) from Ca^{2+} stores such as sarcoplasmic/endoplasmic reticulum (SR/ER), recycling of Ca^{2+} from cell plasma back to the ER and Ca^{2+} influx through plasma membrane (PM) from extracellular space. There are many channels and transporters responsible for the intracellular Ca^{2+} homeostasis in cardiomyocytes.

Firstly, the RyR mediates Ca^{2+} release from SR/ER [5].

Secondly, the ER/SR Ca^{2+}-ATPase (SERCA) pumps Ca^{2+} from the cytosol back into the ER/SR. Plasma membrane Ca^{2+}-ATPase (PMCA) drives Ca^{2+} from the cytosol to the extracellular space [6].

Thirdly, the Ca^{2+} channels or transporters located on the cell membrane allow Ca^{2+} influx across the plasma membrane (PM) from the extracellular space. These channels or transporters include voltage-gated Ca^{2+} channel (VGCC), transient receptor potential channel (TRP), store-operated calcium entry (SOCE) or Ca^{2+} release activated Ca^{2+} channel (CRAC), Na^{+}/Ca^{2+} exchanger (NCX) and purinergic receptor.

Fourthly, mitochondrial Ca^{2+} uniporter (MCU) regulates mitochondrial Ca^{2+} uptake. Besides, there are more channels or transporters on the cell membrane and the ER

membrane involved in the regulation of intracellular Ca^{2+} homeostasis.

The dysregulation of intracellular Ca^{2+} can lead to a wide spectrum of cardiovascular diseases, including but not limited to arrhythmias, cardiac hypertrophy, cardiomyopathy and heart failure (summarized in the following illustrative figure). The first chapter of this dissertation is devoted to a literature review on the intracellular Ca^{2+} in the cardiac system with particular emphasis on SOCE and its machinery components. In Chapter 2, the IP_3-mediated disrupted calcium homeostasis in type 2 diabetes (T2DM) and atrial fibrillation (AF) is examined. In Chapter 3, the role of SOCE in chemotherapy drug epirubicin induced cardiotoxicity is investigated. Finally, in Chapter 4, conclusion will be stated and future directions will be discussed.

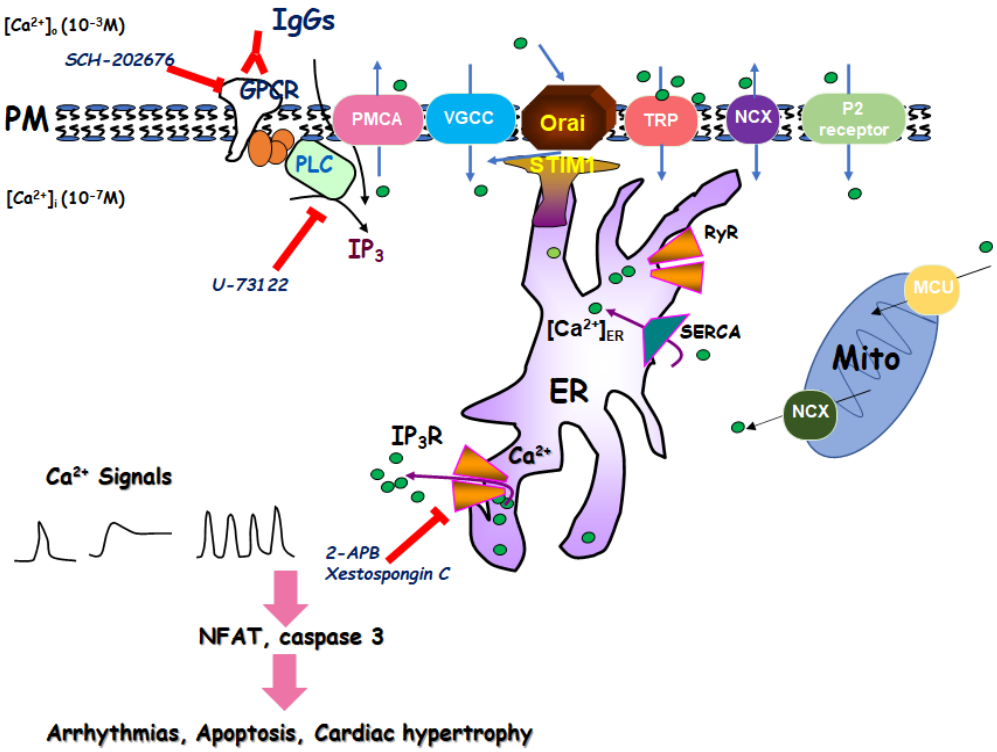

Intracellular Calcium Signaling in Cardiomyocytes

ACKNOWLEDGEMENTS

First and foremost, I would like to express my deepest and most sincere gratitude towards my mentor Dr. Zui Pan. She is not only a great advisor who guides me through my Ph.D. research but also a very supportive supervisor who constantly provides me with guidance for life and personal growth. Without her contributions in time, stimulating ideas, and funding, it would be impossible for me to get through this challenging but exciting journey. Her energetic personality and passion and enthusiasm towards science has been contagious and motivational for me throughout my Ph.D. trajectory.

I appreciate the support and guidance and suggestions from my committee member, Dr. Marco Brotto. He has been extremely supportive. I am very honored to have him as my reference for my grant application. Dr. Brotto has given me a lot of great suggestions for my research. He checks on my research progress and makes sure I stay on track to achieve my goal, which I deeply and sincerely appreciate. And I really appreciate him and Dr. Leticia Brotto for sharing the PTI machine for me to measure the intracellular calcium concentration, which is critical for my research, as the fura-2 based live cell imaging method plays a vital role throughout my dissertation studies.

I would like to thank Dr. Paul Fadel. He has given me many insightful suggestions and significant guidance for my research. I am honored to be able to discuss with him about my study during the research symposium jointly held by College of Nursing and Health Innovation and School of Social work here at UTA. Dr. Fadel's suggestions have always inspired me and guided me in both my experimental design and execution. I also appreciate the weekly research seminar lead by Dr. Fadel, which brings in multiple disciplines and departments on and outside campus. This has definitely broadened my

horizon by exposing me to the cutting-edge research as well as giving me a great deal of inspiration for my own studies.

I would like to express my gratitude towards Dr. Yi Hong from Department of Bioengineering, UTA. He has been incredibly supportive and has provided me with a lot of encouragement and suggestions for my research. Whenever we meet in either SEIR or ERB building, which is quite often, he checks how my research is going and gives me great advice on how to improve it. I also appreciate him for sharing the phalloidin dye, which I have used to demonstrate the epirubicin-induced cellular apoptosis in HL-1 cardiomyocytes in the second part of my dissertation study.

It would have been a much more difficult pursuit for my Ph.D. without all of my committee members' contributions and persistent help. It has been a true honor for me to have the precious opportunity to learn from them.

I would also like to thank Ms. Kim Doubrava for organizing my dissertation defense for me. She has been so kind and supportive. I would like to thank Ms. Cindy Stringer, Mr. Edward Gonzales, Ms. Jitenga Knox, Ms. Myra Martinez, Ms. Tanya Garcia, and Ms. Cynthia Ontiveros, all of whom have been amazing and made my Ph.D. life so much more enjoyable.

I would also like to thank all the faculty in the Department of Kinesiology and College of Nursing and Health Innovation for their kind and generous support. I appreciate that they have passed me their knowledge and passion towards science, which will benefit me for the rest of my life.

I would like to thank all current members of our lab. I thank Dr. Sangyong Choi who I have looked up to as a mentor as well. He always gives great suggestions and asks me

questions, encouraging me to think deeper. He is also a wonderful teacher and when he teaches me an experimental method, he not only states the procedure itself, but also explains the principle and reason behind the procedure very well, making it easy to follow and understand. I also thank Dr. Yan Chang. I have learned a great deal from her. She has also been an incredibly supportive friend who shares my laughter and tears during my time here at UTA. Without her, my Ph.D. life would not have been so fun and delightful. I would like to thank Lam Tran for sharing energetic stories of her life and helping maintain our lab routine, making it easier for us to conduct our experiments. I also thank our lab's previous members, Dr. Yanhong Luo, Dr. Fang Wu and Dr. Chaochu Cui. Their contributions have laid solid foundation for my dissertation studies.

I would like to thank Dr. Jingsong Zhou and Dr. Jianxun Yi who have provided me with guidance and great suggestions for my research. I would also like to thank Dr. Xuejun Li and Dr. Ang Li who have taught me experimental techniques and given me great suggestions and help for my research. I consider myself very fortunate to have them as my teachers and our conversations have contributed a great deal to my research progress.

Special thanks go to Dr. Yigang Wang, Professor of College of Medicine and Director of Regenerative Medicine Division in University of Cincinnati. He has provided me with the iPSCs used for the diabetic atrial fibrillation IgG study. I would also like to acknowledge Dr. Mark Zimering, Chief of Endocrinology in Veterans Affairs New Jersey Health System. He has provided me with the IgGs purified from type 2 diabetic patients.

I would like to thank all former and current graduate students in our department for all of the wonderful memories we have created together.

I would like to express my gratitude to my family and for their unconditional love

and encouragement which has made me an independent and fearless person I am at this moment of my life.

Finally, I would like to acknowledge all the funding sources which have made my Ph.D. work possible.

LIST OF ABBREVIATIONS

2-APB	2-aminoethoxydiphenyl borate
AA	arachidonic acid
AF	atrial fibrillation
ANOVA	one-way analysis of variance
AP	action potential
apoE	apolipoprotein E
AWA	Animal Welfare Act
Ca^{2+}	calcium
CAD	CRAC-activating domain
CaMKII	calmodulin-dependent protein kinase II
CCb9	coiled-coil domain containing region
CHF	congestive heart failure
CICR	calcium-induced calcium release
CPVT	catecholaminergic ventricular tachycardia
CRAC	calcium release-activated channel
CREB	Ca^{2+}/cAMP response element-binding
DAG	diacylglycerol
DCM	dilated cardiomyopathy
DHPR	dihydropyridine receptor
EC	endothelial cell
EGFR	epithelium growth factor receptor
EPC	endothelial precursor cell
EPI	epirubicin
ER	endoplasmic reticulum
ERK1/2	extracellular signal-regulated kinases 1/2
ET-1	endothelin-1
GPCR	G protein-coupled receptor
HDAC	histone deacetylase
hESC-CM	human embryonic stem cell-derived cardiomyocyte
HUVEC	human umbilical vein endothelial cell
IACUC	Institutional Animal Care and Use Committee
I_{Ca}	inward Ca^{2+} current
I_{CRAC}	calcium-release activated current
I_{SOC}	store-operated currents
IP_3R	inositol triphosphate receptor
IRB	Investigational Review Board
KB	Kraft-Brühe

LoCE	local transient Ca^{2+} event
LTC_4	leukotriene C4
M2 receptor	muscarinic cholinergic type 2 receptor
MCU	mitochondrial Ca^{2}+ uniporter
MHC	myosin heavy chain
Na/K-ATPase	sodium-potassium pump
NCX	Na^{+}/Ca^{2+} exchanger
NFAT	nuclear factor of activated T cells
NO	nitric oxide
OASF	Orai-activating small fragment
PAH	pulmonary arterial hypertension
PAR	proteinase-activated receptor
PASMC	pulmonary artery smooth muscle cells
PDGF	plate-derived growth factor
PKG	protein kinase G
PM	plasma membrane
PMCA	plasma membrane Ca^{2+}-ATPase
qRT-PCR	quantitative reverse transcription polymerase chain reaction
RyR	ryanodine receptor
SA	sinoatrial
SAM	sterile alpha motif
SCID	severe combined immune deficiency
SERCA	ER/SR Ca^{2+}-ATPase
shRNA	short hairpin RNA
SOAR	STIM1 Orai-activating region
SOCE	store-operated calcium entry
SR	Sarcoplasmic reticulum
STIM	stromal-interacting molecule
T2DM	type 2 diabetes
TAC	transverse aortic constriction
TG	thapsigargin
TM	transmembrane domain
TRP	transient receptor potential channel
t-tubule	transverse tubule
TXA_2	thromboxane A_2
VANJHCS	Veterans Affairs New Jersey Healthcare System
VEGF	vascular endothelial growth factor
VGCC	voltage-gated Ca^{2+} channel
VSMC	vascular smooth muscle cell

TABLE OF CONTENTS

LIST OF TABLES

LIST OF FIGURES

Chapter 2

Chapter 3

CHAPTER 1

INTRODUCTION

1.1 GENERAL REMARKS

Calcium (Ca^{2+}) is a critical regulator of cardiovascular function. The Ca^{2+} channels, pumps, and exchangers contributing to cytosolic Ca^{2+} signals governing cardiac contraction and vascular tone are well-known. Excitation contraction (EC) coupling is the process where an electrical stimulus triggers the sarcoplasmic reticulum (SR) calcium release, initiating the mechanism of muscle contraction by sarcomere shortening. In addition to those Ca^{2+} components, store-operated calcium entry (SOCE) is a ubiquitous mechanism recently recognized underlying the cardiac function maintenance and disease development and progression. This chapter is devoted to highlight the accumulated knowledge about the presence and potential contribution of Orai/STIM-dependent SOCE to the cardiac function and its role in cardiac pathogenesis and pathology. SOCE consists of two main components of Orai1 and Stromal-Interacting Molecule 1 (STIM1). Orai1 is located on the plasma membrane (PM) and STIM1 is located on the SR membranes. When SR Ca^{2+} stores are reduced, STIM1 is activated and forms patches and induces the aggregation of Orai1, which further triggers the activation of SOCE, leading to the flow of extracellular Ca^{2+} into the cell. This inward current is named calcium-release activated current (I_{CRAC}). Besides I_{CRAC}, another type of store-operated currents (I_{SOC}) not selective for Ca^{2+} has been identified, which requires the presence and interaction among Orai, STIM and transient receptor potential (TRP) cation channels. This chapter will introduce these channels and their roles in the cardiac function maintenance and cardiac disease development in detail.

1.2 CARDIAC EXCITATION-CONTRACTION COUPLING

Ca^{2+} is a ubiquitous cellular second messenger in the cardiomyocytes and controls cardiac EC coupling which is the process from the myocyte electrical excitation to the heart contraction [7]. The heart contracts generating heart beat which involves the synchronized atrial and ventricular contraction in a process called “cardiac cycle” [8]. The cardiac cycle is initiated with the sinoatrial (SA) node formed with a special group of pacemaker myocytes in the right atrial wall. The SA node generates action potentials (APs) which propagate down through the atrial chambers and ventricular chambers, thereby leading to their contraction and generation of the pumping force pushing blood into circulation system throughout the body [7].

On the sarcolemma locates a region penetrating deep into the cell forms the transverse tubule (t-tubule). On the t-tubule locates the L-type VGCCs (also known as dihydropyridine receptors, DHPR), which can be activated by the cardiac AP. During a cardiac AP, Ca^{2+} enters the cardiomyocytes through depolarization-activated DHPR as inward Ca^{2+} current (I_{Ca}), contributing to the AP plateau [9]. This I_{Ca} then binds and activates another receptor called type 2 ryanodine receptor (RyR2) located in the terminal cisternae of SR, which is a calcium store located close to the t-tubule [10]. Activation of RyR2 causes SR to open and release even more calcium into the cell (calcium-induced calcium release, CICR) [11], leading to a calcium spark [12]. Both the Ca^{2+} influx and the CICR contribute to the increased concentration of free intracellular Ca^{2+}, which binds to the myofilament protein troponin C and switches on the contractile machinery [7],

including the interaction between actin and myosin, thereby causing cardiac contraction [13].

1.3 EXPRESSION OF SOCE COMPONENTS IN THE HEART

1.3.1 STIM

Mammals have two STIM homologs, STIM1 and STIM2 [14].

STIM1 is a single-pass transmembrane protein. Human STIM1 is a 90kD phosphoprotein made of 685 amino acids [15]. Despite the majority ubiquitously expressed in the intracellular organelles (e.g. endoplasmic reticulum-ER), about 10-20% of STIM1 is also found localized in the PM, where its functions are unrelated to SOCE [16]. The carboxyl-terminus of STIM1 projects into the cytosol wherever its location (SR or PM), whereas the amino-terminus is located either in the SR lumen (for SR membrane-resident STIM1) or in the extracellular medium (for PM-resident STIM1) [17, 18]. The structure of functional domains of STIM1 has been studied and revealed. The amino-terminal regions include an SR signal peptide, a canonical EF-hand Ca^{2+}-binding motif, a hidden EF-hand, and a sterile alpha motif (SAM) (aa 1-22, 63-96, 97-128, 132-200, respectively) [19, 20], followed by the transmembrane domain (aa 214-234). The ezrin/radixin/moesin domain-containing carboxyl (cytosol) region is highly conserved among the STIM proteins. This region includes three coiled-coil domains, CC1, CC2, CC3 and a calcium release-activated channel (CRAC)-modulatory domain, a proline/serine-rich region, and a polybasic lysine-rich region (aa 238-342, 364-389, 399-423, 470-491,

600-629, 671-685, respectively) [21-23].

Four groups almost simultaneously identified the key region of STIM1 for interaction with store-operated channels [21, 24-26]. This region overlapping with the coiled-coil domains of the cytosol region of STIM1 was given different names: STIM1 Orai-activating region (SOAR), Orai-activating small fragment (OASF), CRAC-activating domain (CAD), coiled-coil domain containing region (CCb9), with aa 344-442 [21], 233-450 [24], 342-448 [25], 339-444 [26].

STIM1 can go through a variety of post-translational modification, including phosphorylation on serine [27] and tyrosine residues [28], and N-linked glycosylation on the SAM domain N^{131} and N^{171} [29].

STIM1 has been well studied in non-excitable cells and to some extent in skeletal muscle cells, but its presence and roleS in cardiomyocytes are much less known [30, 31]. The expression of STIM1 appears much less in the cardiomyocytes. For example, in a study generating a novel cardiomyocyte-restricted STIM1 knockout mouse the whole heart tissue demonstrated approximately a 20% reduction in total STIM1 protein expression in the knockout group compared with control, indicating the rest 80% expressed in cell types other than cardiomyocytes in the heart [32].

STIM1L is a long splice variant of STIM1 and found to be expressed in human skeletal muscle [33], neonatal rat cardiomyocytes [34], and differentiated myotubes [33]. STIM1L is reported expressed in myotubes during human myogenesis. This isoform has extra 106 amino acids on the carboxyl-terminus of the protein and is bound to cortical

actin filaments, localized near the PM, partially explaining the rapid onset of SOCE in this tissue [33]. Evidence has shown that STIM1L forms permanent cluster with Orai1 contributing to the rapid SOCE activation in the skeletal muscle cells when compared with other cell types [35].

STIM2 was identified at a much later time and found to be a transmembrane protein sharing similar structure to that of STIM1. Unlike STIM1, so far there has been no report showing the presence of STIM2 in the PM [18, 36]. However, STIM2 has been observed to be present in the ER membrane and in acidic intracellular stores [14, 37, 38]. The amino-terminal regions of STIM2 include the EF-hand Ca^{2+}-binding motif and SAM domain (aa 67-100, 136-204, respectively). The ezrin/radixin/moesin domain-containing region at the carboxyl terminus is highly conserved with three coiled-coil domains just as STIM1 [38]. Overlapping with these coiled-coil domains is SOAR [39], playing roles in the activation of SOCE [40]. The function of the proline- and histidine-rich region next to the SOAR remains to be further investigated [27, 41]. There is a calmodulin-binding region and a polybasic lysine-rich region close to the end of the carboxyl-terminal region [41, 42]. Both STIM1 and STIM2 can activate Orai1, but STIM2 is a weaker activator likely as a result of the difference in the SOAR [43, 44] and SAM domains [45]. However the lower affinity for Ca^{2+} by the EF hand of STIM2 allows it to activate Orai1 at lower agonist-induced stimulation level and subsequent ER store depletion [46, 47].

Both human and mouse tissues express STIM2 [27, 42], and it is the dominant homolog expressed in the mouse brain, pancreas, placenta and heart but found almost

absent in the skeletal muscle, kidney, liver and lung. The co-expression of STIM1 and STIM2 in many human cell lines [27] as well as cell types [48, 49] demonstrates the co-existence of these two isoforms and potential interaction.

Researchers have found three splice variants of STIM2 to this date: STIM2.1 (STIM2β), STIM2.2 (STIM2α) and STIM2.3. Among these three variants, STIM2.2 is the best described and known [50] and previously-reported STIM2 mainly referred to STIM2.2 [51]. The gene *STIM2* comprises 13 exons with exon 9 absent in the STIM2.2 mRNA, making it encoded by 12 exons and resulting in an 833-amino-acid protein [40]. The eight-residue insert (383-VAASYLIQ-392) within SOAR domain encoded by exon 9 in STIM2.1 was initially considered responsible for impairing the interaction between Orai1 and its activation [40]. Yet, new evidences have shown the opposite. The heterodimer comprising the SOAR regions of STIM1 and STIM2.1 has been shown capable of fully activating Orai1 channel while preventing its crosslinking and clustering [52]. STIM2.1 expressed ubiquitously and might form heterodimer with STIM1 and STIM2.2, attenuating SOCE-mediated Ca^{2+} influx [40]. STIM2.3 expresses an alternative exon 13, leading to translation at the upstream end, encoding a protein 17kD smaller [50]. The expression of STIM2.3 is limited and its function remains to be elucidated [50].

1.3.2 ORAI

The human Orai family consists of three homologs, Orai1, Orai2 and Orai3 and cardiomyocytes express all these three homologs. Orai is the heaven's gate keeper in Greek mythology [53]. In 1992, an intracellular Ca^{2+} store discharge-activated current was

identified and termed as the Calcium-Release Activated Current (I_{CRAC}) which is highly Ca^{2+}-selective and inwardly-rectifying [54]. Orai1, the canonical isoform, was first identified as the channel conducting I_{CRAC} in 2006 through whole-genome screening of *Drosophila* S2 cells and gene mapping in I_{CRAC} deficiency-induced hereditary severe combined immune deficiency (SCID) patients [55-57]. Orai1 is a 33kD protein of 301 amino acids that does not share homology with other known ion channels. It has four transmembrane domains (TM1-TM4) with both the amino and carboxyl terminal tails located in the cytosol [58-61], which are both proved to be essential for STIM1 interaction and regulation [21, 24, 25, 62-64].

Initially studies have demonstrated that a tetramer is the most likely Orai1 subunit stoichiometry of the mammalian CRAC channels [65-67]. However, crystallization of *Drosophila* Orai has identified the hexameric assembly of Orai subunits forming the channel [68]. Despite the unavailability of mammalian crystal structure of Orai1 so far, study analyzing the biophysical properties of hexameric and tetrameric human Orai1 has revealed the difference of these two stoichiometry hypotheses. A tetrameric structure is shown to display highly Ca^{2+}-selective conductance characteristic of $I_{CRAC,}$ whereas the hexameric architecture forms a non-selective cation channel [69]. In the hexameric CRAC channel, six of the TM1 domains of Orai1 subunits form a hexamer with a pore including residues 74-90 (ETON region) of amino terminus at the center, with the ETON essential for STIM1 interaction [62]. Negatively charged residues (D110, D112 and D114) form an external vestibule working as a funnel (the pore) and attract Ca^{2+} to the pore, which is

followed by the selectivity filter (aa E106), contributing to the CRAC channel high Ca^{2+} selectivity [70, 71], a hydrophobic region (aa V102, F99 and L95) and a basic region (aa R91, K87 and R83). The other three transmembrane domains TM2-TM4 surround the pore [68] with residues of these domains essential for regulating CRAC channel function.

Two splice variants of Orai1 (the long Orai1α and the short Orai1β) have been discovered through alternative translation-initiation sites at Methionine 1 and Methionine 64 from the same messenger RNA. Both variants mediate I_{CRAC} [72, 73], but Orai1β shows a much smaller Ca^{2+}-dependent inactivation [73].

All three Orai homologs are able to mediate I_{CRAC} with STIM1 overexpression [74, 75], but Orai2 and Orai3 mediate smaller currents than Orai1 [58], with a few specific exceptional studies [76, 77] and how they mediate native Ca^{2+} entry pathways remains to be explored [78].

1.3.3 TRPC

Besides I_{CRAC}, another type of store-operated currents (I_{SOC}) not selective for Ca^{2+} has been identified. They have different biophysical properties and exhibit a greater conductance than I_{CRAC} [79]. The interaction among STIM1, Orai1 and TRPC1 is required for the activation of I_{SOC} [73, 80-82]. The coiled-coil domains of both the amino and carboxyl termini of TRP channels are relevant with the interaction with STIM1 [83]. TRPC subfamily include seven members, i.e. TRPC1-TRPC7 [84]. The first mammalian TRP protein was TRPC1 and it was identified in both humans [85, 86] and mouse [87].

The involvement of TRP channels in SOCE has been widely investigated and

heated debates have been present, with the TRPC subfamily in particular. Gated by store Ca^{2+} depletion, the TRPC channel's roles have been examined with a variety of tools including endogenously knocking down TRPs, generating TRPC knockout models, as well as overexpression of specific TRPC proteins [88-90]. Researchers have reached consensus that TRPC1, STIM1 and Orai1 form a complex underlying the less selective I_{SOC} current. However, two hypotheses about the molecular basis of I_{SOC} still co-exist. The first hypothesis states that the I_{SOC} equals to I_{CRAC} plus a less selective TRPC-mediated current [91]. Whereas the second hypothesis insists there is still undiscovered component contributing to I_{SOC} besides TRPC1 and Orai1 subunits [92].

Many excellent reviews have summarized the roles of TRPC channels in cardiomyocytes [93, 94], a brief summary is presented here. Several TRPC subfamily proteins are found expressed in the heart [30, 93, 95]. It has been found that TRPC proteins together with L-type voltage-gated calcium channels (VGCCs) form a complex, responsible the developing heart's beat initiation [93]. Correlation has been found between the increased expression of TRPC channels and enhanced SOCE and spontaneous Ca^{2+} waves underlying arrhythmia [95]. During chronic cardiac diseases in both human and animal models increased expression levels of almost all TRPC family members (TRPC1, TRPC 3-7) have been identified [94, 96, 97]. In addition, both the diacylglycerol (DAG)-sensitive (TRPC3/6/7) and the IP_3R-sensitive (TRPC1/4/5) subfamily members have been found responsible for store-dependent activation [96, 98, 99].

1.4 SOCE DURING CARDIAC DEVELOPMENT

At different stages of cardiac maturation, SOCE seems to be playing differentiated roles. In embryonic cardiomyocytes, SOCE appears to be more prominent, whereas with postnatal development it tends to decline. This is manifested by the relatively higher expression of STIM1 in early cardiomyocytes than later in adult cells [34]. Furthermore, the morphology, organization and signaling properties are different in embryonic and neonatal cardiomyocytes compared to those in adult cells [100]. Many of the studies stating SOCE to be functional in cardiomyocytes are done within neonatal cells, and the results do not necessarily correspond to the situation in adult muscle.

However, numerous evidences have demonstrated the expression of molecular components of SOCE (such as STIM, Orai, and TRPC proteins) from embryo to adult.

In fact, STIM1 and Orai1 proteins have been identified by several groups simultaneously in embryonic, neonatal and adult rat ventricular cardiomyocytes [101-105] and demonstrated them to be essential in SOCE. Moreover, a significant amount of a splice variant of STIM1 (STIM1L) whose expression decreases with cardiomyocyte maturation, was found also expressed in neonatal hearts [34]. Sabourin et al. reported a physical interaction between STIM1 and Orai1 induced by Ca^{2+} store depletion in neonatal cardiomyocytes [98]. It has also been reported in neonatal cardiomyocytes the SR Ca^{2+} depletion causes STIM1 to form puncta [103] and interact with Orai1 [105], which recapitulates studies in non-excitable cells. The co-localization of STIM1 and SERCA, phospholamban and RyR has also been reported in neonatal and adult rat hearts [30,

105, 106].

TRPC1, STIM1, and Orai1 were found to be involved in the formation of SOCE channels in human cardiac c-kit^{+} progenitor cells, and can regulate cell cycling and migration [107]. However in a cardiomyocyte-restricted STIM1 knockout mouse model, the cardiac function of the mice didn't decline before they reached 20week age [32]. By 36 weeks, the STIM1-deficient mice demonstrated marked left ventricular dilation. The presence of an inflammatory infiltrate and cardiac fibrosis also appeared from 20weeks and progressively worsened by 36weeks of age. These data demonstrate that deletion of STIM1 does not affect early development of the heart, but precipitates deleterious heart remodeling in postnatal mice. What's more, despite the exhibition of immunodeficiencies, muscular hypotonia, ectodermal dysplasia, autoimmunity, and lymphoproliferative diseases, Orai1-/STIM1-deficient patients or mice don't show overt cardiac muscle-related phenotypes and no prejudice to the cardiovascular function [108]. This is consistent with the idea that SOCE pathway is not indispensible during cardiac muscle development and/or contractility under physiological circumstances. SOCE-associated cardiac dysfunction might be seen with aging, stress stimuli, or prolonged exercise, but couldn't be examined due to the death in utero or in early life of patients or deficient mice. Interestingly, the overexpression of STIM1 in cardiomyocytes also is detrimental. Mice with cardiomyocyte-specific overexpression showed no phenotype until 10 weeks of age when they started demonstrating declined cardiac function [30]. These studies indicate the significance of STIM1 in the cardiomyocyte structure and function; either too little or

too much STIM1 can contribute to pathological changes in cardiomyocytes. However, it is still elusive whether these changes caused by reducing or enhancing STIM1 is due to changes of SOCE.

1.5 SOCE AND THE CARDIAC DISEASES

1.5.1 Cardiac Hypertrophy and Heart Failure

The heart functions to pump blood into and perfuse the peripheral organs, satisfying the demand under both normal and stress conditions. To achieve this goal, the heart and individual cardiomyocytes undergo enlargement (termed as hypertrophy) during increased preload or afterload [109]. Initially cardiac hypertrophy increases contractility by adding sarcomere units in parallel [109]. Then following Laplace's law, the increased left ventricular wall thickness then decreases the left ventricular wall stress, thus maintaining cardiac efficiency [109]. Accompanied by cardiac hypertrophy are also qualitative changes including those in gene expression, which induce changes in metabolism, contractility, and cardiomyocyte survival [109]. Cardiac hypertrophy can be divided into two categories: physiological and pathological, both of which develops as an adaptive response to cardiac stress but their underlying molecular mechanisms, cardiac phenotype and prognosis are quite different. Physiological hypertrophy keeps normal cardiac function over time, while pathological hypertrophy often undergoes deleterious remodeling of cardiomyocytes further progressing to adverse cardiovascular events including but not limited to heart failure, arrhythmias and even sudden cardiac death [94,

110-112]. It is the nature of upstream stimuli and downstream signaling pathways that determine the development of physiological or pathological hypertrophy, not the duration of cardiac stress per se [113-116]. Ca^{2+}-related genes are only changed during pathological hypertrophy but not in physiological hypertrophy [109]. We will mainly focus on pathological hypertrophy in our review.

To match a greater hemodynamic demand or some stress conditions induced by myocardial infarction or hypertension-induced pressure overload, cardiac hypertrophy occurs in preservation of the pump function [117]. Several lines of evidence have demonstrated the involvement of a number of signaling pathways in the hypertrophic growth of cardiomyocytes, and the Ca^{2+} signals have been established as the triggering events. However not all Ca^{2+} signals in the cardiomyocytes can initiate hypertrophic response. For example the global cytosol Ca^{2+} signals accompanying with every contraction are not necessary activator for hypertrophy [118]. It is rather the local signaling action-triggering Ca^{2+} signals from discrete sources that can initiate hypertrophic growth [119]. The IP_3 receptors near the nucleus [119] or on the nuclear envelope generates increased cytosolic Ca^{2+} signals, activating phosphatase calcineurin, which subsequently dephosphorylates nuclear factor of activated T-cells (NFAT) causing it to translocate into the nucleus and activate gene transcription; or activating calmodulin-dependent protein kinase II (CaMKII), which subsequently phosphorylates histone deacetylase (HDAC) [120-122], both of which switch on the fetal genes leading to cardiac hypertrophy [94].

STIM1/Orai-mediates SOCE may serve as the necessary source for local Ca^{2+}

elevation to promote hypertrophic growth [123]. The first study in neonatal rat ventricular myocytes showed that 48hrs administration of IP_3-activating agonists such as phenylephrine and angiotension II increased intracellular Ca^{2+} and cell area and lead to NFAT activation, which were all prevented by the treatment of a nonselective SOC inhibitior SKF-96365 and to a lesser extent by the treatment of LRCC inhibitor [124]. Following this study several lines of evidence found similar results in STIM1 and Orai1 knockdown neonatal cardiomyocytes where 48hr treatment of endothlin-1 or phenylephrine induced SOCE enhancement, NFAT activation and cell size increase were suppressed [101-103]. Another study demonstrated that knockdown of both STIM1 and Orai1 completely abolished phenylephrine-induced hypertrophic growth in rat neonatal cardiomycytes by inhibiting CaMKII and ERK1/2 (extracellular signal-regulated kinases 1/2) signaling pathway, whereas merely Orai1 knockdown prevented phenylephrine-mediated signaling in a calcineurin-dependent manner [102]. On the other hand, when STIM1 was overexpressed in neonatal caridomyocytes the cells showed significantly larger size and enhanced NFAT activity, both of which were prevented by SKF-96365 treatment [103].

These *in vitro* data clearly identify the STIM1/Orai1-mediated Ca^{2+} entry as the fundamental mechanism underlying cardiac hypertrophy development. However, how it contributes to adults and *in vivo* models are still relatively limited. The first *in vivo* study to demonstrate up-regulation of STIM1 protein and enhanced SOC current in the pressure overload-induced left ventricular hypertrophy was carried out in rat [103]. To the contrary,

silencing STIM1 gene expression reduces SOCE and protects the heart from hypertrophy development through decreasing the CnA/NFAT4 signaling pathway [103]. Another study in mice demonstrated that deletion of STIM1 protects the heart from pressure overload-induced cardiac hypertrophy [125]. Other studies have also confirmed that Transverse aortic constriction (TAC)-induced STIM1 up-regulation activates the NFAT and CaMKII signaling pathway through enhancing SOCE, thereby promoting cardiac hypertrophy and arrhythmias [30, 126].

STIM1L has been found predominant at neonatal stages and its expression is decreased in adults and reappears upon hypertrophic agonist application or afterload-induced cardiac stress. Mice undergoing TAC presented increased mRNA and protein expression levels of STIM1L and enhanced SOCE compared with sham animals, in line with the evidence showing reactivation of STIM1L expression enhances SOCE during hypertrophic process [34]. In isolated adult cardiomyocytes with application of phenylephrine induction of STIM1L was also observed [34].

Studies examining the role of Orai1 in cardiac hypertrophy and heart failure remain limited. Human embryonic stem cell-derived cardiomyocytes (hESC-CMs) treated with phenylephrine for 48hrs induced a marked hypertrophy along with increased Orai1 protein expression level [127]. Hypertrophy was inhibited by suppression of Orai1 expression/activity using siRNAs or a dominant-negative construct Orai1 (G98A), or inhibited by nitric oxide (NO) and cyclic guanosine monophosphate (cGMP) via activating PKG. Importantly, when Orai1 is mutated aon serine 34, the anti-hypertrophic responses

were abolished, indicating that hat NO, cGMP, and PKG inhibit the hypertrophy of hESC-CMs via PKG-mediated phosphorylation on Orai1-Ser-34 [127]. As for *in vivo* studies, in a zebrafish model using reverse genetics, the inactivation of the highly conserved zebrafish orthologue of Orai1 resulted in heart failure, reduced ventricular systolic function, bradycardia and skeletal muscle weakness [104]. This is the first study showing Orai1 deficiency in zebrafish causes heart failure. Loss of Orai1 is found to lead to defective signal transduction at the cardiac z-disc [104]. Their findings link Orai1-mediated calcium signaling to sarcomere physiology, in part by affecting z-disc composition and function mediated by the calcineurin-calsarcin-NFAT signaling pathway, shedding light upon the potential role of SOCE in serving as the pharmacological target to modulate Ca^{2+}-dependent pathways to improve the outcome of cardiac hypertrophy. Horton et. al applied a TAC pressure overload model to mice deficient in Orai1 (global heterozygous) and compared their response to wild type mice [31]. After eight weeks of TAC, the Orai1 deficient mice show a significantly reduced survival rate, a much earlier loss of cardiac function, and an earlier, greater dilation of the left ventricle, and significantly higher expression levels of apoptotic markers, indicating that Orai1 deficiency seems to accelerate or exacerbate the progression of the decease, rapidly leading to dilated cardiomyopathy, heart failure and earlier death [31]. Notably, contrary to the above mentioned phenotypes, the authors did not observe any change in the heart weight or rate of increase in heart weight early on, nor in cellular hypertrophy [31]. They attribute this discrepancy to the theory that a maximum rate of hypertrophy has been achieved in

both Orai1-deficient and wild-type mice, but the Orai1-deficient mice are unable to compensate to the overload (to yield equivalent functional compensation to wild-type mice) [31]. A recent *in vivo* study shows that overexpression of SOCE-associated regulatory factor in the heart prevents cardiac hypertrophy probably through suppressing the up-regulation of STIM1 and Orai1 [128]. In an even more recent study, using a novel genetically-modified mouse that specifically disrupts the Orai1 channel in cardiomyocytes, the authors show that even if Orai1 is not instrumental in regulating normal EC coupling and cardiac function, its functional inhibition preserves alterations of Ca^{2+} homeostasis, fibrosis and systolic function without affecting hypertrophy during pressure overload [129].

TRPC family members have also been demonstrated up-regulated in several studies of cardiac hypertrophy and heart failure [130-132]. Seven isoforms (TRPC1-TRPC7) are found to control pathological hypertrophy through signaling effectors including calcineurin and NFAT [94, 130, 132, 133]. TRPC3 and TRPC6 are particularly vital for the development of hypertrophy through calcineurin-dependent signaling pathways [134-136]. Maladaptive hypertrophy induced by pressure overload was suppressed by deletion of either *Trpc3* or *Trpc6* in mice [137]. TRPC6 is phosphorylated by protein kinase G (PKG), which reduces channel conductance, therefore negatively regulating TRPC-mediated hypertrophy [138]. TRPC1 knockout mice are also shown to have the calcineurin-NFAT signaling pathway inhibited, which reduces the transverse aortic constriction (TAC)-induced hypertrophic response and is related to a better survival rate [139]. Knockdown of *Trpc4* also decreased TAC-induced hypertrophy and contractile

dysfunction in response to myocardial infarction [96]. Another study further shows TRPC1/4 double knockout prevents cardiac hypertrophy and fibrotic infiltration after TAC and chronic neurohumoral stimulation [133]. Overexpression of dominant-negative gene variants of certain TRPCs (TRPC3, TRPC4 and TRPC6) is confirmed to have protective effects against TAC-induced hypertrophy [99]. A recent study demonstrates that the mineralocorticoid pathway specifically promotes TRPC1/TRPC5-mediated SOCE in adult rat cardiomyocyte, which might be the underlying mechanism of abnormally enhanced SOCE during cardiac hypertrophy and heart failure [140].

1.5.2 Arrhythmia

As stated above in the EC coupling section, the calcium concentration within the cardiomyocytes experiences dynamic changes following an action potential. However for tens to hundreds of miliseconds after AP, Ca^{2+} remains refractory to the electrical stimuli by returning to diastolic levels mediated by the sarcolemma Ca^{2+}-ATPase and NCX as well as the SR NCX [141].

In humans, normal cardiac sinus rhythm is typically around 60 beats per minute, and this relies on a pacemaker mechanism called “coupled-clock” mechanism which is a coordinated crosstalk between sarcolemma and SR and involves multiple Ca^{2+}-dependent ion transport processes [142, 143]. This mechanism integrates an electric oscillator located on the sarcolemma and an intracellular SR Ca^{2+} cycling mechanism. Cellular Ca^{2+} oscillation requires a Ca^{2+} entry mechanism to compensate the loss of Ca^{2+} that goes extracellular during cytosolic Ca^{2+} transients, and to replenish the Ca^{2+} stores.

The vital role of store-replenishing mechanism in cardiac pacemaking has been clearly reported, and thus the important role of SOCE as one key mechanism for store-filling has been recognized [144]. The search for pacemaker activity regulating SOCE channels was first done in the TRPC family [145] and later in STIM/Orai complexes [146, 147]. The TRPC, STIM and Orai proteins have been found expressed in sinoatrial node cells and involved in SOCE pacemaker activity [145, 147]. In addition, STIM1 has been demonstrated to be crucial in maintaining the Ca^{2+} content of intracellular Ca^{2+} stores, thus contributing to maintaining the regular sinus rhythm of the heart in mouse [146]. The knockdown of STIM1 was found to perturb cell contraction rate and induce irregular spontaneous Ca^{2+} oscillations, thus presenting proarrhythmogenic activities, including early or delayed after depolarizations [148]. In an adult murine model with inducible and myocyte-specific STIM1 depletion, STIM1 was demonstrated to regulate spatially discordant alternans [149]. Early mortality in STIM1-knockdown mice was reported likely related to enhanced susceptibility to ventricular tachycardia/ventricular fibrillation secondary to the pathogenesis of spatially discordant action potential duration alternans [149]. The overexpression of STIM1 *in vivo* (in adult heart) and *in vitro* (in ventricular myocytes) generates spontaneous Ca^{2+} transients, thus causing arrhythmogenic Ca^{2+} waves and cytosolic and SR Ca^{2+} overload, potentially triggering sudden cardiac death [30, 106]. The role of Orai1 and Orai3-activating 2-APB (when applied at high concentration) in initiation of atrial and ventricular arrhythmias has been reported in cardiomyocytes [150]. Application of 2-APB induced a period of tachycardic ectopy and

progressed to spontaneous ventricular depolarization in Langendorff perfused rat heart and sinus rhythm and heart mechanical output was restored upon SKF-96365 application, indicating that activating myocardial voltage-independent calcium channels, possibly the Orais, may be a novel cause of ventricular arrhythmia [150].

In some disease conditions related with arrhythmias, abnormal calcium signals have been reported. During atrial fibrillation, spurious electrical signals can lead to atrial tachycardic with the atrial chamber displaying more than 300 beats per minute [151]. Spontaneous Ca^{2+} signals have been recognized as the cause of such arrhythmic activity [8, 152, 153]. In cardiomyocytes many mechanisms can contribute to the generation of Ca^{2+} spontaneous signals, including increased SR Ca^{2+} content, increased RyR or IP_3R activity, CICR-triggering Ca^{2+} source introduction. Although generating a more modest current than VGCC, Ca^{2+} entry pathway such as SOCE could also lead to arrhythmogenic spontaneous Ca^{2+} signals generation [154]. Notably, TRPC3, although unlikely to function as the primary SOCE channel in pacemakers, was reported to have implication in both sinoatrial and atrial arrhythmias [155]. It has also been demonstrated that SOCE, which is at least partially mediated by TRPC channels, exists in adult mouse ventricular myocytes. TRPC channels and SOCE mechanism are also reported to be involved in cardiac arrhythmogenesis via promotion of spontaneous Ca^{2+} waves and triggered activities under hyperactivated conditions [156]. A recent study demonstrated local transient Ca^{2+} (LoCE) events which comprise cardiac SOCE [157]. These LoCEs were found concentrated at the myocyte periphery from a genetic murine model of arrhythmic

disease (catecholaminergic ventricular tachycardia, CPVT), particularly at the intercalated disk, close to intercellular mechanical junctions. Furthermore, SOCE proteins and LoCEs were found upregulated at the intercalated disk in CPVT and myocytes showed characteristic arrhythmogenic spontaneous Ca^{2+} waves under cholinergic stress, which was effectively prevented by SOCE inhibition, further indicating the role of cardiac SOCE-mediated signaling in arrhythmias and providing more details with the fundamental cardiac SOCE properties.

CHAPTER 2

CIRCULATING IGGS IN TYPE 2 DIABETES WITH ATRIAL FIBRILLATION INDUCE IP_3-MEDIATED CALCIUM ELEVATION IN CARDIOMYOCYTES

Yanhong Luo[1, 4, 7], Xian Liu[2, 3, 7], Ruilian Ma[5], Yigang Wang[5], Mark Zimering[6*], Zui Pan[1, 2, 3, 8*]

AFFILIATIONS:

[1] Davis Heart and Lung Research Institute, Ohio State University-Wexner Medical Center, Columbus, OH, 43210, USA; [2] Department of Kinesiology; [3] College of Nursing and Health Innovation, University of Texas at Arlington, Arlington, TX, 76010, USA; [4] Department of Endocrinology, The Children's Hospital of Chongqing Medical University, Chongqing, P. R. China; [5] Division of Regenerative Medicine Research, Department of Pathology and Laboratory Medicine, University of Cincinnati, Cincinnati, OH, 45219, USA; [6] Endocrinology, Veterans Affairs New Jersey Healthcare System, East Orange, NJ, 07018, USA & Rutgers-Robert Wood Johnson Medical School, New Brunswick, NJ, 08901, USA.

[7] These authors contributed equally.
[8] Lead Contact

[*]Correspondence:
Zui Pan, PhD
Mark Zimering, MD, PhD

A version of this chapter has been published: Luo, Yanhong, Xian Liu, Ruilian Ma, Yigang Wang, Mark Zimering, and Zui Pan. "Circulating IgGs in Type 2 Diabetes with Atrial Fibrillation Induce IP_3-Mediated Calcium Elevation in Cardiomyocytes." *Iscience* (2020): 101036.

2.1 SUBJECT AREAS

Molecular Biology, Calcium signaling, Cardiovascular complications, G protein coupled receptor, IP_3 receptor, cardiac arrhythmias, Phospholipase C

2.2 ABSTRACT

Higher risk of cardiac arrhythmias including atrial fibrillation (AF) associates with type 2 diabetes mellitus (T2DM) with the underlying mechanism largely unknown. The present study reported a subset of circulating immunoglobulin G autoantibodies (IgGs) from T2DM patients with AF (T2DM/AF) induced intracellular calcium elevation in both human induced pluripotent stem cell (iPSC)-derived and mouse atrial cardiomyocytes, while (identical concentrations of) IgGs from T2DM patients without AF could not. The IgG-evoked intracellular calcium elevation was insensitive to verapamil, mibefradil or BTP2, indicating calcium source from neither voltage-gated calcium channels nor store-operated calcium entry. On the other hand, pharmacological antagonism or genetic knock-down of inositol triphosphate (IP_3) receptor significantly decreased T2DM/AF IgG-induced intracellular calcium elevation. Furthermore, pharmacological blockage of G protein-coupled receptor (GPCR), heterotrimeric G protein or Phospholipase C dampened IgG-induced intracellular calcium elevation. Taken together, circulating IgGs from T2DM/AF patients stimulated arrhythmogenic intracellular calcium elevation through IP_3 pathway in atrial cardiomyocytes.

2.3 INTRODUCTION

Diabetes mellitus (DM) affects 30.3 million people in the United States, i.e. 9.4% of the population, according to the 2017 National Diabetes Statistics Report [158]. Type 2 diabetes (T2DM) accounts for 90% to 95% of all diabetic cases [158]. Ischemic and non-ischemic cardiovascular diseases have been recognized for decades as the leading cause for morbidity and mortality in older adult T2DM [159]. Atrial fibrillation (AF) is the most common life-threatening cardiac arrhythmia in aging populations; and AF increases significantly in older persons having hypertension and T2DM [160]. Yet the underlying mechanism for the known association between AF and adult T2DM remains obscure [161].

Type 2 diabetes is not an autoimmune disease. Yet circulating IgG autoantibodies have been reported in advanced T2DM patients in association with specific neurovascular complications [162-164]. For example, in our prior report, IgG autoantibodies purified from T2DM patients suffering with macular edema and albuminuric nephropathy potently induced stress fiber formation and Rho kinase-mediated apoptosis in endothelial cells [163]. Clustering of microvascular diabetic complications, i.e. painful neuropathy, maculopathy and nephropathy triopathy, was observed in adult T2DM patients harboring highly potent endothelial inhibitory autoantibodies [165]. Triopathy diabetic IgG autoantibodies evoked significant intracellular calcium elevation in endothelial cells as well as in differentiated, neuronal-like rat pheochromocytoma PC12 cells. Since many of the same patients manifested non-ischemic cardiomyopathy such as clinically significant AF, and/or left ventricular hypertrophy, the possibility was suggested that IgG

autoantibodies may alter intracellular calcium signals in cardiomyocytes as well. Disturbance in calcium homeostasis has been implicated in the pathogenesis of AF and other cardiovascular diseases [166-168], thus, these IgGs may be arrhythmogenic and play an important role in T2DM non-ischemic cardiomyopathy. The present study provides evidence that circulating IgG autoantibodies from T2DM patients with AF stimulated arrhythmogenic intracellular calcium release and revealed their signaling pathway in cardiomyocytes.

Calcium signaling has been known to be involved in the development of AF. AF often progresses from an intermittent to persistent stage, and finally into permanent AF which lasts for more than a year and remains as chronic [169]. The primary arrhythmia mechanisms underlying AF can be characterized into two major types, the focal ectopic firing and the re-entrant activity, for both of which calcium has been reported to be involved. First of all, both AF animal models and human patient atrial samples show abnormal atrial calcium signaling in AF pathophysiology through contributing to the ectopic activity, conduction block and calcium-induced subcellular alternans mediated by after-depolarization [170]. Secondly, re-entry has been identified as the other predominant mechanism that initiates and maintains arrhythmias [170]. Re-entry requires both a vulnerable substrate and a trigger to act on the substrate and initiate AF [170]. This study seeks to examine the underlying mechanism of how circulating IgG autoantibodies could trigger arrhythmogenic calcium signals in atrial myocytes.

2.4 RESULTS

2.4.1 Purified IgG autoantibodies from T2DM/AF patients induced intracellular calcium elevation in human and mouse cardiomyocytes

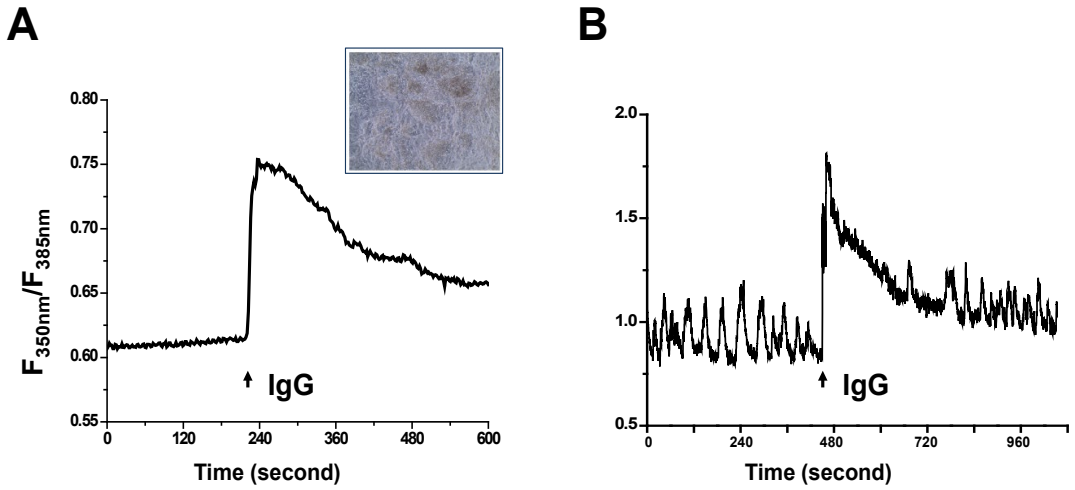

Figure 2-1 Purified IgG autoantibodies from a subset of patients with T2DM and AF induced Ca^{2+} elevation in both human iPSC-differentiated and mouse cardiomyocytes.

Ratio of fluorescence of fura-2 at two excitation wavelengths (F_{350nm}/F_{385nm}) was used to monitor changes in intracellular Ca^{2+} concentration.
A, Representative trace of intracellular Ca^{2+} in iPSC-differentiated cardiomyocytes. The inserted panel is phase contract image of human iPSC-differentiated cardiomyocytes. IgGs: ~30 μg/ml, n=8.
B, Representative trace of intracellular Ca^{2+} in HL-1 cells. The spontaneous Ca^{2+} oscillations could be observed in most of the cardiomyocytes. IgGs: ~30 μg/ml, n=12.
See also **Figure 2-3**.

To test whether IgG autoantibodies purified from T2DM patients with AF (T2DM/AF) could alter intracellular calcium homeostasis in cardiomyocytes, human induced pluripotent stem cells (iPSCs) were differentiated into cardiomyocytes [171]. These cells were loaded with fluorescent calcium indicator Fura-2 acetoxymethyl ester (Fura-2, AM)

and intracellular calcium level (presented as F_{350nm}/F_{385nm}) was monitored using live cell imaging. As shown in **Figure 2-1A**, addition of purified IgG autoantibodies from T2DM/AF patients could induce a rapid intracellular calcium elevation in these human iPSCs-derived cardiomyocytes. This was also seen in isolated adult mouse atrial cardiomyocytes as shown in **Figure 2-3**. Similar effects were observed in HL-1, a cardiomyocyte cell line derived from adult mouse atrium (**Figure 2-1B**)**.** HL-1 cells contained the spontaneous calcium oscillations, and addition of purified IgGs from T2DM/AF patients increased intracellular calcium and altered the oscillations' pattern (**Figure 2-1B**). Since HL-1 cells responded to these IgG autoantibodies similarly to human cardiomyocytes, this mouse cell line was used in the following studies.

2.4.2 HL-1 cells responded to IgG autoantibodies from T2DM/AF but not control subjects

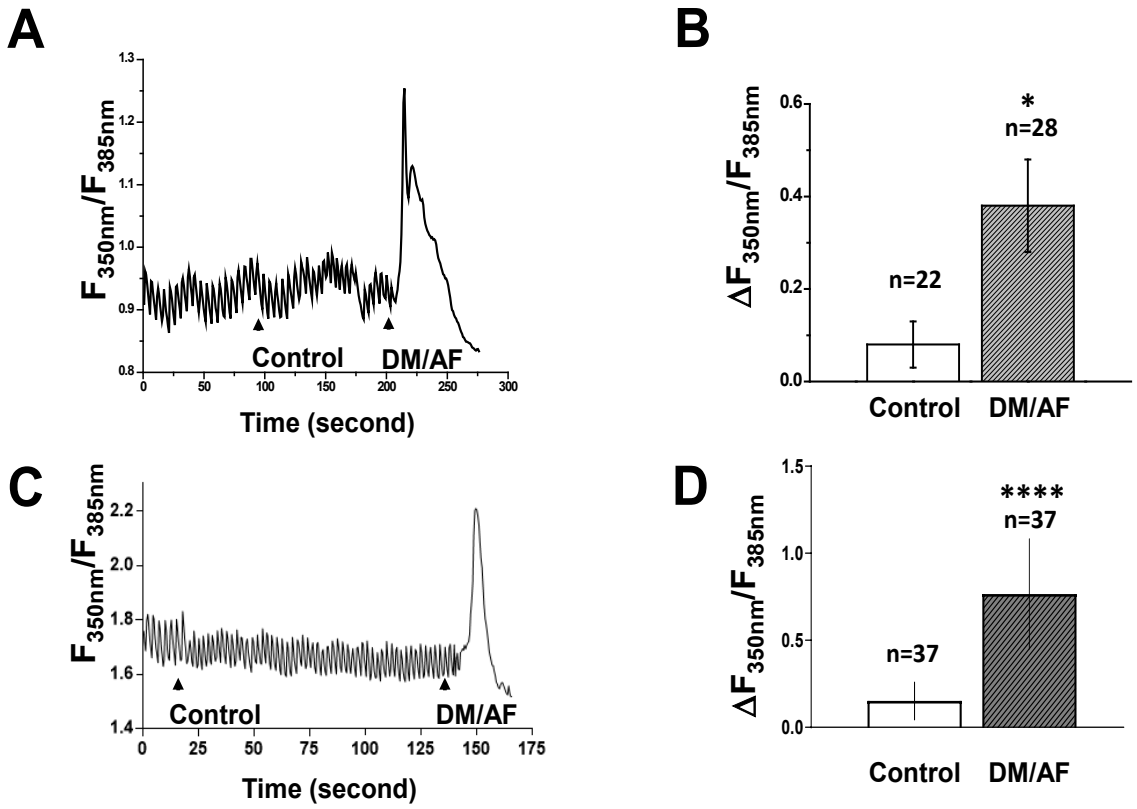

Figure 2-2 Intracellular Ca^{2+} response in HL-1 cells treated with IgG autoantibodies from T2DM patients with or without AF.

A. Representative trace of intracellular Ca^{2+}. The cardiomyocytes presenting spontaneous Ca^{2+} oscillations were selected for experiments. IgGs (2-5 μg/ml) derived from different patients were added at the indicated points (arrows). Control, T2DM without AF; DM/AF, T2DM with AF.

B. Statistics of changes in intracellular Ca^{2+} stimulated by IgGs. * $p< 0.01$. Data are represented as mean ± SEM.

C. Representative trace of intracellular Ca^{2+}. IgGs (30 μg/ml) derived from different patients were added at the indicated points (arrows).

D. Statistics of changes in intracellular Ca^{2+} stimulated by IgGs. **** $p< 0.0001$. Data are represented as mean ± SEM.

See also **Figure 2-3**.

To examine whether the intracellular calcium homeostasis disturbing-IgG autoantibodies are specific for T2DM/AF patients, intracellular calcium levels in cultured HL-1 cells were compared using purified IgG autoantibodies from T2DM patients with AF and T2DM patients without non-ischemic cardiomyopathy, i.e. no AF or left ventricular

hypertrophy (control subjects). Addition of 5 μg/ml of IgG autoantibodies purified from control subjects failed to stimulate significant intracellular calcium elevation in HL-1 cells, while IgG autoantibodies from T2DM/AF patients at the same concentration could induce a rapid calcium elevation (**Figure 2-2A**). IgG autoantibodies purified from 24 out of 28

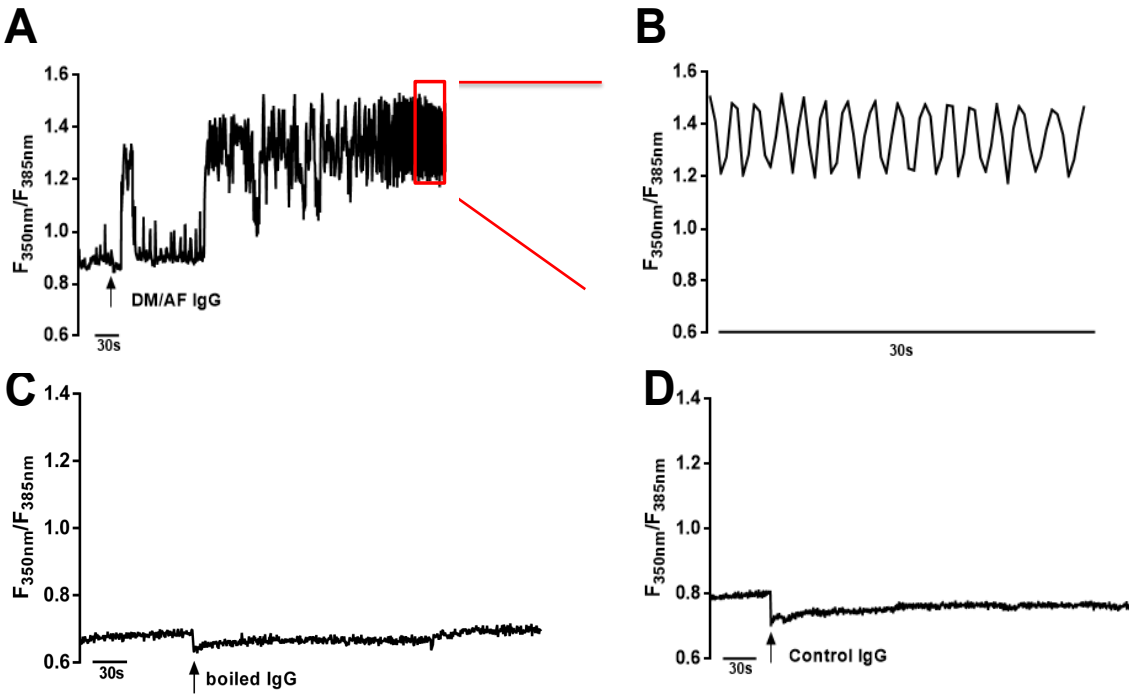

Figure 2-3 Intracellular calcium response in isolated adult mouse atrial myocytes treated with IgGs from T2DM patients with and without AF, **Related to Figure 2-1 and Figure 2-2.**

A. Representative trace of intracellular calcium signal. IgGs (5 μg/ml) derived from T2DM/AF patients were added at the indicated point (arrow).

B. Enlarged calcium oscillation signals in the red rectangle of **A**.

C. Representative trace of intracellular calcium signal treated with boiled IgGs (same as used in **A**) as negative control.

D. Representative trace of intracellular calcium signal treated with 5 μg/ml IgG from diabetic patients without AF. The same cells were later treated with 5 μg/ml T2DM/AF IgGs and demonstrated similar trace as in **A**.

T2DM/AF patients had significant responses while IgG autoantibodies from 21 out of 22 of control subjects failed to do so. The mean level of intracellular calcium elevation (presented as $\Delta F_{350nm}/F_{385nm}$) in the autoantibodies from T2DM/AF (0.38 ± 0.01) significantly exceeded the mean level (0.08 ± 0.05) in control subjects (**Figure 2-2B**. * $p<$ 0.01).

2.4.3 Pharmacological characterization of IgG autoantibody-induced calcium elevation in HL-1 cells

To understand the mechanism underlying the IgG autoantibody-induced intracellular calcium elevation, the calcium sources were examined first using various pharmacological inhibitors. Incubation of verapamil up to 20 μM, which is known to almost completely inhibit L-type calcium channel in HL-1 cells [172], failed to block these IgG autoantibody-induced intracellular calcium elevation (**Figure 2-4A**). Mibefradil is an antagonist for both L-type and T-type calcium channels and has IC_{50} at 0.4 μM for external K^+ induced-calcium influx in HL-1 cells. Up to 25 μM mibefradil failed to block the IgG autoantibody-induced intracellular calcium elevation (**Figure 2-4B**). BTP2 has been shown to block store-operated calcium entry (SOCE)-mediated calcium influx in cardiomyocytes [173]. Again, BTP2 at concentration of 5 μM failed to block the IgG autoantibody-induced intracellular calcium elevation in HL-1 cells (**Figure 2-4C**). Interestingly, 100 μM concentration of 2-aminoethoxydiphenyl borate (2-APB) completely blocked the IgG-induced intracellular calcium elevation (**Figure 2-4D**). Addition of 20 mM

caffeine at the end of experiments could induce a rapid calcium elevation (second arrow) indicating the sarcoplasmic reticulum (SR) calcium stores were intact. The quantification of the IgG autoantibody-induced calcium elevation is shown in **Figure 2-4E**. These data suggested that the IgG autoantibody-induced intracellular calcium elevation is independent of calcium influx from L-type, T-type calcium channels or SOCE.

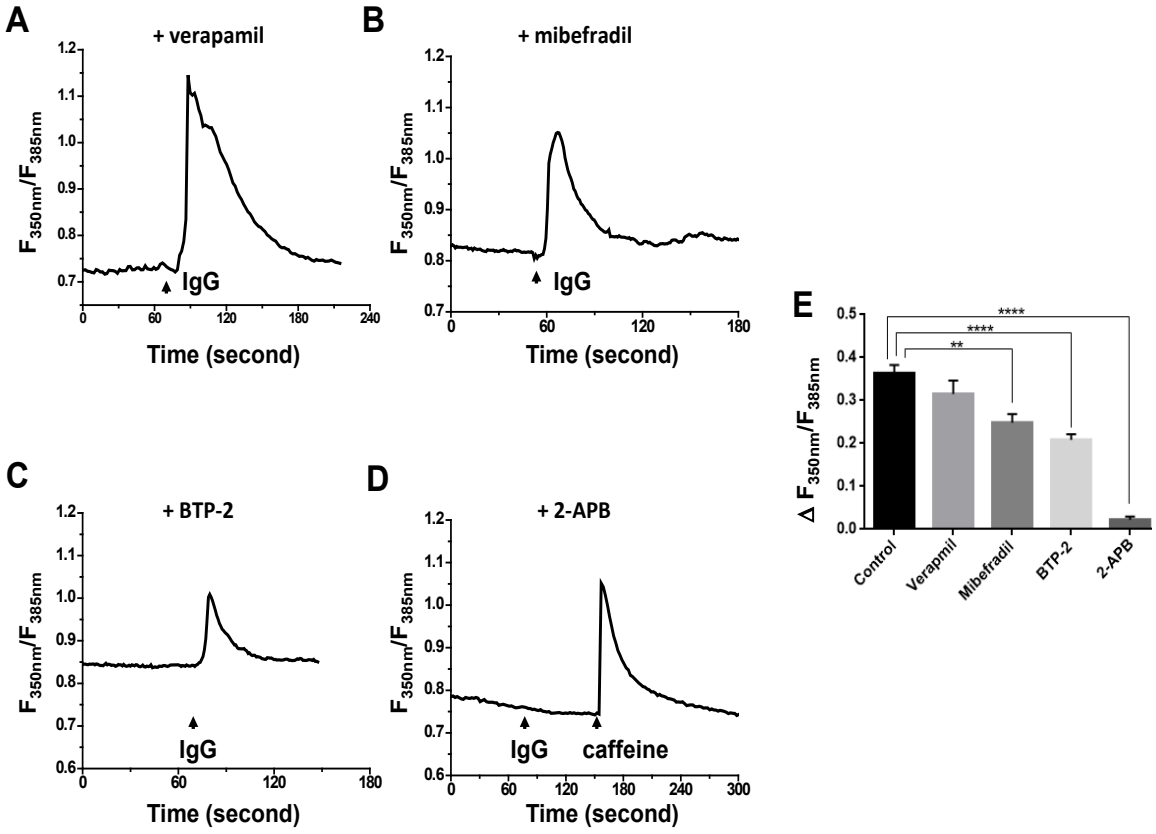

Figure 2-4 Pharmacological characterization of IgG autoantibody-induced Ca^{2+} elevation in HL-1 cardiomyocytes.

IgGs (2 μg/ml) derived from DM/AF patients resulted intracellular Ca^{2+} elevation in HL-1 cells treated with mibefradil (**A**, 25 μM), verapamil (**B**, 20 μM) and BTP-2 (**C**, 5 μM), but not in cells treated with 2-APB (**D**, 100 μM). 20 mM caffeine was added at the end of experiments to test whether SR Ca^{2+} stores were intact. n ≥ 3. **E.** Statistical data of IgGs induced changes in intracellular Ca^{2+} in HL-1 cells.
**: p=0.0014. ****: p<0.0001(based on One Way ANOVA and Bonferroni *post-hoc* analysis). Data are represented as mean ± SEM.

2.4.4 IgG autoantibody-induced intracellular calcium elevation was through IP_3 receptor

Since 2-APB at 100 μM could block both SOCE and IP_3 receptor (IP_3R) [174], an IP_3-mediated mechanism for IgG autoantibody-induced calcium elevation was tested using a more specific antagonist for IP_3R, i.e. xestosphongin C [175]. Incubation of HL-1

cells with 10 μM xestospongin C nearly completely blocked the IgG autoantibody-induced intracellular calcium elevation (**Figure 2-5B**), which was unaffected in HL-1 cells treated with vehicle alone (**Figure 2-5A**). The peak of intracellular calcium elevation responding to 20 mM caffeine indicated the intact SR calcium stores in both groups. To further examine the possible involvement of IP_3R in the IgG autoantibody-induced intracellular calcium elevation, the genes encoding IP_3R type 1 or type 2 were knocked down using a short hairpin RNA (shRNA) probe targeting the common sequences on the mouse mRNAs for IP_3R1 and IP_3R2 [176]. The efficacy of knocking down IP_3R1 and IP_3R2 proteins has been confirmed previously [176] and currently by qRT-PCR (**Figure 2-6**) . IgG autoantibodies from T2DM/AF failed to induce intracellular calcium elevation in HL-1 cells transfected with plasmids containing shRNA specifically targeting $IP_3R1\&2$ (**Figure 2-5E**), but they were still able to do so in cells transfected with control plasmids (**Figure 2-5D**). Statistically, the averaged intracellular calcium changes presented as $\Delta F_{350nm}/F_{385nm}$ were 0.08 ± 0.02 in cells transfected with shRNA against $IP_3R1\&2$ compared with 0.23 ± 0.02 in control cells (**Figure 2-5F**. ** $p< 0.001$**)**.

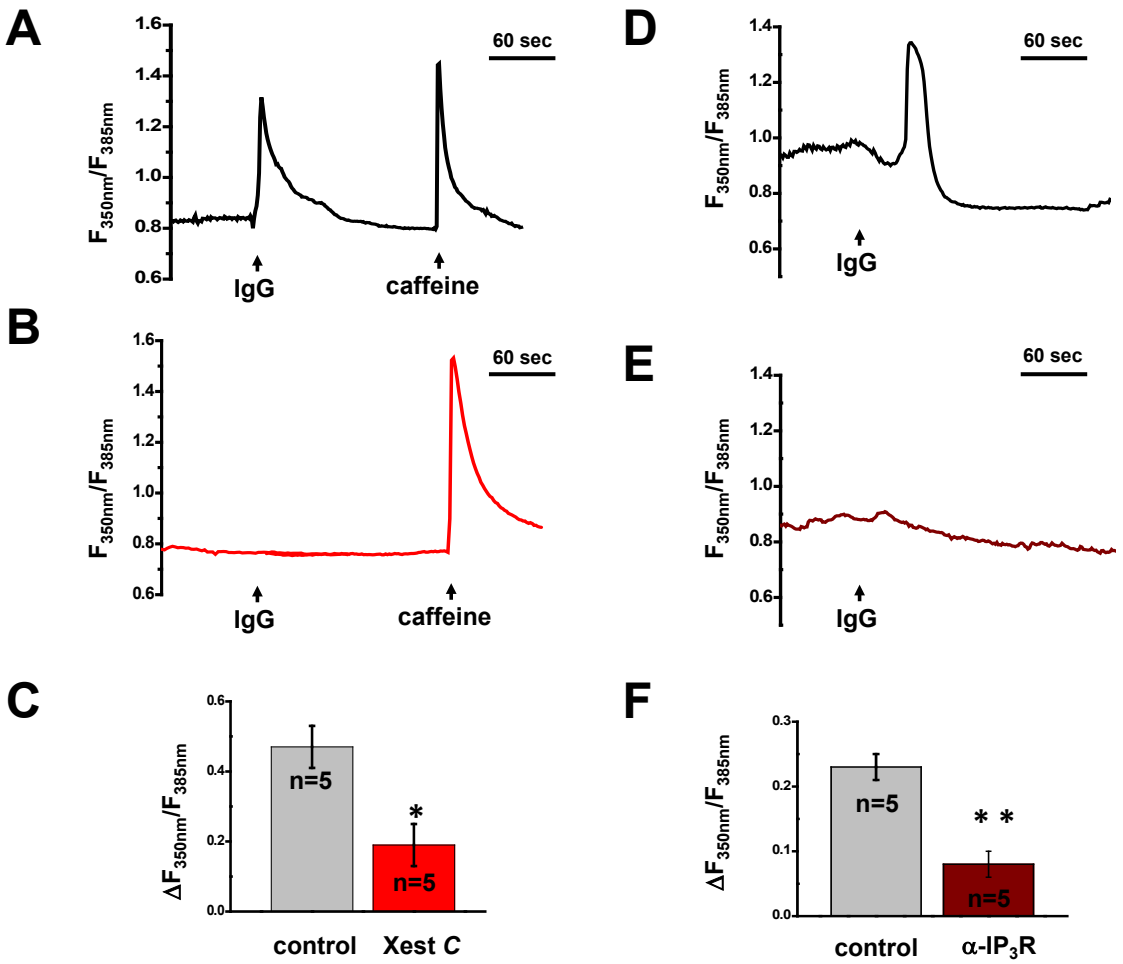

Figure 2-5 Inhibition or knockdown of IP_3R diminished IgG autoantibody-induced Ca^{2+} elevation in HL-1 cardiomyocytes.

IgGs purified from DM/AF patients were applied at the concentration of 2 μg/ml. The intracellular Ca^{2+} was recorded in HL-1 cells pre-treated with vehicle (**A,** control) or 10 μM xestospongin C (**B,** Xest C). 20 mM caffeine was added at the end of experiments to test whether SR Ca^{2+} stores were intact. **C**. Statistical data of IgGs induced changes in intracellular Ca^{2+} in HL-1 cells treated with vehicle or Xest C. *p<0.01. Data are represented as mean ± SEM. **D-E**. Representative traces of intracellular Ca^{2+} in HL-1 cells transfected with plasmids containing shRNA-control (**D,** control) or shRNA-α-IP_3R (**E,** α-IP_3R). **F**. Statistical data of IgGs induced changes in intracellular Ca^{2+} in HL-1 cells transfected with control or α-IP_3R plasmids. **: p<0.001. Mean ± SEM.
See also **Figure 2-6** and **Table 2-1**.

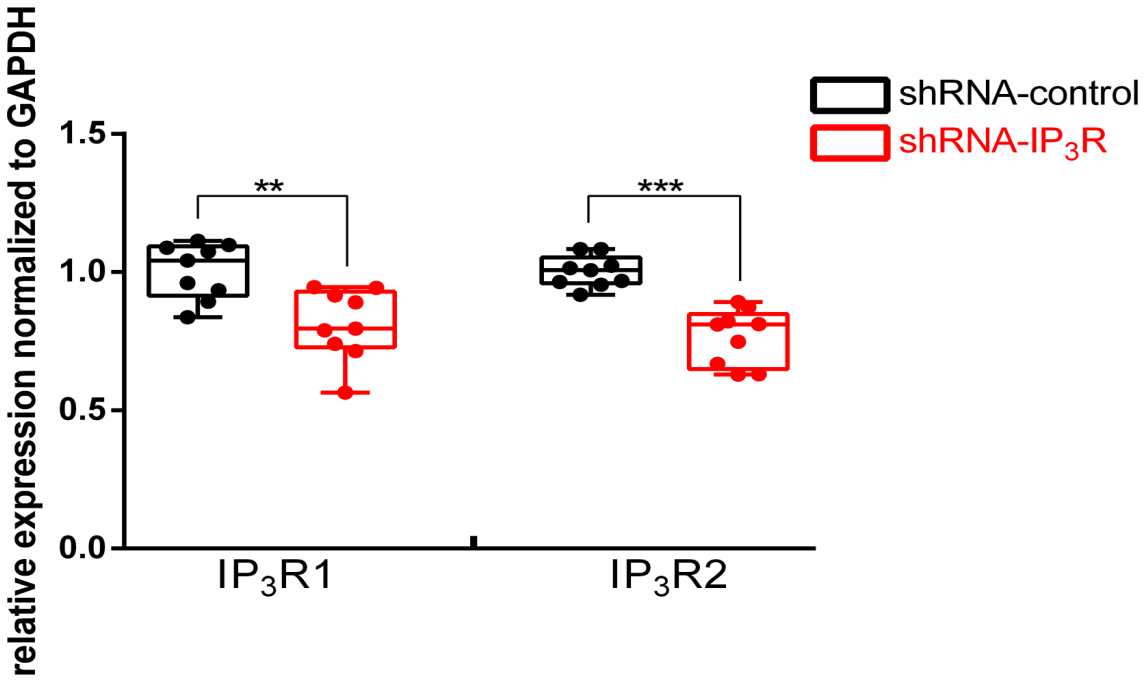

Figure 2-6 shRNA-mediated knockdown of IP_3R1 and IP_3R2 in HL-1 cells, Related to Figure 2-5.

shRNA-IP_3R was designed to target a common sequence on IP_3R1 and IP_3R2. Quantitative RT-PCR was performed using total RNAs from HL-1 cells two days after plasmid DNA transfection and showed that shRNA-IP_3R resulted in significant knockdown of IP_3R1 and IP_3R2 in HL-1 cells. n=3, **: p=0.0013. ***: p=0.0001.

Table 2-1 Primer sequences for qRT-PCR, Related to Figure 2-5.

Gene Name	Forward Primer (5'-3')	Reverse Primer (5'-3')
IP_3R1	CGTTTTGAGTTTGAAGGCGTTT	CATCTTGCGCCAATTCCCG
IP_3R2	CCTCGCCTACCACATCACC	TCACCACTCTCACTATGTCGT
GAPDH	AGGTCGGTGTGAACGGATTTG	TGTAGACCATGTAGTTGAGGTCA

2.4.5 PLC and GPCRs mediated IgG autoantibody-induced calcium elevation in HL-1 cells

To reveal the mechanism underlying IgG autoantibody-induced IP_3R-mediated intracellular calcium elevation, the pharmacological compounds, i.e. U-73122 [177] and SCH-202676 [178] were used to block PLC and GPCR, respectively. As shown in **Figure 2-7A & B**, treatment with both U-73122 (10 μM) and SCH-202676 (50 μM) could significantly reduce IgG autoantibody-induced intracellular calcium elevation. Statistical data were summarized in **Figure 2-7C**.

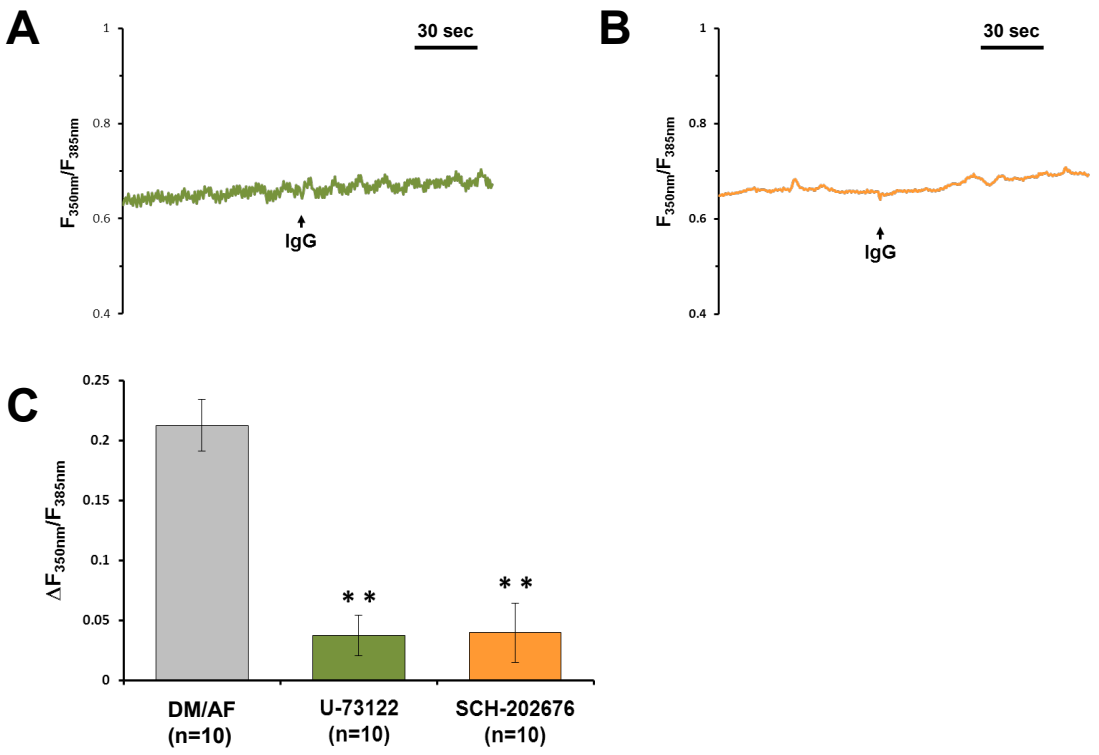

Figure 2-7 PLC and GPCR are involved in IgG autoantibody-induced Ca^{2+} elevation in HL-1 cardiomyocytes.

IgGs from DM/AF patients were applied at the concentration of (30 μg/ml).
A. Representative trace of IgG-induced Ca^{2+} in HL-1 cells treated with 10 μM U-73122 (right panel).
B. Representative trace of IgG-induced Ca^{2+} in HL-1 cells treated with 50 μM SCH-202676 (right panel).
C. Statistical data. n≥5, **: p<0.001. Data are represented as mean ± SEM.

2.5 DISCUSSION

In this study, we showed that circulating IgG autoantibodies from T2DM/AF patients were able to induce intracellular calcium elevation in both human iPSC-differentiated cardiomyocytes and mouse adult atrial cardiomyocytes (**Figure 2-1 and Figure 2-3**). Such effects were not observed in the IgG autoantibodies from a control group of age-matched T2DM without atrial fibrillation, or left ventricular hypertrophy (**Figure 2-2**). The IgG autoantibody-induced intracellular calcium elevation was insensitive to L-type or T-type calcium channel blockers or SOCE blocker but was sensitive to either xestospongin c or knocking down of IP_3Rs, indicating that the IgG autoantibody-induced intracellular calcium elevation was not dependent on voltage-gated calcium channel nor store-operated calcium channel, but rather dependent upon IP_3Rs pathway. Both PLC and GPCR blockers were able to diminish IgG autoantibody-induced intracellular elevation, indicating the involvement of PLC and GPCR in the IgG autoantibody-induced arrhythmogenic effects (**Figure 2-7**). This is the first report, to our knowledge, of circulating IgG autoantibodies with activity of stimulating intracellular calcium signals in diabetic patients with AF. Taken together, these results demonstrated that the IgG autoantibodies purified from older T2DM patient with AF could target an unknown GPCR, triggering IP_3R-dependent pathways. This discovery suggested the circulating IgG autoantibodies might play an important role in AF (**Figure 2-8**).

This study revealed that IgG autoantibodies from T2DM patients could trigger intracellular calcium elevation in both human iPSC-differentiated cardiomyocytes and

mouse atrial cardiomyocytes. The altered intracellular calcium signals could contribute to the onset or development of AF. The significant association between intracellular calcium release in atrial cardiomyocytes evoked by IgG autoantibodies in T2DM with, but not without co-morbid AF (**Figure 2-2B**) suggests a possible role for the IgG autoantibodies in AF causation. However, the exact contribution of these circulating IgG autoantibodies to the development of AF at different stages requires further investigation.

IP_3 receptor-dependent pathways have been reported to play an important role in hypertrophy and remodeling of cardiomyocytes. Many key factors known to induce arrhythmogenic calcium signals occur through IP_3 receptor-dependent pathways, and thus regulate atrial structural and electrical remodeling associated with AF, such as angiotensin II and endothelin-1 [179]. For example, endothelin increases the formation of IP_3 leading to enhanced calcium signaling, thus contributing to the development of atrial arrhythmias, which can ultimately lead to sudden cardiac death [180]. Up-regulation of IP_3R expression has been found in atrial tissues of patients with chronic AF [181]. The G-protein signaling regulator RGS4 has been reported to be the molecular substrate for predisposition of AF [182]. Mice with global RGS4 deletion show higher frequency of AF development, calcium spark under basal condition as well as upon endothelin treatment, and abnormal spontaneous calcium release events after field stimulation in the atrial cells isolated from them, compared with the control littermates. RGS4 inhibits the $G_{q/11}$ which activates the PLCβ that generates IP_3 [183]. The role of IP_3 in calcium signaling and the development of AF has also been reported in rat atrial myocytes [184]. The 2-APB-

induced IP_3R inhibition at 2 μM specifically suppresses the endothelin and IP_3-evoked increase of calcium signal amplitude and extra calcium transients, which are absent under control conditions in rat atrial myocytes. Furthermore, in an animal study using the IP_3R2-deficient mice, arrhythmogenic effects are abolished in the atrial myocytes isolated from IP_3R2-deficient mice compared to those in the cells isolated from the wild type littermates [180]. This study revealed that IP_3-IP_3R pathways mediate intracellular calcium elevation triggered by IgG autoantibodies from T2DM/AF patients. Data suggest that pharmacologic blockers targeting IP_3R pathways could be new drugs to neutralize harmful effects of IgG autoantibodies in treatment or prevention of AF in T2DM patients.

Emerging evidence has implicated the involvement of autoimmunity in the development of AF in many autoimmune diseases, together with other factors contributing to the pathogenesis of AF, ranging from electrical, structural, neurohumoral to inflammatory processes [185]. Several autoantibodies that play roles in the pathogenesis of AF include autoantibodies against GPCR superfamily proteins such as myosin heavy chain (MHC), sodium-potassium pump (Na/K-ATPase), the muscarinic cholinergic type 2 (M2) receptors, and the β1-adrenergic receptor [186]. The implications of autoantibody as upstream indicators of paroxysmal AF was shown in patients with congestive heart failure (CHF) [187]. In this cohort study of 95 CHF patients and 48 age-matched control patients with hypertension, circulating autoantibodies against Na/K-ATPase are suggested to be an independent risk factor for the occurrence of paroxysmal AF. Autoantibodies against M2 receptors may play roles in the development of AF in patients

with dilated cardiomyopathy (DCM) [188]. M2 autoantibodies are also found in patients with idiopathic AF [188]. M2 autoantibodies are confirmed to be independent predictors of the presence of AF in the patients indicated by multivariable analysis [188]. Autoantibodies against β1 and M2 facilitate the development of AF in patients with Graves' hyperthyroidism [189]. T2DM is not an autoimmune diseases, yet, accumulating evidence showed that circulating IgGs from T2DM patients, especially patients at advanced diseases stage or aged, present autoimmunity [163, 165]. In this study, blocking GPCR could eliminate IgG autoantibody-triggered arrhythmogenic calcium signals, suggesting that these IgGs could target GPCRs. However, the exact GPCR and whether other antigens are involved in these IgG autoantibody-mediated effects in T2DM/AF patients warrant further study.

In summary, this report highlighted that circulating IgGs from T2DM/AF patients could induce arrhythmogenic calcium signals in cardiomyocytes. The results reported here shed light upon a possible mechanism underlying the association between increased risk of AF and T2DM. The circulating IgGs may serve as a biomarker for identifying a subset of T2DM patients with an increased risk for the development of AF. Further identification of the receptors or antigens involved in IgG autoantibody-mediated IP_3R activation could result in sentinel biomarkers to assess the risk factors for AF and/or novel approaches for AF prevention in T2DM patients.

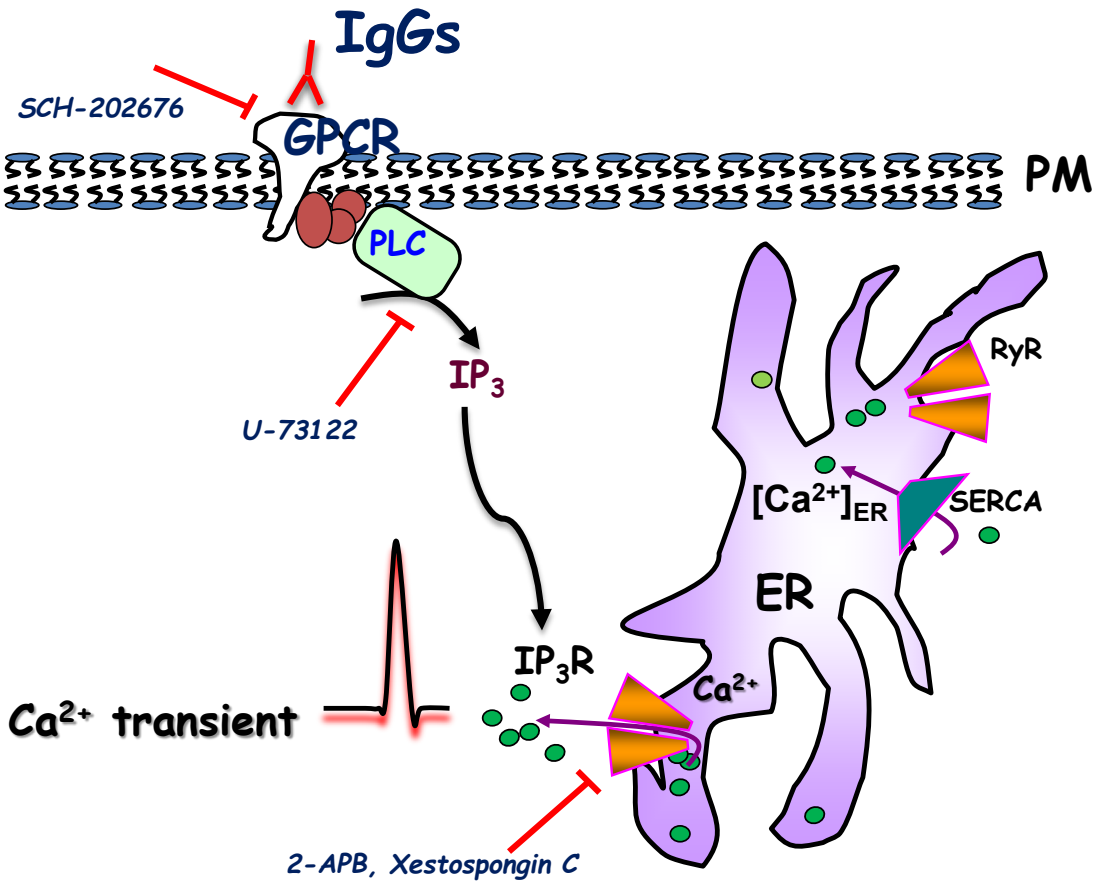

Figure 2-8 Working model for arrhythmogenic calcium signaling induced by circulating IgG autoantibodies in T2DM/AF patients.

Pharmacological data suggest that intracellular calcium elevation is through GPCR-PLC-IP_3-IP_3R pathway.

2.6 LIMITATION OF THE STUDY

Some limitations to our findings must be acknowledged. First of all, this study revealed a possible mechanism for the arrhythmogenic role of IgG autoantibodies purified from T2DM patients with AF in which they could trigger intracellular calcium elevation in human iPSC-differentiated, immortalized mouse atrial cardiomyocytes and isolated adult

mouse atrial myocytes. However, we do not know whether the same effects can be recapitulated *in vivo* as well. Secondly, our findings showed that the T2DM/AF IgGs could target GPCR and trigger IP_3R-dependent pathway, however the specific GPCR involved is currently unknown and remains to be further investigated.

2.7 MATERIALS AND METHODS

*2.7.*1 Subjects

All participants signed a local Veterans Affairs New Jersey Healthcare System (VANJHCS) Investigational Review Board (IRB)-approved informed consent prior to blood drawing for the study. Participants included twenty-one adult T2DM patients from the Veterans Affairs Diabetes Trial [163, 190]; and twenty-nine adult T2DM participants enrolled in a VANJHCS study of diabetic complications. Patients having diabetes with AF were excluded if they had a co-morbid condition associated with an independent increased risk of AF (severe pulmonary disease, heavy alcohol use, valvular heart disease or AF-onset following episode of ischemic heart disease). Diabetes without AF was excluded for these same co-morbidities or for having left ventricular hypertrophy, or sinus arrythmia on a recent electrocardiogram. Diabetes (with or without atrial fibrillation) did not differ significantly in their baseline age, glycosylated hemoglobin or presence of nephropathy or retinopathy (**Table 2-2**). Diabetes with atrial fibrillation had significantly higher baseline prevalence of insulin use (64% vs 35%, p=0.45) compared to diabetes without atrial fibrillation (**Table 2-2**). The circulating IgGs were purified from each patient's

stored serum samples using protein-A columns as previously described [164]. The purified IgG samples were coded and shipped on dry ice to Dr. Pan's laboratory. Dr. Pan was blinded to the study participants' diagnosis until the conclusion of the calcium elevation experiments.

2.7.2 Cell lines and cell culture

HL-1 cells were maintained in Claycomb medium supplemented with 10% FBS, 100 U/ml penicillin, 100 μg/ml streptomycin, 0.1 mM norepinephrine, 2 mM L-glutamine [191]. The cell line was cultured at 37°C in a humidified 5% CO_2 incubator. Human induced pluripotent stem cells (iPSCs) were cultured and differentiated into cardiomyocytes following the published procedure [171].

*2.7.*3 Measurement of intracellular calcium concentration

Intracellular calcium concentration in HL-1 cell line, human iPSCs and isolated adult mouse atrial myocytes was monitored by fluorescence microscopy with a 40x objective (Nikon TE200 Super Fluo, N.A. 1.3) in a dual-wavelength spectrofluorometer (Photon Technology International, Monmouth Junction, NJ), with excitation wavelengths at 350 and 385 nm and emission at 510 nm [164]. Purified IgGs from T2DM AF patients were added into bath saline solution (140 mM NaCl, 2.8 mM KCl, 2 mM $MgCl_2$, 2 mM $CaCl_2$, 10 mM HEPES, pH 7.2) at indicated time. The intracellular calcium elevation was presented as $\Delta F_{350nm}/F_{385nm}$.

2.7.4 Plasmids and shRNAs

The plasmid containing RFP reporter gene and a short hairpin RNA (shRNA) probes targeting common sequences of mouse mRNAs for both IP_3R1 and IP_3R2 were transfected into HL-1 cells. Same plasmids containing scramble shRNA were used as control. The efficacy in knocking down IP_3R1 and IP_3R2 protein has been confirmed previously verified by Western blotting analysis [176] and by current experiment examining the mRNA levels using quantitative reverse transcription polymerase chain reaction (qRT-PCR) two days after plasmid DNA transfection.

2.7.5 Statistical analysis

Data were analyzed using Origin Pro 7 and Graphpad 6 software. Values are Mean ± SEM or otherwise indicated. Significance was determined by one-way analysis of variance (ANOVA) followed by Bonferroni *post-hoc* analysis examining the differences among groups. A value of $p<0.01$ was used as criterion for statistical significance.

2.7.6 Quantitative reverse transcription polymerase chain reaction (qRT-PCR)

Total RNAs were extracted from HL-1 cells using Illustra RNAspin MiniRNA Isolation Kit and measured photometrically at 260/280 nm. Primers were obtained from Sigma Aldrich. 200ng of total RNA was applied for reverse transcription using qScript microRNA Synthesis Kit (QuantaBio) according to the manufacturer's protocol. cDNA was diluted 1:5 in DNase-, RNase- and protease-free water and 2 µl template was used. Primer pairs of IP_3R1, IP_3R2 and GAPDH were used. The sequences are indicated in

Table 2-1. For qRT-PCR QuantaBio PerfecTa SYBR Green FastMix ROX was used based on the manufacturer's procedure. Signals generated by integration of SYBR Green into the amplified DNA were detected in a real-time PCR system (StepOnePlus) and normalized to GAPDH gene expression. Data were expressed as $2^{-\Delta\Delta CT}$.

2.7.7 Adult mouse atrial myocyte isolation

All animal protocols were approved by the University of Texas at Arlington Institutional Animal Care and Use Committee (IACUC) in accordance with the Animal Welfare Act (AWA) and PHS Policy on Humane Care and Use of Laboratory Animals of United States. C57BL/6J mice with both genders, at age of 5-16 months old were used. Primary atrial myocytes were isolated according to the published protocol [192] using a combination of enzymatic digestion and mechanical dissociation of these tissues. Briefly, the mouse atrial appendage was excised and put into modified Tyrode's pH 7.4 solution and cut into 8-10 strips and then transferred into 2.5 ml modified Tyrode's pH 6.9 solution and incubated for 5 min. The atrial tissues were washed three times in 2.5 ml modified Tyrode's pH 6.9 solution, followed by enzymatic digestion for 30 min in 5 ml Enzymatic solution. Three washes were then performed in 2.5 ml Kraft-Brühe (KB) solution (HEPES balanced, pH 7.2) followed by 5 min incubation in 2.5 ml KB solution. The atrial myocytes were then triturated for 7.5 min in 2.5 ml KB solution and incubated for 1 hr at room temperature in 29 mm glass-bottom dishes pre-coated with laminin overnight. Right before calcium measurement, the external solution was changed to BSS-Ca^{2+} solution.

Table 2-2 Baseline clinical characteristics in participants

Risk factor	Diabetes		
	AF (N=28)	No AF (N =22)	*p*-value^, *
Age (years)	63.9± 8.1	65.0 ± 11.5	0.57
HbA_1c (%)	8.0 ± 1.4	8.2 ± 1.8	0.39
HTN (%)	82	77	0.73
Insulin use (%)	64	35	0.045
ME, AMD (%)	29	23	0.75
Nephropathy (%)	18	14	1.00

HbA_1c- glycosylated hemoglobin

ME-macular edema

AMD- age-related macular degeneration

HTN-hypertension

p-value: ^T-test for continuous variables (age, glycosylated hemoglobin)

*Fischer's exact test for dichotomous variables (HTN, insulin use, ME, AMD, Nephropathy)

CHAPTER 3

BLOCKING STORE-OPERATED CA^{2+} ENTRY TO PROTECT CARDIOMYOCYTES FROM EPIRUBICIN-INDUCED CARDIOTOXICITY

3.1 INTRODUCTION

Anthracyclines listed in the 21st (the latest) version of World Health Organization (WHO) model list of essential medicines [193] are among the most efficacious and widely used chemotherapy drugs since the late 1960s [194, 195]. Epirubicin (EPI) belongs to the anthracycline family and combined with new-generation targeted drugs continue to play a major role in the modern era of cancer treatment, making great contribution to the improvement of cancer outcomes. However, dose-limiting cardiotoxicity hinders their clinical application, which often leads to requirement for regimen modification or even discontinuation [196]. The anthracycline-induced cardiotoxicity can be manifested either acutely during the treatment period or chronically several weeks to even years after treatment has stopped [2]. The associated cardiac dysfunction has a broad range of symptoms including cardiac hypertrophy, cardiomyopathy and ultimately congestive heart failure [3-6, 197, 198].

Cardiac hypertrophy is the enlargement of the heart. Cardiac hypertrophy can be divided into two categories: physiological and pathological, both of which develop as an adaptive response to cardiac stress but their underlying molecular mechanisms, cardiac phenotype and prognosis are quite different. Several lines of evidence have demonstrated the involvement of signaling pathways in the cardiomyocyte hypertrophic growth, however Ca^{2+}-related genes are only changed during pathological hypertrophy but not in physiological hypertrophy [109]. Studies have demonstrated that intracellular calcium regulates calcineurin-NFAT signaling pathway and thus initiating hypertrophy-

related gene transcription [101-103, 124]. A rise in intracellular calcium leads to the activation of the phosphatase activity of calcineurin, the dephosphorylation of NFAT family members, and their translocation to the nucleus to initiate transcription [124].

Store-operated calcium entry (SOCE) is a ubiquitous calcium entry pathway activated in response to the depletion of endoplasmic reticulum Ca^{2+} stores. Although SOCE is well-studied in non-excitable cells and skeletal muscles, the understanding of its important role in cardiomyocytes is emerging [9, 124, 199-201]. Dysregulated Ca^{2+} signaling has been reported to be underlying EPI-induced cardiotoxicity [197, 198, 202], with the specific role of SOCE in this process currently not fully understood. However there have been evidences linking enhanced SOCE with cardiac hypertrophy and heart failure [101-103], yet its role in EPI-induced cardiotoxicity remains to be further elucidated. Thus, the objective of the present study is to determine the mechanism underlying how SOCE contributes to EPI-induced cell apoptosis and hypertrophy in cardiomyocyte.

3.2 RESULTS

3.2.1 BTP2 inhibited EPI-induced hypertrophy in HL-1 cardiomyocytes

SOCE has recently be associated with cardiac hypertrophy [203], and heart failure [204] and EPI can cause cardiotoxicity including hypertrophy in cardiomyocytes. Thus, we first examined whether BTP2, a known SOCE blocker, can inhibit EPI-induced hypertrophy in HL-1 cardiomyocytes. These cells were treated with vehicle control, 1 μM EPI, or co-treated with 1 μM EPI and 20 μM BTP2 for 4 hrs, followed by drug withdrawal

and cells put back in normal culture media and allowed to grow for 24 hrs. Phase contrast images were then taken on these cells and the surface area of HL-1 cardiomyocytes was measured and quantified. EPI treatment increased the size of cardiomyocytes almost twice as large as vehicle-treated control cardiomyocytes (**Figure 3-1A** and **Figure 3-1B**,

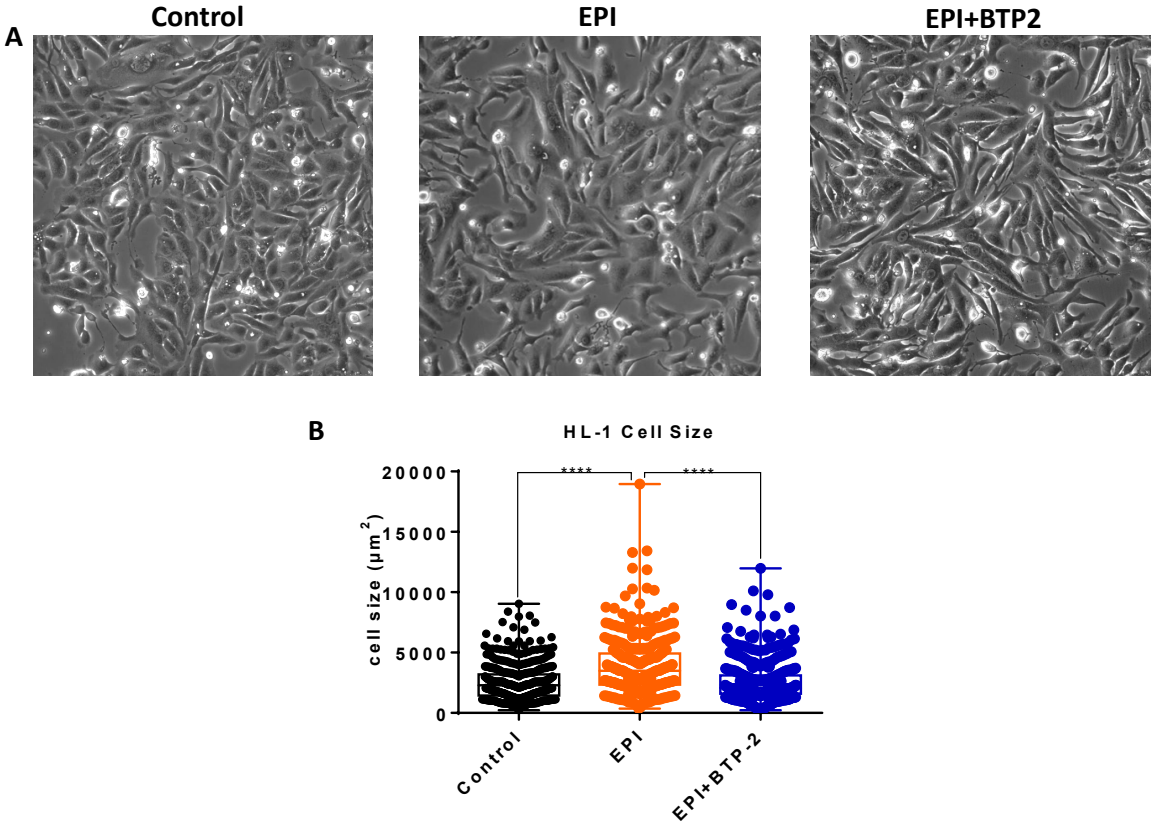

Figure 3-1 BTP2 inhibited epirubicin-induced hypertrophy in HL-1 cardiomyocytes.

HL-1 cells with 1 μM epirubicin 4 hr treatment followed by fresh media culture for 24 hrs showed significantly increased cell size compared with the vehicle-treated control cells. This EPI-induced cell size increase was abolished by 20 μM BTP2 co-treatment.
(A) Phase contrast images of HL-1 cells treated with 1 μM epirubicin, 1 μM epirubicin together with 20 μM BTP2, or vehicle-treated control.
(B) Quantification of the cell surface area of HL-1 cardiomyocytes. Mean ± SEM, n=581. ****: p<0.0001. (based on One Way ANOVA and Bonferroni *post-hoc* analysis).

Mean ± SEM, n=581, EPI vs. Control, ****: p<0.0001). Co-treatment with BTP2 and EPI,

the size of HL-1 cells was significantly reduced compared to that in EPI treated group (**Figure 3-1A** and **Figure 3-1B**, Mean ± SEM, n=581, EPI vs. EPI+BTP2, ******:** $p<0.0001$). This data indicates that BTP2 was able to reduce EPI-induced hypertrophy in HL-1 cardiomyocytes.

3.2.2 EPI-increased SOCE could be blocked by BTP2 in HL-1 cardiomyocytes

Next, we examined whether EPI increases SOCE in HL-1 cardiomyocytes. First, HL-1 cells were loaded with 5 μM fluorescent calcium indicator fura-2 AM at 37°C in the dark together with vehicle control of 20 μM BTP2 for 30 min. The intracellular calcium level (presented as F_{350nm}/F_{385nm}) was monitored using live cell imaging. The cellular endoplasmic reticulum (ER) Ca^{2+} stores were depleted by 10 μM thapsigargin (TG) in 0.5 mM EGTA dissolved in basal saline solution, followed by re-introduction of 2 mM $CaCl_2$. As shown in **Figure 3-2**, the mean level of intracellular calcium in HL-1 cells with BTP2 treatment (0.142 ± 0.064) was significantly decreased compared with that of the vehicle-treated control cells (0.188 ± 0.058, n=35. **: $p=0.0051$). This data validated the presence of SOCE in HL-1 cardiomyocytes, and that BTP2 was able to inhibit SOCE in these cells, thus providing us with a valuable cellular model to examine the influence of EPI treatment in these cells.

We next evaluated whether EPI could enhance SOCE in these cells, and to further determine the effects of blocking SOCE with BTP2 on that. As shown in **Figure 3-2**, HL-1 cells treated with 1 μM EPI demonstrated significantly enhanced SOCE (0.254 ± 0.069) compared to those treated with vehicle control (0.188 ± 0.058, n=37. ****: p<0.0001). When co-treated with BTP2 along with EPI, SOCE was significantly decreased (0.045 ± 0.027) compared to that in EPI-alone-treated (0.254 ± 0.069, n=36, ****: p<0.0001) HL-

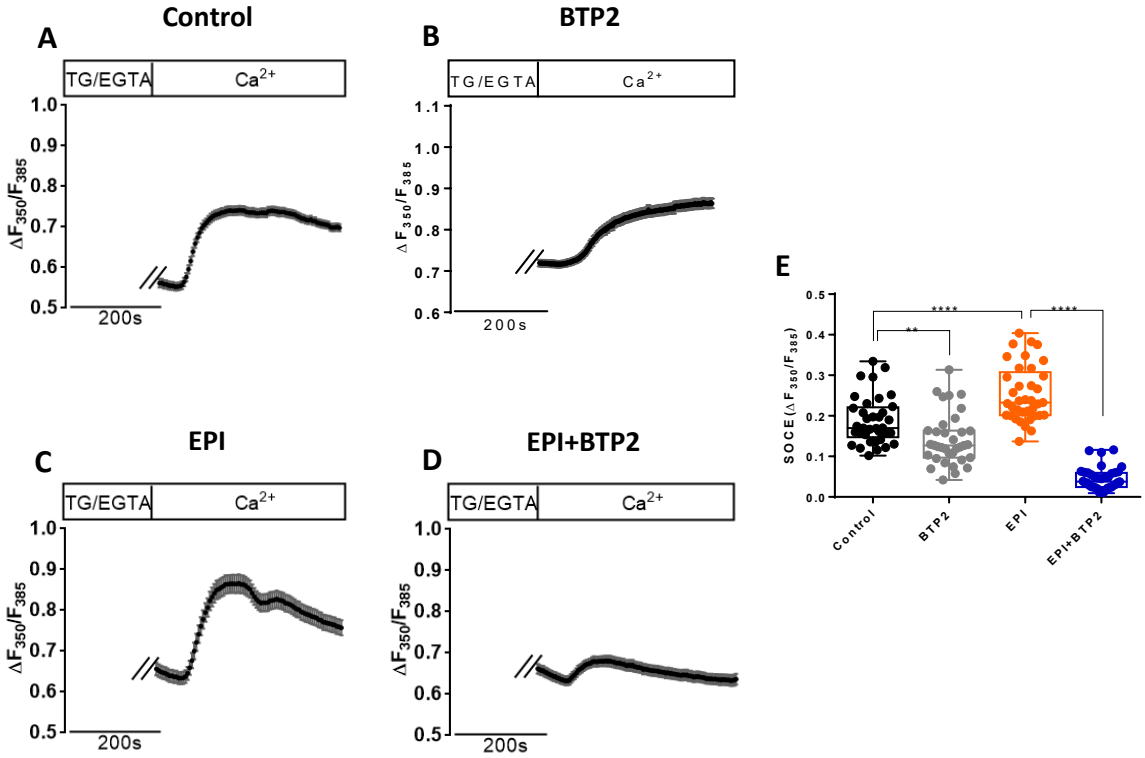

Figure 3-2 Epirubicin-increased SOCE could be blocked by BTP2 in HL-1 cardiomyocytes.

Ratio of fluorescence of fura-2 AM at two excitation wavelengths (F_{350nm}/F_{385nm}) was used to monitor changes in intracellular Ca^{2+} concentration.

(A-D) Representative traces of intracellular Ca^{2+} in HL-1 cells treated with vehicle control, 20 μM BTP2, 1 μM epirubicin or 20 μM BTP2 plus1 μM epirubicin for 30 min.

(E) Statistics of changes in intracellular Ca^{2+} in HL-1 cells with the treatment.

Mean ± SD, n=35. **: p=0.0056. ****: p<0.0001. (based on One Way ANOVA and Bonferroni *post-hoc* analysis).

1 cells, indicating that pharmacologically inhibiting SOCE with BTP2 can reduced the EPI-induced SOCE enhancement in HL-1 cells.

3.2.3 BTP2 inhibited EPI-induced NFAT4 nuclear translocation and BNP upregulation in HL-1 cardiomyocytes

Nuclear factor of activated T-cells (NFAT) is reported to be a critical nuclear transcriptional factor regulating cardiac hypertrophy [94]. Since we observed anti-hypertrophic effect of BTP2 treatment in HL-1 cardiomyocytes, we wanted to further gain insight into the molecular mechanism underlying this anti-hypertrophic effect of BTP2 treatment. Therefore, we continued to investigate whether NFAT nuclear translocation is underlying the EPI-induced cardiomyocyte hypertrophy, and whether pharmacologically inhibiting SOCE by BTP2 treatment can reduce it. Cardiomyocytes express five subtypes

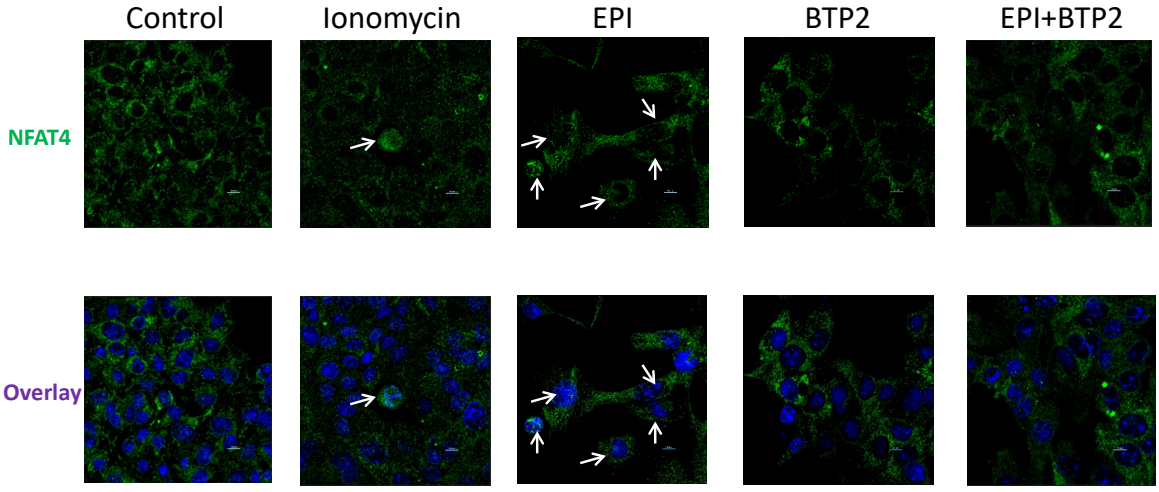

Figure 3-3 BTP2 inhibited epirubicin-induced nuclear translocation of NFAT4 in HL-1 cardiomyocytes.

HL-1 were treated with vehicle, 1 μM epirubicin, 20 μM BTP2 or 1 μM epirubicin combined with 20 μM BTP2 for 4 hrs, followed by drug withdrawal and culture for 24 hrs and stained for NFAT4. Cells treated with 10 μM ionomycin for 15 min were used as positive control.

of NFAT with NFAT4 being the most highly expressed and likely the most important subtype [205]. HL-1 cardiomyocytes were treated with vehicle, 1 μM EPI, 20 μM BTP2 or 1 μM EPI combined with 20 μM BTP2 for 4 hrs, and then the drugs were withdrawn and cells cultured in complete growth media for 24 hrs until fixation and immunostaining with NFAT4 primary antibody. Cardiomyocytes treated with 10 μM ionomycin for 15 min were used as positive control for the immunostaining since ionomycin is a strong activator for NFAT-signaling [202]. The nuclear translocation of NFAT4 was examined by confocal imaging. As shown in **Figure 3-3**, EPI treatment induced NFAT4 nuclear translocation, indicated by the white arrows, whereas co-treatment with BTP2 showed little NFAT4 nuclear translocation. This data suggests that the EPI-induced nuclear translocation of NFAT4 can be inhibited when blocking SOCE of the HL-1 cardiomyocytes.

Activated NFAT has been shown to stimulate the brain natriuretic peptide (BNP) expression increase [206, 207]. To confirm the effect of SOCE blockade on the hypertrophic growth in cardiomyocytes, mRNA level of BNP, the specific marker of cardiac hypertrophy was also examined. As shown in **Figure 3-4**, In line with the result of NFAT4 nuclear translocation, the mRNA expression level of BNP was significantly increased upon 1 μM EPI treatment (4.861 ± 0.697) compared to that of vehicle-treated Control cells (1.010 ± 0.155, n=3, ****: $p<0.0001$). However, when co-treated with 20 μM BTP2 and 1 μM EPI, the increased BNP expression level induced by EPI treatment (4.861 ± 0.697) was significantly inhibited (3.054 ± 0.260, n=3, ****: $p<0.0001$) in HL-1 cardiomyocytes.

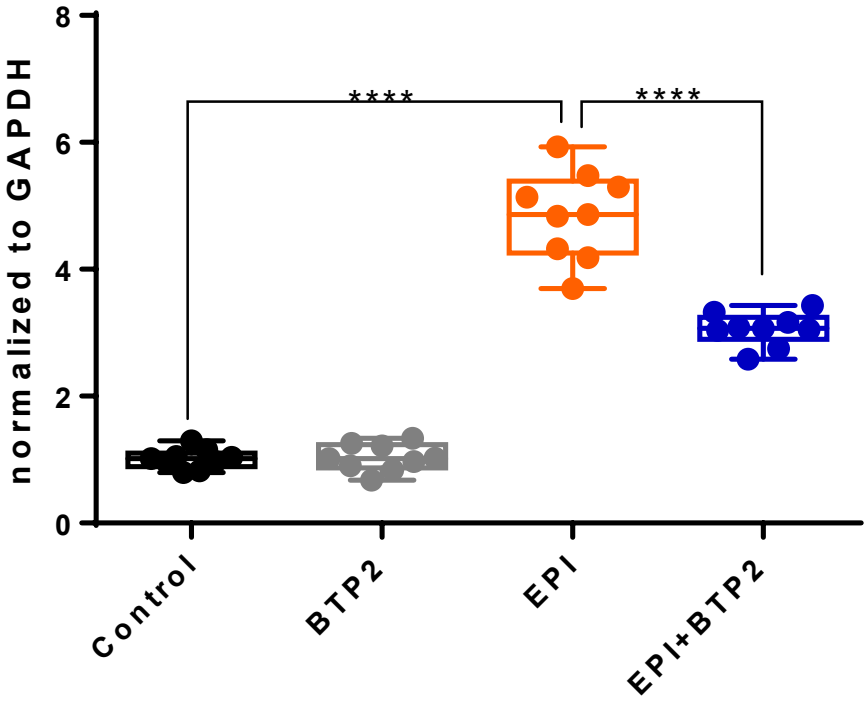

Figure 3-4 BTP2 reduced epirubicin-induced hypertrophy marker BNP transcript increase in HL-1 cardiomyocytes.

BTP2 rescued HL-1 cells from epirubicin-induced BNP transcript increase. Quantitative reverse transcriptase PCR expression level of BNP was normalized to GAPDH and plotted relative to the level in the vehicle-treated control cells.
n=3, Mean ± SD. ****: $p<0.0001$. (based on One Way ANOVA and Bonferroni *post-hoc* analysis).

There results taken together indicate that pharmacologically inhibiting SOCE by BTP2 can inhibit the EPI-induced NFAT4 nuclear translocation and BNP transcript increase in HL-1 cardiomyocytes.

3.2.4 BTP2 inhibited EPI-induced apoptosis in HL-1 cardiomyocytes

Degradation of F-actin is a hallmark for apoptosis [208]. To further examine the

EPI-induced apoptosis in HL-1 cardiomyocytes, we then went on to examine the F-actin expression using the phalloidin dye to stain the cells. After treatment of 10 μM EPI for 5 hrs, a reduced expression of F-actin was observed (**Figure 3-5A**) compared to that of vehicle-treated Control cells, which suggests that EPI induced apoptosis in HL-1 cardiomyocytes. When co-treated with 20 μM BTP2, the EPI-induced degradation of F-actin was partially rescued (**Figure 3-5A**), indicating that BTP2 inhibited EPI-induced F-actin degradation. We also observed nuclear condensation in HL-1 cells with 10 μM EPI

treatment for 5 hrs, which was largely absent when cells were co-treated with 10 μM EPI and 20 μM BTP2 (**Figure 3-5B**). This further confirmed EPI induced cellular apoptosis and it was partially rescued with BTP2 co-treatment.

Anthracyclines have also been implicated in inducing cardiotoxicity through apoptosis in HL-1 cardiomyocytes mediated by caspase-3 [209]. To evaluate the specific

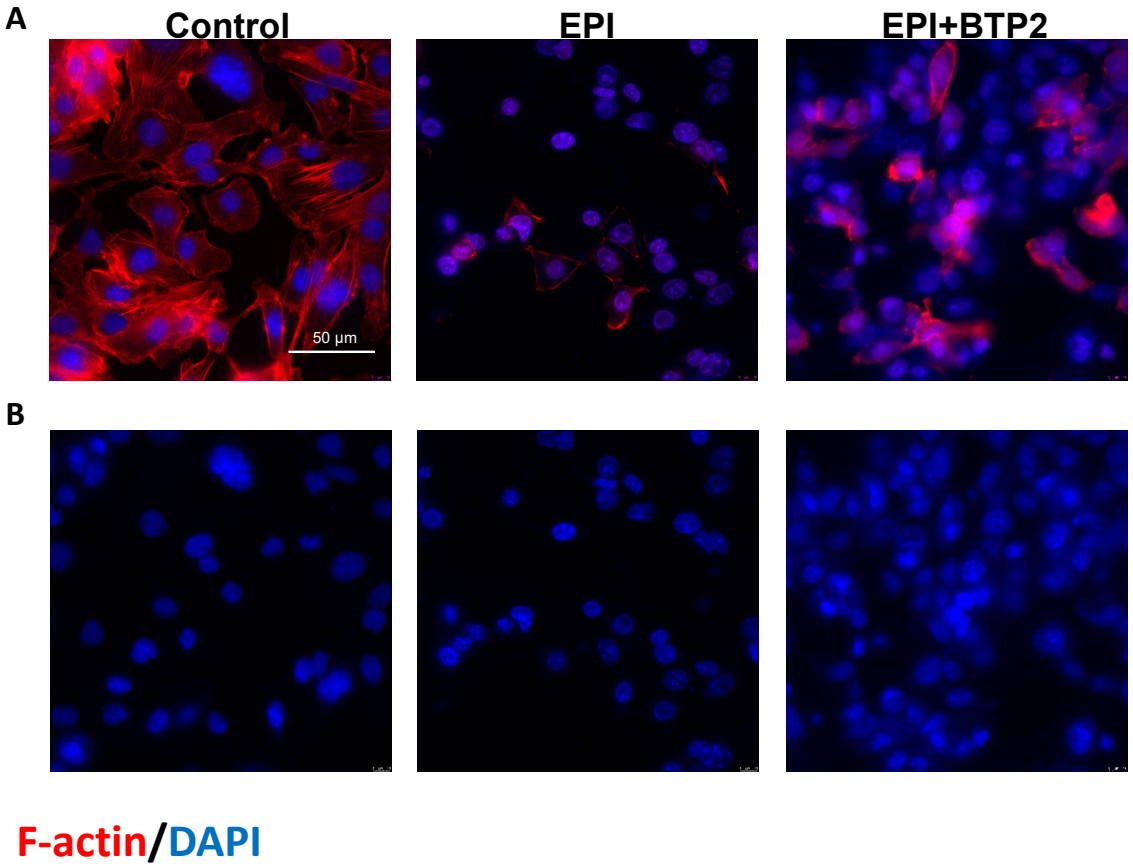

Figure 3-5 BTP2 inhibited epirubicin-induced apoptosis (F-actin degradation) in HL-1 cardiomyocytes.

Cell nuclei were stained with DAPI (blue) and F-actin was stained with phalloidin (red). With 10 μM EPI treatment for 5 hrs, the F-actin degradation was observed. With 20 μM BTP2 co-treatment, the EPI-induced F-actin degradation was partially rescued.

mechanism underlying SOCE inhibition rescuing EPI-induced cardiomyocyte apoptosis,

we continued by examining the expression level of cleaved caspase-3 in HL-1 cells. After treated with 1 μM EPI for 72 hrs, the cleaved caspase-3 protein level in HL-1 cells increased compared to that of the vehicle-treated control cells (**Figure 3-6)**, whereas when co-treated with 20 μM BTP2 the EPI-increased cleaved caspase-3 protein expression level was decreased. This indicates that EPI induced caspase-3-mediated apoptosis in HL-1 cardiomyocytes, which could be inhibited by BTP2 treatment.

These data taken together suggest that pharmacologically inhibition SOCE with BTP2 treatment can inhibit EPI-induced apoptosis in HL-1 cardiomyocytes mediated by caspase-3.

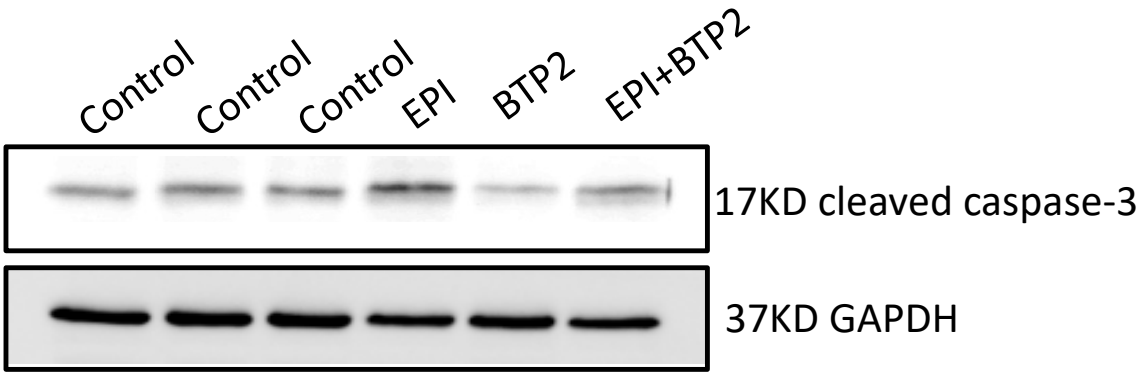

Figure 3-6 BTP2 inhibited epirubicin-induced apoptosis (cleaved caspase-3) in HL-1 cardiomyocytes.

Western blotting analysis of cleaved caspase-3 expression in HL-1 cardiomyocytes after treatment with vehicle, 1 μM epirubicin, 20 μM BTP2 or 1 μM epirubicin combined with 20 μM BTP2 for 72 hrs. GAPDH expression is shown as a loading control.
EPI: 1 μM epirubicin; BTP2: 20 μM BTP2; E+B: 1 μM epirubicin+20 μM BTP2.

3.3 MATERIALS AND METHODS

3.3.1 Chemicals and reagents

Claycomb cell culture medium was purchased from Sigma-Aldrich. Fetal Bovine Serum, PBS, HBSS, and penicillin/streptomycin antibiotic were purchased from Invitrogen/Thermofisher scientific. Other reagents used include BTP2 (Millipore Sigma, MO, USA), epirubicin (Alfa Aesar), thapsigargin (TG, Adipogen), fura-2 AM (Biotium 50033), DAPI (Invitrogen D357), phalloidin (Enzo BML-T111).

3.3.2 Cell culture

HL-1 cardiomyocytes were maintained in Claycomb medium supplemented with 10% FBS, 100 U/ml penicillin, 100 ug/ml streptomycin, 0.1 mM norepinephrine and 2 mM L-glutamine [191]. The cell line was cultured at 37^{o}C in a humidified 5% CO_2 incubator.

3.3.3 Measurement of intracellular calcium concentration

Intracellular calcium concentration in HL-1 cell line was measured following previously published procedures [210]. In brief, the intracellular Ca^{2+} was measured by the fluorescence microscope with a SuperFluo 40x objective (N.A. 1.3) connected to a dual-wavelength spectrofluorometer (Horiba Photon Technology International, NJ, USA). The excitation wavelengths were set at 350 nm and 385 nm respectively and the emission wavelength was set at 510 nm. Cells were loaded with 5 μM fura-2 acetoxymethyl ester (Biotium, Fremont, CA, USA) for 30 min at 37°C in the dark. Cellular endoplasmic reticulum (ER) Ca^{2+} stores were depleted by 10 μM thapsigargin (TG) in 0.5 mM EGTA dissolved in basal saline solution (140 mM NaCl, 2.8 mM KCl, 2 mM $MgCl_2$, 10 mM HEPES, pH 7.2). SOCE was observed upon the rapid exchange of extracellular solution to bath saline containing 2 mM $CaCl_2$ at indicated time. The intracellular calcium elevation

was presented as $\Delta F_{350nm}/F_{385nm}$.

3.3.4 Cytotoxicity assay

HL-1 cells seeded at $1.5x10^5$ cells per well in a 29 mm glass-bottom dish were treated with vehicle, 20 μM BTP2, 10 μM EPI, 20 μM BTP2 plus 10 μM EPI for 5 hrs. Then the culture medium was removed and cells were fixed with 4% paraformaldehyde for 10min at room temperature. The paraformaldehyde was removed and then cells were immersed into 0.1% of Triton X-100 in PBS for 10 min and washed with PBS twice, followed by incubation with PBS containing 6.6 μM phalloidin (Enzo, USA) for 15min, washing with PBS three times, and then counter staining with PBS containing 1u μg/ml DAPI (1:500) for 5 min at room temperature in the dark. The cells were then washed with PBS twice and immersed in Prolong™ Gold antifade reagent (Life Technologies Corporate, Eugene, OR, USA). The fluorescence signals were observed under DMi8 inverted microscope (Leica, Germany) with 40x objective (NA 1.3). The excitation/emission wavelengths set for DAPI and phalloidin were 405/430 nm and 547/572nm, respectively. The imaging was performed at room temperature.

3.3.5 Western blotting analysis

HL-1 cardiomyocytes were lysed in modified RIPA buffer (150 mM NaCl, 50 mM Tris-Cl, 1 mM EGTA, 1% Triton X-100, 0.1% SDS and 1% sodium deoxycholate, pH 8.0) containing protease inhibitors cocktail (Sigma-Aldrich, US) as previously described [211, 212]. Protein concentration was quantified using a BCA kit (Thermo, USA). Equal amounts of proteins were loaded onto SDS polyacrylamide gels, and the separated

proteins were transferred to PVDF membranes (Bio-Rad, Hercules, CA, USA). The blot was incubated with 5% non-fat dry milk blocking buffer (Bio-Rad, Hercules, CA, USA) for 1hr at room temperature and probed with specific primary antibodies in blocking buffer at 4°C overnight. Primary antibodies used in this study included anti-caspase-3 (1:1000, catalog #9662, Cell Signaling Technology, USA), anti-GAPDH (1:1000, GeneTex, USA). The next day, the blots were washed with PBST three times followed by incubation with secondary antibodies including the appropriate horse radish peroxidase (HRP)-conjugated goat anti-rabbit IgG (1:5000, Cell Signaling Technology, USA) and anti-mouse IgG (1:5000, Cell Signaling Technology, USA). Signals were detected using ECL detection method on ChemiDoc instrument.

3.3.6 Cell size measurement

HL-1 cells seeded at $1x10^6$ cells per well in a 6-well plate were treated with vehicle or 20 μM BTP2, 1 μM EPI, 20 μM BTP2 plus 1 μM EPI for 2 hrs followed by switching to normal culture media for 24 hrs. The cells were then observed and imaging under the DMi8 inverted microscope (Leica, Germany) and phase contrast imaging was conducted. The cell surface area was quantified using ImageJ and Graphpad 6 software.

3.3.7 Quantitative reverse transcription polymerase chain reaction (qRT-PCR)

Total RNAs were extracted from HL-1 cells using Illustra RNAspin MiniRNA Isolation Kit and measured photometrically at 260/280 nm. Primers were obtained from Sigma Aldrich. 400 ng of total RNA was applied for reverse transcription using qScript microRNA Synthesis Kit (QuantaBio) following the manufacturer's protocol. cDNA was

diluted 1:5 in DNase-, RNase- and protease-free water and 2 µl template was used. Primer-pairs of BNP and GAPDH were used. The sequences for BNP primers are forward (5'→3') GCCAGTCTCCAGAGCAATTC and reverse (5'→3') TCTTTTGTGAGGCCTTGGTC. The sequences for GAPDH primers are forward (5'→3') AGGTCGGTGTGAACGGATTTG and reverse (5'→3') TGTAGACCATGTAGTTGAGGTCA. For qRT-PCR QuantaBio PerfecTa SYBR Green FastMix ROX was used according to the manufacturer's procedure. Signals generated by integration of SYBR Green into the amplified DNA were detected in a real-time machine (StepOne Plus Real-Time PCR System). Data were expressed as $2^{-\Delta\Delta CT}$ relative to GAPDH gene expression.

3.3.8 Immunofluorescence staining

Cells were seeded into 29 mm glass-bottom dish. The cells were fixed with 4% paraformaldehyde for 10 min at room temperature. The paraformaldehyde was then removed and cells were immersed in PBS containing 0.1% of Triton X-100 for 10 min. After washing with PBS three times, cells were blocked in PBS containing 0.1% of Triton X-100 supplemented with 10% horse serum for 30min at room temperature. Then, the cells were incubated with rabbit anti-NFAT4 primary antibody (1:100, ProteinTech, USA) in blocking solution at 4°C overnight. The next day cells were taken out and washed with PBS three times, then incubated with Alexa Fluor 488-labelled secondary antibody (1:500, Abcam) at room temperature in the dark for 1 hr to visualize the expression and localization of NFAT4. Cells were then counter-stained with PBS containing 1ug/ml DAPI

(1:500) for 5 min at room temperature in the dark and immersed in Prolong™ Gold antifade reagent (Life Technologies Corporate, Eugene, OR, USA). Images were taken under Nikon A1R HD25 LSM confocal microscope with 40x oil immersion objective (NA 1.3) with GFP and DAPI filter (Ex:488/405; Em: 509/430nm).

3.3.9 Statistical Analysis

Data were analyzed using Graphpad Prism 6 software. Results were presented as mean ± standard deviation (SD) or otherwise indicated. Comparisons between two groups were analyzed using a Student's *t*-test. Comparisons among >two groups were analyzed using one-way analysis of variance (ANOVA) followed by Bonferroni *post-hoc* analysis. A p value of <0.05 was considered statistically significant.

3.4 DISCUSSION

In this study, we observed and confirmed that EPI-induced cell size increase could be decreased by SOCE blocker BTP2 when treated together with EPI in HL-1 cardiomyocytes (**Figure 3-1**). We further found SOCE was enhanced in HL-1 cardiomyocytes when treated with EPI. However, when co-treated with BTP2, this EPI-induced SOCE enhancement could be reduced (**Figure 3-2**). HL-1 cardiomyocytes demonstrated activated NFAT4 signaling upon EPI treatment indicated by NFAT4 translocating into the nuclei. BTP2 co-treatment with EPI was able to decrease the number of cells showing NFAT4 nuclear translocation (**Figure 3-3**). The EPI-triggered BNP up-regulation was also decreased by co-treating the cells with SOCE blocker BTP2

(**Figure 3-4**), further confirming the rescuing effects of SOCE inhibition achieved by BTP2 treatment in HL-1 cells. Last but not the least, BTP2 co-treatment with EPI was able to inhibit EPI-induced apoptosis (F-actin degradation, nuclear condensation and cleaved caspase-3 protein expression increase) in HL-1 cardiomyocytes (**Figure 3-5 & Figure 3-6**). Taken together, these results demonstrated that EPI treatment enhanced SOCE in HL-1 cardiomyocytes, triggering the NFAT4-mediated cardiomyocyte hypertrophy and caspase-3-mediated cardiomyocyte apoptosis (**Figure 3-7**).

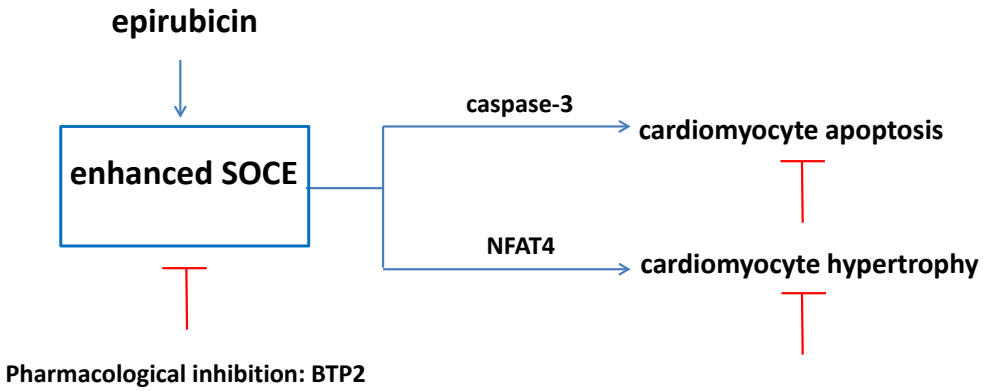

Figure 3-7 Working hypothesis.

SOCE has been reported to be associated with cardiac hypertrophy *in vitro*. The first study was carried out in neonatal cardiomyocytes and demonstrated phenylephrine and angiotensin II, both of which are IP_3-activating agonists, increased the intracellular Ca^{2+} and cell area and lead to NFAT activation, which were all prevented by treating the cells with nonselective SOC inhibitor SKF-96365 and to a lesser extent with LRCC inhibitor [124]. Following this study several lines of evidence found similar results in STIM1 and Orai1 knockdown neonatal cardiomyocytes. In these cells treatment of

endothlin-1 or phenylephrine for 48hrs induced enhanced SOCE, NFAT activation and cell size enlargement in the wild type cells were suppressed [101-103]. Our current findings are in line with these previous reports, indicating that EPI-induced cardiomyocyte hypertrophy could also be inhibited by SOCE blocker.

Some limitations of the current study must be recognized. First, this study is limited by *in vitro* evidence. Although we have used HL-1 mouse atrial cardiomyocyte cell line to reveal the role of SOCE in EPI-induced cardiac hypertrophy and apoptosis, we do not know if the same effects can be recapitulated *in vivo* as well. Secondly, the specific molecular component involved (i.e. Orai1 or STIM1) remains to be further investigated.

The previous studies of our lab have demonstrated that SOCE is an effective chemotherapy drug target [211-215]. The findings of the present study have shown that SOCE contributes to EPI-induced cardiotoxicity, indicating that SOCE blocker was able to protect cardiomyocytes from side effects of anthracycline chemotherapy drugs. These combined results suggest that targeting SOCE might function both as chemotherapy and cardio-protection, shedding light to the dual-function drug administration and combined systematic chemotherapy strategy design to delay the onset, progression or even prevent chemotherapy- induced cardiovascular diseases.

CHAPTER 4

CONCLUSION AND FUTURE DIRECTIONS

4.1 SUMMARY

First of all, a working model in which circulating IgG autoantibodies purified from type 2 diabetic (T2DM) patients with atrial fibrillation (AF) induced arrhythmogenic calcium signals in both human iPSC-differentiated and adult mouse atrial cardiomyocytes was first described in Chapter 2. The IgG autoantibody-induced intracellular calcium elevation did not respond to L-type or T-type calcium channel blockers or store-operated calcium entry (SOCE) blocker but did respond to both pharmacologically and genetically knocking down IP_3Rs, indicating that the IgG autoantibody-induced intracellular calcium elevation was independent of voltage-gated calcium channel and SOC channel, but rather dependent on IP_3R-mediated signaling pathway. Both PLC and GPCR blockers reduced IgG autoantibody-induced intracellular calcium elevation, indicating the involvement of PLC and GPCR in the IgG autoantibody-induced arrhythmogenic effects in the cardiomyocytes. Taken together, these results demonstrated that the circulating IgG autoantibodies from older T2DM patient with AF could target an unknown GPCR, triggering IP_3R-dependent pathways. Our discovery suggested the vital role of circulating IgG autoantibodies in AF.

Subsequently, the role of SOCE in epirubicin (EPI)-induced cardiotoxicity was discussed in Chapter 3. In this study, we observed and confirmed the EPI-induced cell size increase was reduced with treatment of the SOCE blocker BTP2 when co-treated with EPI in HL-1 cardiomyocytes. Furthermore, we observed SOCE enhancement in HL-1 cardiomyocytes induced by EPI treatment, which was reduced when co-treated with BTP2. EPI also triggered activated NFAT4 signaling demonstrated by the nuclear

translocation of NFAT4 in HL-1 cardiomyocytes. BTP2 co-treatment with EPI then decreased the number of cells undergoing NFAT4 nuclear translocation. SOCE blocker BTP2 co-treatment with EPI rescued the EPI-increased hypertrophy marker BNP mRNA expression level, which further confirmed that SOCE inhibition could rescue the EPI-induced cardiac hypertrophy in HL-1 cells. Last but not the least, the EPI-induced cellular apoptosis (indicated by the degraded F-actin, condensed nuclei and increased protein expression level of cleaved caspase-3) in HL-1 cells was inhibited when the cells were co-treated with BTP2 and EPI. Taken together, these results demonstrated that EPI treatment lead to the SOCE enhancement in HL-1 cardiomyocytes, which subsequently triggered the NFAT4-mediated cardiomyocyte hypertrophy and caspase-3-mediated cell apoptosis.

Cardiovascular diseases are associated with Ca^{2+} dysregulation not only in the cardiomyocytes but also in the vascular tissues. This dissertation study has been focused on the aspect of cardiomyocytes. Since the evidence of dysregulated SOCE in vascular tissues is emerging, the future work is warranted to reveal the role of SOCE in vascular function and its contribution to the vascular aspect in the cardiovascular diseases.

4.2 SOCE IN THE VASCULAR SYSTEM

The blood vessel walls mainly consist of two cell types, the vascular smooth muscle cells (VSMCs) and endothelial cells (ECs). The majority of VSMCs are in the tunica, especially for muscular arteries and arterioles. Despite of VSMCs being

maintained in a partially constricted state, the dynamic regulation of intracellular Ca^{2+} concentrations has the ability to rapidly adjust to the vascular tone and maintain hemodynamic stability [216]. Normally VSMCs are quiescent and contractile and infrequently divide, however they can switch to a proliferative and migratory state in certain circumstances, such as arterial injury or inflammation [217-219]. This change is reckoned as a critical step in the pathogenesis of multiple vascular diseases, including arterial stenosis in atherosclerosis, neointimal hyperplasia following angioplasty or stent placement, and arteriolar remodeling in hypertension. ECs are most abundant in the intimal layer of the blood vessel and are involved in various functions, such as selective barrier formation for cellular and nutrient trafficking, local blood flow and vascular tone modulation, as well as oxidative stress and inflammation, thrombosis, hemostasis and VSMC proliferation resistance [220]. Notably, ECs demonstrate distinctive diversity, indicated by their significantly heterogeneous structural and functional phenotypes throughout the cardiovascular system [221]. Similar to VSMCs, ECs display proliferative and migratory phenotypes under pathological conditions [222]. Understanding the signaling pathways underlying the switch of phenotypes in VSMCs and ECs is essential for the development of targeted therapies against vascular diseases.

Thrombin is physiological agonist for proteinase-activated receptor (PAR) located on both VSMCs and ECs. Despite of the limited expression of the PARs on healthy artery VSMCs, an increased expression of these receptors is seen in vascular lesions [223]. The activation of thrombin is crucial to mediate VSMC contraction, proliferation, migration,

hypertrophy and extracellular matrix production [224], therefore its signaling in VSMCs contributes importantly to the pathogenesis of vascular occlusive diseases. Synthetic VSMCs stimulated with thrombin *in vitro* is reported to enable the activation of an innovative non-SOCE/CRAC but STIM1/Orai1/Orai3-requiring and highly selective Ca^{2+} entry pathway [225], similar to the arachidonic acid (AA)-modulated Ca^{2+} (ARC) channels [226, 227]. Thrombin activates store-independent leukotrieneC4 (LTC_4)-regulated Ca^{2+} entry (LTC) channels in VSMCs [225]. The involvement of either ER or plasma membrane STIM1 pools, the oligomeric state of functional STIM1 and the nature of the interactions between STIM1 and Orai1/3 LRC channels remains to be further elucidated. The LRC channels are the first store-independent Orai channels reported to be stimulated with a physiological agonist in the vasculature. On the other hand, thrombin in ECs has been reported to activate store-dependent CRAC channels [228]. In conclusion, not only can we see distinct effects of different agonists in the same cell type, but the same agonist can result in diverse Ca^{2+} entry pathways in different cell types.

4.2.1 SOCE in Vascular Smooth Muscle Cells

The contribution of SOCE to vascular smooth muscle cell (VSMC) growth, proliferation and migration has been demonstrated in studies using vasoactive agonists and growth factors. The growth and proliferation of aortic VSMCs have been reported to me mediated by STIM1 and Orai1-dependent SOCE when stimulated by angiotensin-II [229, 230]. In addition, treatment of urotensin-II promotes VSMCs proliferation and

Ca^{2+}/cAMP response element-binding protein (CREB) activation. These require a complex signaling pathway involving on the one hand SOCE mediated by STIM1, Orai1 and TRPC1, and on the other hand epithelium growth factor receptor (EGFR), extracellular signal-regulated kinase (ERK) and CaMK activation [231]. Meanwhile, the paracrine release of plate-derived growth factor (PDGF) by VSMCs, ECs and macrophages promotes VSMC migration, while induction of intimal proliferation is considered as secondary phenomenon [232]. STIM1- and Orai1-(but not TRPC1/4/6- nor Orai2/3-) mediated SOCE specifically contributes to the PDGF-induced Ca^{2+} entry [233], with STIM1 and Orai1 being the essential components for VSMCs and airway smooth muscle migration when stimulated with PDGF *in vitro* [233, 234]. On the contrary, in smooth muscle-specific STIM1 knockout mice, PDGF-induced VSMC proliferation is strongly reduced as a result of SOCE-dependent NFAT activation reduction [235]. Similarly, studies using PDGF receptor inhibitors demonstrate neointima formation attenuation in animal models of restenosis [236-238].

Although the contribution of SOCE to VSMC growth, proliferation and migration has been well established as shown above, its role in VSMC contractility remains contentious. A number of studies have used non-specific SOCE inhibitors like 2-Aminoethoxydiphenyl borate (2-APB) and lanthanides to examine the role of SOCE in VSMC contractility [239-241]. In freshly isolated contractile VSMCs compared with cultured synthetic proliferative VSMCs, minimal SOCE/CRAC activity and STIM1/Orai1 protein expression levels have been reported [225, 242-244]. However, the contribution

of CRAC channels to vascular tone can be achieved by their vasorelaxation roles mediated by ECs, delivered by Ca^{2+}-modulated nitric oxide (NO) production [245]. Vasoactive agonists increase cytosolic endothelial Ca^{2+} concentrations, activate endothelial No synthase and initiate NO-dependent vasodilation [246]. In porcine aortic ECs STIM1 inhibition blocked SOCE and was associated with thrombin-induced partial NO production decrease [247]. Meanwhile, in mouse aortic ECs the reduced SOCE activity is associated with impaired acetylcholine-induced vasorelaxation [248]. In addition, in diabetic mice, decreased STIM1 protein expression-caused Impaired ER Ca^{2+} refilling, attenuates endothelium-dependent vasorelaxation in coronary arteries, while STIM1 overexpression has a beneficial and therapeutic effect on coronary endothelial dysfunction in diabetes [249].

Interestingly, although detectable in cultured human aortic VSMCs, Orai1 is much less expressed than the abundant Orai2 and Orai3 when normalized to expression levels in lymphocytes [244]. Orai2 and Orai3 expression levels are also higher in cultured synthetic aortic VSMCs than in contractile cells [225, 241]. Despite of the high expression levels, Orai2 and Orai3 being silenced *in vitro* did not change the SOCE amplitude in synthetic VSMCs, indicating only Orai1 as the component of CRAC channels in these cells [243]. However, after carotid injury the expression level of Orai3 was increased and in vivo knockdown of Orai3 significantly inhibited neointima formation [225], indicating the contribution of Orai3 in channels or signaling pathways other than SOCE (namely store-independent LTC channels), thus promoting VSMC synthetic phenotypes.

In addition to the above mentioned *in vitro* data, the important contrition of SOCE to VSMC proliferation and migration on luminal side of injured vessels to form neointima has also been demonstrated *in vivo*, taking advantage of the animal model of angioplasty, accomplished by mechanical injury procedure of rat carotid arteries [250]. In fact, in the medial and neointimal layer, the lentivirus-mediated STIM1 and Orai1 inhibition reduces the formation of neointima and prevents the increase of these two proteins fourteen days after injury. Furthermore, knockdown of STIM1 and Orai1 blocks VSMC proliferation reduction-associated NFAT activation [242]. Similarly, angiotensin-II significantly up-regulates STIM1 and Orai1 expression levels in the neointimal layer [230, 251]. When STIM1 and Orai1 are silenced, the angiotensin-II-induced VSMCs proliferation and accelerated neointimal growth are suppressed [230, 251]. In line with this, after carotid artery ligation, the smooth muscle-specific STIM1 knockout mice demonstrate significantly reduced neointimal formation compared with control mice [235]. A recent study identifies the scaffolding protein Homer1 (which can bind to several Ca^{2+}-signaling molecules [252]) as a binding partner for Orai1 and TRPC channels forming SOC complexes in the neointima and that Homer1 can regulates the migration and proliferation of VSMCs [253].

4.2.2 SOCE in Endothelial Cells

Endothelial cells can produce both potent vasoconstrictor endothelin-1 (ET-1) and vasodilator NO. When there is damage in the vessels (for example caused by tissue

hypoxia [222]), they need to be replaced by newly grown ones either from preexisting blood vessels or from bone marrow-generated endothelial precursor cells (EPCs). However, the growth of new vessels is also a contributor to the development of tumor growth and metastasis-promoting vascular networks [222]. Upon stimulation of various growth factors, vascular endothelial growth factor (VEGF) in particular, signaling pathways are activated and induce the proliferation and migration of endothelial cells (ECs) [222]. The activation of VEGF receptor triggers IP_3-mediated Ca^{2+} release and induces a low Ca^{2+} conductance across the plasma membrane, which is essential for EC proliferation [254, 255]. This conductance was initially difficult to measure due to its relatively low and variable amplitude in endothelial cells. The first evidence demonstrates that ECs can activate store-operated small inward rectifying CRAC-like current induced by IP_3, thapsigargin or Ca^{2+} ionophores [256]. Following that, in human umbilical vein ECs (HUVECs) STIM1 and Orai1 are shown to be required in mediating CRAC currents post passive store depletion, and CRAC channels are shown to contribute to EC proliferation [228]. Genetic inhibition of Orai1 using siRNA or a dominant negative Orai1 mutant, as well as pharmacological inhibition of Orai1 using the CRAC channel blocker S66, are both able to inhibit prevent the endothelial tube from forming *in vitro* [257]. Conversely, in primary HUVECs STIM1 , TRPC1 and TRPC4, but not Orai1, are associated with the endothelial tube formation [258], indicating a potential dissociation of STIM1 from Orai1 in tubulogenesis. Meanwhile, knockdown of STIM1 or STIM2 only shows mild inhibitory effects compared to that from knockdown of Orai1 [228]. Consistently, when STIM1 is

knocked down specifically in EC in the mice, no abnormal endothelial migration or vasculogensis is observed [259].

EPCs exist in postnatal circulation and they proliferate, migrate and development into mature EC phenotype [260]. The expression of SOCE in EPC was first demonstrated in 2010 [261]. The SOCE in EPC was further characterized by evidence showing enhanced STIM1-mediated SOCE upon stimulation of hepatocyte grow factor [262], with STIM1 being essential for EPC proliferation and migration [251, 262, 263]. SOCE-mediated IP_3-dependent calcium oscillations are seen when EPCs are treated with VEGF [264]. All these data provide evidence demonstrating the involvement of CRAC channels in EPC Ca^{2+} signaling pathways regulating the proliferation and tubulogenesis.

SOCE is identified as a key mechanism in tissue vascularization, vascular repair and vasculogenesis, which is de novo formation of new blood vessels.

Angiogenesis is the expansion of existing vascular system, which first takes place during embryonic development, and also continues in the mature animals most commonly seen in either wound healing [265] or tumor metastasis[266]. In angiogenesis the sprouting of endothelial cells are mainly controlled by two categories of tyrosine receptors, the VEGF-receptors and the tie and tek kinases [267]. Cells surrounding the vessels synthesize and secrete angiopoitein-1 and angiopoietin-2, whose endothelial receptors are tie-2 [268]. The tie-2/angiopoietin signaling pathway is able to induce the production of growth factors like PDGF and VEGF, which triggers the mesenchymal cells to differentiate into pericytes or smooth muscle cells to form vessel wall [269]. Interestingly,

angiopoietin-1 inhibits VEGF-triggered SOCE, thus negatively regulating and protecting the endothelial cells from growth factor-induced hyperpermeability [270].

Vasculogenesis is the de novo formation of the vascular system in the early embryo, while in the mature organism a similar process is responsible for vascular repair. At the initial stage, both vascular and hematopoietic tissue development occur simultaneously, involving angioblasts and hematopoietic stem cells. Then endodermal cells secrete growth factors to induce vasculogenesis in the embryo [271-273]. Angioblasts and endothelial progenitor cells have also been identified in the adult [260], suggesting the vasculogenesis does not only occur during the embryonic development. Endothelial repair involves a heterogeneous population of endothelial progenitors existing in both peripheral blood and within specific niches of the vessel wall. When transplanted into immunodeficient mice, a subtype of endothelial progenitor cells, cells that can form endothelial colony, display great ability to proliferate and form de novo blood vessels [274]. These cells may play roles in neointima hyperplasia and vascular repair after injury. Endothelial repair accomplished by progenitor cells is tightly modulated by specific growth factors, with the underlying signaling pathways likely associated with SOCE. Dysfunctional SOCE has been found to contribute to impaired proliferation of endothelial progenitor cells in an atherosclerosis mouse model [275]. Similar to mature endothelium, the CRAC channels' contribution to growth hormone and mediator signaling pathways are also dependable on the developmental stage and differentiation. Notably, in certain phenotypical stages during ex vivo proliferation of progenitor cell clusters, TRPC3

expression level has been shown increased [276].

The involvement of this classical SOCE and STIM1/Orai1 as the core of Ca^{2+} entry pathway in particular progenitor populations and stages of vasculogenesis remains to be further validated. The proliferation and differentiation of endothelial precursors seem to be regulated by multiple Ca^{2+} entry signaling pathways in a highly cooperative manner. In addition, these pathways appear to have differential influences dependent on different vasculogenesis or vascular endothelial repair stages.

4.3 SOCE AND VASCULAR DISEASES

Vascular diseases include systemic and pulmonary arterial hypertension and a number of vascular occlusive diseases such as restenosis, thrombosis, atherosclerosis. Evidences have strongly supported that dysregulated SOCE being a crucial contributor to the development of vascular diseases [217, 233, 244, 277-281].

4.3.1 Thrombosis

Thrombosis is a pathological process of thrombus formation within the blood vessels. It is a defense mechanism against post-traumatic blood loss at sites of vascular injury when platelets and fibrin are drawn to the injured location, forming clots to prevent the bleeding. However, under severe circumstances, a process called embolism occurs. The thrombus formed gets released into the circulation system, traveling freely in the blood vessels, leading to infarction and stroke. In addition, thrombosis causes the

narrowing of blood vessels, thus obstructing blood flow. The obstruction of coronary arteries leads to myocardial infarction and further to heart attack, while the obstruction of cerebral arteries causes ischemic brain infarction and ultimately leads to stroke.

During thrombus formation, a key step is the platelet activation achieved through the binding of agonists such as thrombin, thromboxane A_2 (TXA_2), and ADP to PLC-coupled receptors, which leads to increased cytosolic Ca^{2+} concentration inside the platelets [282, 283]. This elevation of cytosolic Ca^{2+} concentration is essential for platelet aggregation at the thrombus formation [282].

The identification of Orai1 as the platelet SOC channels was reported to be essential for thrombus formation [284]. The authors showed strongly expressed Orai1 in human and mouse platelets. To examine the role of Orai1 in blood clotting, Orai1-deficient ($Orai1^{-/-}$) mice were generated and their platelets demonstrated severely defective SOCE, agonist (thrombin, ADP, collagen-related peptide-CRP, collagen)-induced Ca^{2+} responses, along with impaired activation and thrombus formation compared with wild type mice under flow *in vitro*. Further *in vivo* results showed that $Orai1^{-/-}$ chimeras (wild type mice infused with the bone marrow of an Orai1 knockout mouse) were protected from cerebral ischemia without displaying major bleeding [284]. The involvement of Orai1 in platelet SOCE was also supported by another study using chimeric mice expressing a mutated inactive form of Orai1 in blood cells only ($Orai1^{R93W}$, a naturally occurring mutation found in patients with severe combined immunodeficiency, SCID) [285]. Reduced integrin activation and impaired degranulation was shown in these $Orai1^{R93W}$ platelets when

stimulated with low agonist (collagen) concentrations under static conditions. However, the Orai1^{R93W} platelets' ability to aggregate or adhere to collagen was not significantly affected under arterial flow conditions *ex vivo*. In contrast, these adherent Orai1^{R93W} platelets were defective in surface phosphatidylserine exposure, indicating Orai1 as a crucial component for the platelets' pro-coagulant response rather than for other Ca^{2+}-dependent cellular responses [285].

Accumulating evidences supporting the role of STIM1 in platelet Ca^{2+} concentration elevation and thrombosis occurrence are strong. STIM1 is implicated to be required for platelet activation in a study using a gain of function STIM1 mutant mouse model (STIM1^{D84G}), which constitutively expresses active STIM1 [286]. The platelets in these mice with STIM1 mutation showed premature activation and these mice demonstrated symptoms of macrothrombocytopenia. Furthermore, another gain of function mouse model with mutant STIM1^{R304W} showed impaired platelet activation, likely as a result of decreased expression of STIM1 in platelets [287, 288]. STIM1 is also shown to be a critical participant in thrombus stability. A platelet-specific conditional STIM1 knockout mouse model was generated to display thrombosis induced by laser injury [289]. The platelets in these mice showed reduced ability to generate fibrin at the injury site, indicating less stable thrombi in these mice compared to wild type mice. The ability to express phosphatidylserine at the plasma membrane of the platelets was reduced when STIM1 was knocked out, lowering the thrombus stability [289, 290]. Collectively, these data have established the crucial role of STIM1 in thrombus formation and stability. In

addition, human patients with Orai1 and STIM1 mutations and abrogated SOCE did not demonstrate prolonged bleeding time compared with control patients [291, 292]. Cyclophilin-A was identified as an important regulator of SOCE by regulating STIM1 phosphorylation [293].

Although there is consensus about the involvement of Orai1 and STIM1 in thrombosis, whether TRPCs are functioning similarly is a contentious issue. Varga-Szabo group revealed that TRPC1 does not contribute to platelet SOCE nor to their activation and function [294]. The authors used mice lacking TRPC1 and platelets from these mice display normal SOCE compared to wild type mice. Furthermore, platelet function both in vitro and in vivo did not change in the absence of TRPC1. In addition human platelets SOCE was not altered when treated with presumably inhibitory anti-TRPC1 antibodies [294]. $TRPC1^{-/-}$ mice platelets SOCE mediated by thapsigargin, thrombin, and CRP was shown to be independent of TRPC1 [284]. Taken together, TRPC1 neither contributes to physiological function of platelets nor to pathological thrombosis. Contrary to this, Galan et al. reported both Orai1 and TRPC1 are involved in platelet SOCE and aggregation [295]. Interestingly, it has been hypothesized that platelets contain two mechanisms of Ca^{2+} entry and phophatidylserine exposure, with only one depending on STIM1-Orai1 interaction, and the other being receptor-operated Ca^{2+} entry pathway [290]. Interestingly, STIM2 is shown not to play significant roles in thrombus formation as $STIM2^{-/-}$ reacted normally to collagen treatment [290].

4.3.2 Restenosis

Restenosis is the pathological remodeling and reoccurrence of arteries (most often coronary arteries) causing restricted blood flow. This is usually following percutaneous angioplasty or stenting. Restenosis happens in 1% to 3% of patients and often leads to acute myocardial infarction of even acute cardiac arrest [296, 297]. Two most important contributors to restenosis are thrombosis (see the above section) and neointima formation, which is due to VSMC proliferation and migration into the lumen of vessels (see the VSMC section).

4.3.3 Atherosclerosis

The pathogenesis of atherosclerosis is the narrowing of the blood vessel lumen caused by the sub-endothelial deposition of lipids on the blood vessel wall. The stimulation of the lipid accumulation leads to chronic inflammation of the arterial wall, which is a hallmark of atherosclerosis. Monocytes and macrophages migrate into the plaques between ECs and VSMCs upon lipid stimulation. These immune cells engulf the excessive fatty materials and turn into foam cells, promoting a chronic inflammatory environment in the vasculature. This chronic inflammation triggers VSMC remodeling and further causes endothelial dysfunction, thus leading to the final blood vessel narrowing. Diet is also a key factor during atherosclerosis development and progression.

Emerging evidences have implicated involvement of Orai1 and STIM1 in atherosclerosis. A study using apolipoprotein E (apoE) knockout mouse model reported these mice are prone to hyperlipidemia and atherosclerosis and demonstrate higher

SOCE induced by ATP in endothelial denuded aortic rings. Notably, the enhancement of SOCE in VSMCs occurred in apoE knockout mice before the significant development of atherosclerosis plaques, indicating that SOCE and VSMC remodeling might be early events in atherosclerosis development [277]. Another study also using apoE knockout mouse model demonstrated when these mice are fed with high fat diet the Orai1 expression both at mRNA and protein levels are increased in isolated aortic tissue [277]. The atherosclerosis plaque size was decreased when Orai1 knocked down by either siRNA or SOCE pharmacological inhibitor SKF96365 application [298]. This study did not identify specific cell type and thus further studies are needed for clarification. Similarly, in pigs fed with pro-atherosclerosis high-calorie diet, enhanced SOCE, STIM1 and Orai1 expression levels are observed in isolated VSMCs compared to those in pigs fed with normal chow, though Orai1 increase was not significant [299]. Interestingly, exercise decreased the expression level of STIM1 as well as SOCE [299], indicating that SOCE and its related protein expression level together with coronary atherosclerosis can be attenuated with proper diet and exercise. A recent study identified miR-185 as a modulator of STIM1 in atherosclerosis models both *in vitro* and *in vivo*. The authors demonstrated SIMT1 was a potential target gene of miR-185 in atherosclerosis, the progression of which was promoted by knocking down of miR-185 through enhancing cell proliferation, migration and invasion via targeting STIM1. This provides insight of miR-185/STIM1 axis function in atherosclerosis development [300].

Endothelial dysfunction is an early step promoting vascular inflammation which

further contributes to the formation of atherosclerosis plaques. There is an excellent review about the endothelial cell dysfunction and the pathobiology of atherosclerosis [301]. EPCs also play vital roles in the regeneration of healthy intima and the proliferation and migration of EPCs are attenuated when apoE is knocked out in mice [302]. The EPCs in these mice also displayed reduction in SOCE, Orai1 and STIM1 protein expression levels [302]. The same group also demonstrated protective effects of SOCE from ox-LDL-induced cellular proliferation decrease in EPCs [303].

The recruitment of monocytes and neutrophils by the endothelium at injury sites is one key step in the atherosclerosis plaque formation. In other occlusive diseases the recruitment of these cells has been reported at the early stage of disease development [304]. Orai1 is shown as a necessary component for neutrophil and monocytes migration into inflammatory vascular endothelium [305]. Orai1 has also been demonstrated important for the formation of foam cells from macrophages upon stimulation of lipids accumulation [298]. Macrophage Ca^{2+} entry was mediated by Orai1 when treated with ox-LDL. The authors showed this ox-LDL-triggered Ca^{2+} entry activates calcineurin, which activates c-Jun N-terminal kinase and p38 kinase enhancing the scavenger receptor A expression, and further induces LDL uptake, thus promoting the transition from macrophage to foam cells [298].

4.3.4 Systemic Arterial Hypertension

The association between arterial hypertension and elevated intracellular Ca^{2+} levels as well as abnormal expression of Ca^{2+}-handling proteins has been well

characterized [306-308]. In mouse model with STIM1 specifically knocked out in the smooth muscle partial protection against endothelial dysfunction and hypertension development after infusion of angiotensin II has been reported [309, 310]. Increased Ca^{2+} has also been demonstrated in hypertensive rat models and human patients [311, 312]. Elevated SOCE-mediated Ca^{2+} influx with STIM1/Orai1 as the molecule involved has been reported to contribute to potentiating vascular activity [313, 314], vascular tone and force generation [307, 308, 315]. Male rats spontaneous hypertensive rats treated with high concentrations of SOCE blockers (either 2-APB and Gd^{3+}, or STIM1 and Orai1 neutralizing antibodies) in their aortic rings lead to reduced spontaneous tone and force generation to levels close to those in normotensive rats [314]. These spontaneous hypertensive rats also displayed higher expression levels of Orai1 and STIM1 at both mRNA and protein levels [314]. However, these data should be interpreted with caution due to the neutralizing antibodies non-specific effects. In addition, the high concentration of SOCE inhibitors have been reported to influence other ion channels, including ER Ca^{2+} release channels and pumps such as IP_3 receptor-mediated channels and various TRP channels [316], which can further inhibit SOCE [314, 317]. The SOCE inhibitors Gd^{3+} and SKF96365 have also been reported to inhibit systemic hypertension in rats [318]. Similarly, rats subjected to chronic ethanol consumption for 30days demonstrated higher systemic blood pressure, enhanced SOCE and increased STIM1 expression [319].

The gender difference in hypertension susceptibility has been supported, showing male having higher rate of incidence than female [320]. More contractile force, higher

mRNA and protein expression levels of Orai1 and STIM1 are found in the aortic rings of male spontaneous hypertensive rats compared with female rats [313]. The differences in Orai and STIM isoform expression in male and female patients with hypertension warrants further investigation. Studies examining the influence of sex hormones on regulating SOCE-related molecular components have been done. Estrogen has been shown to increase Orai3 but not Orai1 in estrogen-positive breast cancer cells [76]. Since Orai3 is an essential component of heteromeric ARC channels, it might be an important triggering downstream signaling pathways distinct from SOCE [226].

4.3.5 Pulmonary Arterial Hypertension

Despite being a relatively rare disease, pulmonary arterial hypertension (PAH) can lead to major complications like dyspnea, heart failure and even death. Similar to systemic arterial hypertension, PAH also has idiopathic pathogenesis. Yet the etiologies of PAH and systemic arterial hypertension are different, with the pathological hallmark of PAH being smooth muscle and endothelial proliferation and migration together with thrombosis [321]. The dysfunction of endothelium is proposed to drive PAH, though in systemic arterial hypertension endothelium only plays a supporting role. Orai1-mediated SOCE has been found as a result of STIM1 activation in mouse pulmonary artery smooth muscle cells (PASMCs) [322]. Fernandez et al. have shown that STIM2 , Orai2, and TRPC6 expression levels, as well as SOCE, are upregulated in the proliferative cultured PASMCs compared with the contractile PASMSC isolated from rat pulmonary artery rings with denuded endothelium [323]. The upregulation of STIM2 is also found by the same group

in PASMCs from patients with idiopathic PAH and contributes to enhanced SOCE [324]. Increased SOCE and expression levels of Orai1 and Orai2 (but not Orai3 and STIM1) were observed in both rat distal pulmonary arteries and PASMCs under chronic hypoxia [325, 326]. This upregulation is selectively in pulmonary only and not in coronary under hypoxia [325]. The expression level of Orai3 has been measured, yet its function in PAH warrants further investigation [326]. STIM1 has been shown to play a key role in hypoxia-induced PAH [327]. When STIM1 was knocked down in PASMCs, SOCE was inhibited; NFAT nuclear translocation was reduced; hypoxia-induced proliferation and cell cycle progression of PASMCs were decreased [327]. Another group used smooth muscle-specific STIM1 knockout mouse model to demonstrate the essential role of STIM1 in hypertension [310]. The authors show that wild type mice infused with angiotensin II develop hypertension and cardiovascular dysfunction with enhanced expression of STIM1 in both heart and vessels. All these pathologies were significantly blunted in mice lacking STIM1 specifically in smooth muscle. The angiotensin II-induced hypertension was found associated with enhanced ER stress through pathways mediated by TGF-β and NADPH oxidase [310].

All the SOCE-associated cardiovascular diseases are listed in **Table 4-1**.

Table 4-1 Summary of published papers reporting the roles of Orai, STIM, and TRPC in various cardiovascular pathophysiology

Disease	Cell/Tissue Type	Species	Main Findings	References
Thrombosis				
	platelet	mouse	Strong Orai1 expression present. Orai1$^{-/-}$ mice show defective SOCE, agonist-induced Ca^{2+} responses, and thrombus activation and formation. Orai1$^{-/-}$ chimeras protected from cerebral ischemia.	284
	platelet	mouse	Orai1^{R93W} mice demonstrate integrin activation reduction and degranulation impairment. Orai1^{R93W} platelets aggregation or adherence to collagen unaffected. Orai1^{R93W} platelets defective in surface phosphatidylserine exposure	285
	platelet	mouse	The platelets in mouse model constitutively expressing STIM1 demonstrate premature activation and these mice demonstrate symptoms of macrothrombocytopenia	286
	platelet	mouse	gain of function mouse model with mutant STIM1^{R304W} shows impaired platelet activation	287, 288
	platelet	mouse	Platelets of mice with specific conditional STIM1 knockout less likely to generate fibrin at laser-induced injury site. STIM1 knockout lowers thrombus stability	289, 290
		human	No prolonged bleeding time in patients with Orai1 and STIM1 mutations and abrogated SOCE compared with control patients.	291, 292
	platelet	mouse	TRPC1 not a contributor to platelet SOCE not its activation and function.	294
	platelet	human	Both Orai1 and TRPC1 are involved in platelet SOCE and aggregation.	295
	platelet	mouse	STIM2 not involved in thrombus formation.	290

Table 4-1 Cont.

Atherosclerosis				
	VSMCs in endothelial denuded aortic rings	mouse	apolipoprotein E (apoE) knockout mice more prone to hyperlipidemia and atherosclerosis, higher ATP-induced SOCE occurring before the significant development of atherosclerosis plaques.	277
	isolated aortic tissue	mouse	ApoE knockout mice fed with high fat diet demonstrate increased Orai1 mRNA and protein levels. Orai1 knockdown demonstrate decreased atherosclerosis plaque size.	277, 298
	Isolated VSMCs	pig	Higher SOCE, STIM1 and Orai1 (not significantly) expression levels found in pigs fed with pro-atherosclerosis high-calorie diet. SOCE and STIM1 expression level decreased with exercise.	299
	Aortic VSMCs & Aortic tissue	mouse	Ox-LDL promotes proliferation, migration and invasion of mouse aortic VSMCs, increases STIM1 expression and decreases miR-185 expression. 3'-UTR of STIM1 contains miR-185 binding site. miR-185 silencing or STIM1 overexpression promotes ox-LDL-induced mouse aortic VSMC viability, migration and invasion, while miR-185 overexpression or STIM1 silencing shows opposite effect. miR-185 silencing increases VEGF and MMP-9 *levels in vitro*, and increases the lesions of arterial wall tissues and STIM1 positive rate *in vivo*. STIM1 silencing reverses these effects.	300
	EPC	mouse	ApoE knockout mice demonstrate attenuated EPC proliferation and migration. EPCs of these mice show reduced SOCE, Orai1 and STIM1 protein levels.	302

Table 4-1 Cont.

Atherosclerosis	EPC	mouse	SOCE showing protective effect from ox-LDL-induced EPC proliferation decrease.	303
	Polymorpho-nuclear leukocytes (PMN)	human	Orai1 shown necessary for neutrophil and monocytes migration into inflammatory vascular endothelium.	305
	macrophages	Human mouse	Macrophage Ca^{2+} entry mediated by Orai1 when treated with ox-LDL. ox-LDL-triggered Ca^{2+} entry activates calcineurin, which activates c-Jun N-terminal kinase and p38 kinase enhancing the scavenger receptor A expression, and further induces LDL uptake, thus promoting the transition from macrophage to foam cells.	298
Systemic Arterial Hypertension				
	Endothelial smooth muscle	mouse	Smooth muscle STIM1 specific knockout mice show partial protection against endothelial dysfunction and hypertension development after AngII infusion.	309, 310
	VSMCs	rat human	Increased Ca^{2+} found in hypertensive rat models and human patients.	311, 312
	endothelium-denuded aortic rings	rat	STIM1/Orai1 involved in elevated SOCE-mediated Ca^{2+} entry contributes to potentiating vascular activity.	313, 314
	basilar artery	rat	STIM1/Orai1 involved in elevated SOCE-mediated Ca^{2+} entry contributes to vascular tone and force generation.	307, 308, 315
	VSMCs	rat	The SOCE inhibitors Gd^{3+} and SKF96365 reported to inhibit systemic hypertension in rats	318

Table 4-1 Cont.

Systemic Arterial Hypertension		rat	Rats subjected to chronic ethanol consumption for 30days demonstrated higher systemic blood pressure, enhanced SOCE and increased STIM1 expression.	319
	aortic rings	rat	Male spontaneous hypertensive rats show more contractile force, higher Orai1 and STIM1 mRNA and protein levels than female.	313
Pulmonary Arterial Hypertension				
	PASMCs	mouse	STMI1 activation leads to Orai1-mediated SOCE.	322
	Proliferative PASMCs & Contractile PASMCs isolated from pulmonary artery rings with denuded endothelium	rat	STIM2, Orai2 and TRPC6 expression levels as well as SOCE higher in proliferative cultured PASMCs.	323
	PASMCs	human	STIM2 higher in idiopathic PAH patient PASMCs and contributes to SOCE enhancement.	324
	distal pulmonary arteries & PASMCs	rat	Increased SOCE and Orai1 and Orai2 expression levels.	325, 326
	PASMCs	rat	PASMCs STIM1 knockdown leads to inhibition of SOCE and decrease of hypoxia-induced proliferation and cell cycle progression.	327

Table 4-1 Cont.

Pulmonary Arterial Hypertension	heart and vessels	mouse	Wild type mice infused with Ang II develop hypertension and cardiovascular dysfunction with enhanced expression of STIM1 in both heart and vessels, whereas this development is absent in mice with STIM1 specifically knocked out in smooth muscle.	310
Cardiac Hypertrophy & Heart Failure				
	neonatal ventricular myocytes	rat	Cells treated with phenylephrine and angiotensin II showed increased intracellular Ca^{2+} and cell area and NFAT activation, which were all prevented by SOC inhibitor SKF-96365 and to a lesser extent by LRCC inhibitor.	124
	neonatal cardiomyocytes	rat	Endothelin-1 treatment for 48h enhanced TRPC1 expression, SOCE, and NFAT activation without upregulating STIM1. However, STIM1 KD suppressed these effects.	101
	neonatal ventricular myocytes	rat	KD of both STIM1 and Orai1 completely abolished phenylephrine-induced hypertrophic growth in neonatal cardiomyocytes by inhibiting CaMKII and ERK1/2 signaling pathway, whereas merely Orai1 KD prevented phenylephrine-mediated signaling in a calcineurin-dependent manner.	102
	neonatal cardiomyocytes	rat	Neonatal cardiomyocytes with STIM1 overexpression showed significantly larger size and increased NFAT activity, and both were prevented by SKF-96365.	103

Table 4-1 Cont.

Cardiac Hypertrophy & Heart Failure	adult heart	rat	Up-regulation of STIM1 protein and enhanced SOC current in the pressure overload-induced left ventricular hypertrophy. silencing STIM1 gene expression reduces SOCE and protects the heart from hypertrophy development through decreasing the CnA/NFAT4 signaling pathway.	103
	heart	mouse	Deletion of STIM1 protects the heart from pressure overload-induced cardiac hypertrophy.	125
	heart	mouse	STIM1 transgenic (overexpression) mice exhibited sudden cardiac death, while surviving mice developed heart failure with hypertrophy, induction of the fetal gene program, histopathology and mitochondrial structural alterations, loss of ventricular functional performance and pulmonary edema.	30
	adult cardiomyocytes	mouse	Cardiac myocytes isolated from STIM1 transgenic mice displayed spontaneous Ca^{2+} transients that were prevented by SOCE blocker SKF-96365, increased LTCC current, and enhanced Ca^{2+} spark frequency.	30
		mouse	Mice undergoing TAC presented increased mRNA and protein STIM1L levels and enhanced SOCE compared with sham animals.	34
	adult cardiomyocytes	mouse	Phenylephrine induced of STIM1L expression.	34
	embryonic stem cell-derived cardiomyocytes	human	Phenylephrine treatment for 48hrs induced a marked hypertrophy along with increased Orai1 protein expression level.	234
		zebrafish	Inactivation of Orai1 resulted in heart failure, reduced ventricular systolic function, bradycardia and skeletal muscle weakness.	98

Table 4-1 Cont.

Cardiac Hypertrophy & Heart Failure		mouse	After 8 weeks of TAC, Orai1 deficient mice showed a significantly reduced survival rate, a much earlier loss of cardiac function, and an earlier, greater dilation of the left ventricle, and significantly higher expression levels of apoptotic markers, indicating that Orai1 deficiency seems to accelerate or exacerbate the progression of the decease, rapidly leading to dilated cardiomyopathy, heart failure and earlier death.	18
		mouse	Overexpression of SOCE-associated regulatory factor in the heart prevents cardiac hypertrophy through suppressing the up-regulation of STIM1 and Orai1.	128
		mouse	In a novel genetically-modified mouse model that specifically disrupts Orai1 in cardiomyocytes, Orai1 functional inhibition preserves alterations of Ca2+ homeostasis, fibrosis and systolic function without affecting hypertrophy during pressure overload.	129
	heart	mouse	TRPC6 functions as a positive regulator of calcineurin-NFAT signaling and a key component of a calcium-dependent regulatory loop driving pathologic cardiac remodeling.	134
	cardiomyocytes	rat	DAG-induced Ca^{2+} signaling pathway through TRPC3 and TRPC6 is essential for angiotensin II-induced NFAT activation and cardiac hypertrophy.	135
		rat	TRPC3 expression was up-regulated in spontaneous hypertensive heart failure (SHHF) rat model through activation of calcineurin and its downstream effector NFAT.	136
	ventricular cardiac tissue	human	TRPC5 expression is induced in failing human heart.	136
		mouse	Maladaptive hypertrophy induced by pressure overload was suppressed by deletion of either *Trpc3* or *Trpc6* in mice.	137

Table 4-1 Cont.

Cardiac Hypertrophy & Heart Failure		mouse	TRPC1 KO mice are shown to have the calcineurin-NFAT signaling pathway inhibited, which reduces TAC-induced hypertrophic response and is related to a better survival rate.	139
	cultured adult feline myocytes	cat	KD of *Trpc4* decreased TAC-induced hypertrophy and contractile dysfunction in response to myocardial infarction.	96
		mouse	TRPC1/4 double KO prevents cardiac hypertrophy and fibrotic infiltration after TAC and chronic neurohumoral stimulation.	133
		mouse	Overexpression of dominant-negative gene variants of TRPC3, TRPC4 and TRPC6 is confirmed to have protective effects against TAC-induced hypertrophy.	99
	adult cardiomyocyte	rat	The mineralocorticoid pathway specifically promotes TRPC1/TRPC5-mediated SOCE in adult rat cardiomyocytes.	140
Arrhythmia				
	isolated sinoatrial nodes (SAN)	mouse	Mouse SAN exhibits SOC activity which may be attributable to TRPC expression, and SOCCs may be involved in regulating pacemaker firing rate.	145
		mouse	STIM1 is demonstrated to be crucial in maintaining the Ca^{2+} content of intracellular Ca^{2+} stores, thus contributing to maintaining the regular sinus rhythm of the heart in mouse.	146
	HL-1 cells	mouse	STIM1 KD could perturb cell contraction rate and induce irregular spontaneous Ca^{2+} oscillations, thus presenting proarrhythmogenic activities, including early or delayed after depolarizations.	148

Table 4-1 Cont.

Arrhythmia		mouse	Early mortality in STIM1-KD (inducible and myocyte-specific) mice was reported likely related to enhanced susceptibility to ventricular tachycardia/ventricular fibrillation secondary to the pathogenesis of spatially discordant action potential duration alternans.	149
	ventricular myocytes	rat	The overexpression of STIM1 generates spontaneous Ca^{2+} transients, thus causing arrhythmogenic Ca^{2+} waves and cytosolic and SR Ca^{2+} overload, potentially triggering sudden cardiac death.	106
	heart	rat	Application of 2-APB induced a period of tachycardic ectopy and progressed to spontaneous ventricular depolarization in Langendorff perfused rat heart and sinus rhythm and heart mechanical output was restored upon SKF-96365 application.	150
		mouse	TRPC3, although unlikely to function as the primary SOCE channel in pacemakers, was reported to have implication in both sinoatrial and atrial arrhythmias.	155
	ventricular myocytes	mouse	TRPC channels and SOCE mechanism are involved in cardiac arrhythmogenesis via promotion of spontaneous Ca^{2+} waves and triggered activities under hyperactivated conditions.	156

REFERENCES

1. Wallace, K.B., *Doxorubicin-induced cardiac mitochondrionopathy.* Pharmacol Toxicol, 2003. **93**(3): p. 105-15.
2. Mitry, M.A. and J.G. Edwards, *Doxorubicin induced heart failure: Phenotype and molecular mechanisms.* Int J Cardiol Heart Vasc, 2016. **10**: p. 17-24.
3. Cardinale, D., et al., *Anthracycline-induced cardiomyopathy: clinical relevance and response to pharmacologic therapy.* J Am Coll Cardiol, 2010. **55**(3): p. 213-20.
4. Steinherz, L.J., et al., *Cardiac toxicity 4 to 20 years after completing anthracycline therapy.* JAMA, 1991. **266**(12): p. 1672-7.
5. Praga, C., et al., *Adriamycin cardiotoxicity: a survey of 1273 patients.* Cancer Treat Rep, 1979. **63**(5): p. 827-34.
6. Bonadonna, G., et al., *Clinical evaluation of adriamycin, a new antitumour antibiotic.* Br Med J, 1969. **3**(5669): p. 503-6.
7. Bers, D.M., *Cardiac excitation-contraction coupling.* Nature, 2002. **415**(6868): p. 198-205.
8. Bers, D.M., *Calcium cycling and signaling in cardiac myocytes.* Annu Rev Physiol, 2008. **70**: p. 23-49.
9. Pan, Z., M. Brotto, and J. Ma, *Store-operated Ca2+ entry in muscle physiology and diseases.* BMB Rep, 2014. **47**(2): p. 69-79.
10. MacLeod, K.T., *Recent advances in understanding cardiac contractility in health and disease.* F1000Res, 2016. **5**.
11. Roderick, H.L., M.J. Berridge, and M.D. Bootman, *Calcium-induced calcium release.* Curr Biol, 2003. **13**(11): p. R425.
12. Cheng, H., et al., *Calcium sparks and [Ca2+]i waves in cardiac myocytes.* Am J Physiol, 1996. **270**(1 Pt 1): p. C148-59.
13. Berridge, M.J., *Cardiac calcium signalling.* Biochem Soc Trans, 2003. **31**(Pt 5): p. 930-3.
14. Liou, J., et al., *STIM is a Ca2+ sensor essential for Ca2+-store-depletion-triggered Ca2+ influx.* Curr Biol, 2005. **15**(13): p. 1235-41.
15. Manji, S.S., et al., *STIM1: a novel phosphoprotein located at the cell surface.* Biochim Biophys Acta, 2000. **1481**(1): p. 147-55.
16. Thompson, J.L. and T.J. Shuttleworth, *A plasma membrane-targeted cytosolic domain of STIM1 selectively activates ARC channels, an arachidonate-regulated store-independent Orai channel.* Channels (Austin), 2012. **6**(5): p. 370-8.
17. Lopez, J.J., et al., *Interaction of STIM1 with endogenously expressed human canonical TRP1 upon depletion of intracellular Ca2+ stores.* J Biol Chem, 2006. **281**(38): p. 28254-64.
18. Spassova, M.A., et al., *STIM1 has a plasma membrane role in the activation of store-operated Ca(2+) channels.* Proc Natl Acad Sci U S A, 2006. **103**(11): p. 4040-5.

19. Stathopulos, P.B., et al., *Structural and mechanistic insights into STIM1-mediated initiation of store-operated calcium entry.* Cell, 2008. **135**(1): p. 110-22.
20. Baba, Y., et al., *Coupling of STIM1 to store-operated Ca2+ entry through its constitutive and inducible movement in the endoplasmic reticulum.* Proc Natl Acad Sci U S A, 2006. **103**(45): p. 16704-9.
21. Yuan, J.P., et al., *SOAR and the polybasic STIM1 domains gate and regulate Orai channels.* Nat Cell Biol, 2009. **11**(3): p. 337-43.
22. Li, Z., et al., *Mapping the interacting domains of STIM1 and Orai1 in Ca2+ release-activated Ca2+ channel activation.* J Biol Chem, 2007. **282**(40): p. 29448-56.
23. Muik, M., et al., *Dynamic coupling of the putative coiled-coil domain of ORAI1 with STIM1 mediates ORAI1 channel activation.* J Biol Chem, 2008. **283**(12): p. 8014-22.
24. Muik, M., et al., *A Cytosolic Homomerization and a Modulatory Domain within STIM1 C Terminus Determine Coupling to ORAI1 Channels.* J Biol Chem, 2009. **284**(13): p. 8421-6.
25. Park, C.Y., et al., *STIM1 clusters and activates CRAC channels via direct binding of a cytosolic domain to Orai1.* Cell, 2009. **136**(5): p. 876-90.
26. Kawasaki, T., I. Lange, and S. Feske, *A minimal regulatory domain in the C terminus of STIM1 binds to and activates ORAI1 CRAC channels.* Biochem Biophys Res Commun, 2009. **385**(1): p. 49-54.
27. Williams, R.T., et al., *Identification and characterization of the STIM (stromal interaction molecule) gene family: coding for a novel class of transmembrane proteins.* Biochem J, 2001. **357**(Pt 3): p. 673-85.
28. Lopez, E., et al., *STIM1 tyrosine-phosphorylation is required for STIM1-Orai1 association in human platelets.* Cell Signal, 2012. **24**(6): p. 1315-22.
29. Williams, R.T., et al., *Stromal interaction molecule 1 (STIM1), a transmembrane protein with growth suppressor activity, contains an extracellular SAM domain modified by N-linked glycosylation.* Biochim Biophys Acta, 2002. **1596**(1): p. 131-7.
30. Correll, R.N., et al., *STIM1 elevation in the heart results in aberrant Ca(2)(+) handling and cardiomyopathy.* J Mol Cell Cardiol, 2015. **87**: p. 38-47.
31. Horton, J.S., et al., *The calcium release-activated calcium channel Orai1 represents a crucial component in hypertrophic compensation and the development of dilated cardiomyopathy.* Channels (Austin), 2014. **8**(1): p. 35-48.
32. Collins, H.E., et al., *Stromal interaction molecule 1 is essential for normal cardiac homeostasis through modulation of ER and mitochondrial function.* Am J Physiol Heart Circ Physiol, 2014. **306**(8): p. H1231-9.
33. Darbellay, B., et al., *STIM1L is a new actin-binding splice variant involved in fast repetitive Ca2+ release.* J Cell Biol, 2011. **194**(2): p. 335-46.
34. Luo, X., et al., *STIM1-dependent store-operated Ca(2)(+) entry is required for pathological cardiac hypertrophy.* J Mol Cell Cardiol, 2012. **52**(1): p. 136-47.

35. Rosado, J.A., et al., *STIM and Orai1 Variants in Store-Operated Calcium Entry.* Front Pharmacol, 2015. **6**: p. 325.
36. Jardin, I., et al., *The polybasic lysine-rich domain of plasma membrane-resident STIM1 is essential for the modulation of store-operated divalent cation entry by extracellular calcium.* Cell Signal, 2013. **25**(5): p. 1328-37.
37. Zbidi, H., et al., *STIM1 and STIM2 are located in the acidic Ca2+ stores and associates with Orai1 upon depletion of the acidic stores in human platelets.* J Biol Chem, 2011. **286**(14): p. 12257-70.
38. Soboloff, J., et al., *STIM2 is an inhibitor of STIM1-mediated store-operated Ca2+ Entry.* Curr Biol, 2006. **16**(14): p. 1465-70.
39. Wang, J.Y., et al., *STIM1 overexpression promotes colorectal cancer progression, cell motility and COX-2 expression.* Oncogene, 2015. **34**(33): p. 4358-67.
40. Rana, A., et al., *Alternative splicing converts STIM2 from an activator to an inhibitor of store-operated calcium channels.* J Cell Biol, 2015. **209**(5): p. 653-69.
41. Ercan, E., et al., *Di-arginine signals and the K-rich domain retain the Ca(2)(+) sensor STIM1 in the endoplasmic reticulum.* Traffic, 2012. **13**(7): p. 992-1003.
42. Bauer, M.C., et al., *Calmodulin binding to the polybasic C-termini of STIM proteins involved in store-operated calcium entry.* Biochemistry, 2008. **47**(23): p. 6089-91.
43. Wang, X., et al., *Distinct Orai-coupling domains in STIM1 and STIM2 define the Orai-activating site.* Nat Commun, 2014. **5**: p. 3183.
44. Zheng, S., et al., *Identification of molecular determinants that govern distinct STIM2 activation dynamics.* PLoS Biol, 2018. **16**(11): p. e2006898.
45. Zheng, L., et al., *Auto-inhibitory role of the EF-SAM domain of STIM proteins in store-operated calcium entry.* Proc Natl Acad Sci U S A, 2011. **108**(4): p. 1337-42.
46. Brandman, O., et al., *STIM2 is a feedback regulator that stabilizes basal cytosolic and endoplasmic reticulum Ca2+ levels.* Cell, 2007. **131**(7): p. 1327-39.
47. Subedi, K.P., et al., *STIM2 Induces Activated Conformation of STIM1 to Control Orai1 Function in ER-PM Junctions.* Cell Rep, 2018. **23**(2): p. 522-534.
48. Oh-Hora, M., et al., *Dual functions for the endoplasmic reticulum calcium sensors STIM1 and STIM2 in T cell activation and tolerance.* Nat Immunol, 2008. **9**(4): p. 432-43.
49. Darbellay, B., et al., *Human muscle economy myoblast differentiation and excitation-contraction coupling use the same molecular partners, STIM1 and STIM2.* J Biol Chem, 2010. **285**(29): p. 22437-47.
50. Miederer, A.M., et al., *A STIM2 splice variant negatively regulates store-operated calcium entry.* Nat Commun, 2015. **6**: p. 6899.
51. Berna-Erro, A., et al., *Role of STIM2 in cell function and physiopathology.* J Physiol, 2017. **595**(10): p. 3111-3128.
52. Zhou, Y., et al., *Cross-linking of Orai1 channels by STIM proteins.* Proc Natl Acad Sci U S A, 2018. **115**(15): p. E3398-E3407.
53. Guo, R.W. and L. Huang, *New insights into the activation mechanism of store-*

operated calcium channels: roles of STIM and Orai. J Zhejiang Univ Sci B, 2008. **9**(8): p. 591-601.
54. Hoth, M. and R. Penner, *Depletion of intracellular calcium stores activates a calcium current in mast cells.* Nature, 1992. **355**(6358): p. 353-6.
55. Feske, S., et al., *A mutation in Orai1 causes immune deficiency by abrogating CRAC channel function.* Nature, 2006. **441**(7090): p. 179-85.
56. Vig, M., et al., *CRACM1 is a plasma membrane protein essential for store-operated Ca2+ entry.* Science, 2006. **312**(5777): p. 1220-3.
57. Zhang, S.L., et al., *Genome-wide RNAi screen of Ca(2+) influx identifies genes that regulate Ca(2+) release-activated Ca(2+) channel activity.* Proc Natl Acad Sci U S A, 2006. **103**(24): p. 9357-62.
58. Mercer, J.C., et al., *Large store-operated calcium selective currents due to co-expression of Orai1 or Orai2 with the intracellular calcium sensor, Stim1.* J Biol Chem, 2006. **281**(34): p. 24979-90.
59. Peinelt, C., et al., *Amplification of CRAC current by STIM1 and CRACM1 (Orai1).* Nat Cell Biol, 2006. **8**(7): p. 771-3.
60. Prakriya, M., et al., *Orai1 is an essential pore subunit of the CRAC channel.* Nature, 2006. **443**(7108): p. 230-3.
61. Soboloff, J., et al., *Orai1 and STIM reconstitute store-operated calcium channel function.* J Biol Chem, 2006. **281**(30): p. 20661-5.
62. Derler, I., et al., *The extended transmembrane Orai1 N-terminal (ETON) region combines binding interface and gate for Orai1 activation by STIM1.* J Biol Chem, 2013. **288**(40): p. 29025-34.
63. Palty, R. and E.Y. Isacoff, *Cooperative Binding of Stromal Interaction Molecule 1 (STIM1) to the N and C Termini of Calcium Release-activated Calcium Modulator 1 (Orai1).* J Biol Chem, 2016. **291**(1): p. 334-41.
64. Palty, R., C. Stanley, and E.Y. Isacoff, *Critical role for Orai1 C-terminal domain and TM4 in CRAC channel gating.* Cell Res, 2015. **25**(8): p. 963-80.
65. Penna, A., et al., *The CRAC channel consists of a tetramer formed by Stim-induced dimerization of Orai dimers.* Nature, 2008. **456**(7218): p. 116-20.
66. Maruyama, Y., et al., *Tetrameric Orai1 is a teardrop-shaped molecule with a long, tapered cytoplasmic domain.* J Biol Chem, 2009. **284**(20): p. 13676-85.
67. Mignen, O., J.L. Thompson, and T.J. Shuttleworth, *Orai1 subunit stoichiometry of the mammalian CRAC channel pore.* J Physiol, 2008. **586**(2): p. 419-25.
68. Hou, X., et al., *Crystal structure of the calcium release-activated calcium channel Orai.* Science, 2012. **338**(6112): p. 1308-13.
69. Thompson, J.L. and T.J. Shuttleworth, *How many Orai's does it take to make a CRAC channel?* Sci Rep, 2013. **3**: p. 1961.
70. Peinelt, C., et al., *2-Aminoethoxydiphenyl borate directly facilitates and indirectly inhibits STIM1-dependent gating of CRAC channels.* J Physiol, 2008. **586**(13): p. 3061-73.

71. Yamashita, M., et al., *Orai1 mutations alter ion permeation and Ca2+-dependent fast inactivation of CRAC channels: evidence for coupling of permeation and gating.* J Gen Physiol, 2007. **130**(5): p. 525-40.
72. Fukushima, M., et al., *Alternative translation initiation gives rise to two isoforms of Orai1 with distinct plasma membrane mobilities.* J Cell Sci, 2012. **125**(Pt 18): p. 4354-61.
73. Desai, P.N., et al., *Multiple types of calcium channels arising from alternative translation initiation of the Orai1 message.* Sci Signal, 2015. **8**(387): p. ra74.
74. Frischauf, I., et al., *Molecular determinants of the coupling between STIM1 and Orai channels: differential activation of Orai1-3 channels by a STIM1 coiled-coil mutant.* J Biol Chem, 2009. **284**(32): p. 21696-706.
75. Lis, A., et al., *CRACM1, CRACM2, and CRACM3 are store-operated Ca2+ channels with distinct functional properties.* Curr Biol, 2007. **17**(9): p. 794-800.
76. Motiani, R.K., et al., *Orai3 is an estrogen receptor alpha-regulated Ca(2)(+) channel that promotes tumorigenesis.* FASEB J, 2013. **27**(1): p. 63-75.
77. Vaeth, M., et al., *ORAI2 modulates store-operated calcium entry and T cell-mediated immunity.* Nat Commun, 2017. **8**: p. 14714.
78. Trebak, M. and J.P. Kinet, *Calcium signalling in T cells.* Nat Rev Immunol, 2019. **19**(3): p. 154-169.
79. Parekh, A.B. and J.W. Putney, Jr., *Store-operated calcium channels.* Physiol Rev, 2005. **85**(2): p. 757-810.
80. Ambudkar, I.S., L.B. de Souza, and H.L. Ong, *TRPC1, Orai1, and STIM1 in SOCE: Friends in tight spaces.* Cell Calcium, 2017. **63**: p. 33-39.
81. Jardin, I., et al., *Orai1 mediates the interaction between STIM1 and hTRPC1 and regulates the mode of activation of hTRPC1-forming Ca2+ channels.* J Biol Chem, 2008. **283**(37): p. 25296-304.
82. Sabourin, J., et al., *Store-operated Ca2+ Entry Mediated by Orai1 and TRPC1 Participates to Insulin Secretion in Rat beta-Cells.* J Biol Chem, 2015. **290**(51): p. 30530-9.
83. Lee, K.P., et al., *Molecular determinants mediating gating of Transient Receptor Potential Canonical (TRPC) channels by stromal interaction molecule 1 (STIM1).* J Biol Chem, 2014. **289**(10): p. 6372-82.
84. Flockerzi, V. and B. Nilius, *TRPs: truly remarkable proteins.* Handb Exp Pharmacol, 2014. **222**: p. 1-12.
85. Wes, P.D., et al., *TRPC1, a human homolog of a Drosophila store-operated channel.* Proc Natl Acad Sci U S A, 1995. **92**(21): p. 9652-6.
86. Zhu, X., et al., *Molecular cloning of a widely expressed human homologue for the Drosophila trp gene.* FEBS Lett, 1995. **373**(3): p. 193-8.
87. Petersen, C.C., et al., *Putative capacitative calcium entry channels: expression of Drosophila trp and evidence for the existence of vertebrate homologues.* Biochem J, 1995. **311 (Pt 1)**: p. 41-4.

88. Huang, G.N., et al., *STIM1 carboxyl-terminus activates native SOC, I(crac) and TRPC1 channels.* Nat Cell Biol, 2006. **8**(9): p. 1003-10.
89. Pani, B., et al., *Impairment of TRPC1-STIM1 channel assembly and AQP5 translocation compromise agonist-stimulated fluid secretion in mice lacking caveolin1.* J Cell Sci, 2013. **126**(Pt 2): p. 667-75.
90. Jardin, I., et al., *Functional relevance of the de novo coupling between hTRPC1 and type II IP3 receptor in store-operated Ca2+ entry in human platelets.* Cell Signal, 2008. **20**(4): p. 737-47.
91. Cheng, K.T., et al., *Local Ca(2)+ entry via Orai1 regulates plasma membrane recruitment of TRPC1 and controls cytosolic Ca(2)+ signals required for specific cell functions.* PLoS Biol, 2011. **9**(3): p. e1001025.
92. Ong, E.C., et al., *A TRPC1 protein-dependent pathway regulates osteoclast formation and function.* J Biol Chem, 2013. **288**(31): p. 22219-32.
93. Sabourin, J., E. Robin, and E. Raddatz, *A key role of TRPC channels in the regulation of electromechanical activity of the developing heart.* Cardiovasc Res, 2011. **92**(2): p. 226-36.
94. Eder, P. and J.D. Molkentin, *TRPC channels as effectors of cardiac hypertrophy.* Circ Res, 2011. **108**(2): p. 265-72.
95. Dominguez-Rodriguez, A., et al., *Proarrhythmic effect of sustained EPAC activation on TRPC3/4 in rat ventricular cardiomyocytes.* J Mol Cell Cardiol, 2015. **87**: p. 74-8.
96. Makarewich, C.A., et al., *Transient receptor potential channels contribute to pathological structural and functional remodeling after myocardial infarction.* Circ Res, 2014. **115**(6): p. 567-580.
97. Kirschmer, N., et al., *TRPC4alpha and TRPC4beta Similarly Affect Neonatal Cardiomyocyte Survival during Chronic GPCR Stimulation.* PLoS One, 2016. **11**(12): p. e0168446.
98. Sabourin, J., et al., *Transient Receptor Potential Canonical (TRPC)/Orai1-dependent Store-operated Ca2+ Channels: NEW TARGETS OF ALDOSTERONE IN CARDIOMYOCYTES.* J Biol Chem, 2016. **291**(25): p. 13394-409.
99. Wu, X., et al., *TRPC channels are necessary mediators of pathologic cardiac hypertrophy.* Proc Natl Acad Sci U S A, 2010. **107**(15): p. 7000-5.
100. Bootman, M.D., et al., *Atrial cardiomyocyte calcium signalling.* Biochim Biophys Acta, 2011. **1813**(5): p. 922-34.
101. Ohba, T., et al., *Essential role of STIM1 in the development of cardiomyocyte hypertrophy.* Biochem Biophys Res Commun, 2009. **389**(1): p. 172-6.
102. Voelkers, M., et al., *Orai1 and Stim1 regulate normal and hypertrophic growth in cardiomyocytes.* J Mol Cell Cardiol, 2010. **48**(6): p. 1329-34.
103. Hulot, J.S., et al., *Critical role for stromal interaction molecule 1 in cardiac hypertrophy.* Circulation, 2011. **124**(7): p. 796-805.
104. Volkers, M., et al., *Orai1 deficiency leads to heart failure and skeletal myopathy in*

zebrafish. J Cell Sci, 2012. **125**(Pt 2): p. 287-94.
105. Zhu-Mauldin, X., et al., *Modification of STIM1 by O-linked N-acetylglucosamine (O-GlcNAc) attenuates store-operated calcium entry in neonatal cardiomyocytes.* J Biol Chem, 2012. **287**(46): p. 39094-106.
106. Zhao, G., et al., *STIM1 enhances SR Ca2+ content through binding phospholamban in rat ventricular myocytes.* Proc Natl Acad Sci U S A, 2015. **112**(34): p. E4792-801.
107. Che, H., et al., *Roles of store-operated Ca2+ channels in regulating cell cycling and migration of human cardiac c-kit+ progenitor cells.* Am J Physiol Heart Circ Physiol, 2015. **309**(10): p. H1772-81.
108. Feske, S., *CRAC channelopathies.* Pflugers Arch, 2010. **460**(2): p. 417-35.
109. Nakamura, M. and J. Sadoshima, *Mechanisms of physiological and pathological cardiac hypertrophy.* Nat Rev Cardiol, 2018. **15**(7): p. 387-407.
110. Ljubojevic, S., et al., *Early remodeling of perinuclear Ca2+ stores and nucleoplasmic Ca2+ signaling during the development of hypertrophy and heart failure.* Circulation, 2014. **130**(3): p. 244-55.
111. Iemitsu, M., et al., *Physiological and pathological cardiac hypertrophy induce different molecular phenotypes in the rat.* Am J Physiol Regul Integr Comp Physiol, 2001. **281**(6): p. R2029-36.
112. Umar, S., et al., *Cardiac structural and hemodynamic changes associated with physiological heart hypertrophy of pregnancy are reversed postpartum.* J Appl Physiol (1985), 2012. **113**(8): p. 1253-9.
113. Maillet, M., J.H. van Berlo, and J.D. Molkentin, *Molecular basis of physiological heart growth: fundamental concepts and new players.* Nat Rev Mol Cell Biol, 2013. **14**(1): p. 38-48.
114. Shimizu, I. and T. Minamino, *Physiological and pathological cardiac hypertrophy.* J Mol Cell Cardiol, 2016. **97**: p. 245-62.
115. Tham, Y.K., et al., *Pathophysiology of cardiac hypertrophy and heart failure: signaling pathways and novel therapeutic targets.* Arch Toxicol, 2015. **89**(9): p. 1401-38.
116. Bernardo, B.C., et al., *Molecular distinction between physiological and pathological cardiac hypertrophy: experimental findings and therapeutic strategies.* Pharmacol Ther, 2010. **128**(1): p. 191-227.
117. Samak, M., et al., *Cardiac Hypertrophy: An Introduction to Molecular and Cellular Basis.* Med Sci Monit Basic Res, 2016. **22**: p. 75-9.
118. Molkentin, J.D., *Dichotomy of Ca2+ in the heart: contraction versus intracellular signaling.* J Clin Invest, 2006. **116**(3): p. 623-6.
119. Lipp, P., et al., *Functional InsP3 receptors that may modulate excitation-contraction coupling in the heart.* Curr Biol, 2000. **10**(15): p. 939-42.
120. Nakayama, H., et al., *The IP3 receptor regulates cardiac hypertrophy in response to select stimuli.* Circ Res, 2010. **107**(5): p. 659-66.

121. Hohendanner, F., et al., *Calcium and IP3 dynamics in cardiac myocytes: experimental and computational perspectives and approaches.* Front Pharmacol, 2014. **5**: p. 35.
122. Higazi, D.R., et al., *Endothelin-1-stimulated InsP3-induced Ca2+ release is a nexus for hypertrophic signaling in cardiac myocytes.* Mol Cell, 2009. **33**(4): p. 472-82.
123. Collins, H.E., et al., *STIM1/Orai1-mediated SOCE: current perspectives and potential roles in cardiac function and pathology.* Am J Physiol Heart Circ Physiol, 2013. **305**(4): p. H446-58.
124. Hunton, D.L., et al., *Capacitative calcium entry contributes to nuclear factor of activated T-cells nuclear translocation and hypertrophy in cardiomyocytes.* J Biol Chem, 2002. **277**(16): p. 14266-73.
125. Parks, C., et al., *STIM1-dependent Ca(2+) microdomains are required for myofilament remodeling and signaling in the heart.* Sci Rep, 2016. **6**: p. 25372.
126. Troupes, C.D., et al., *Role of STIM1 (Stromal Interaction Molecule 1) in Hypertrophy-Related Contractile Dysfunction.* Circ Res, 2017. **121**(2): p. 125-136.
127. Wang, Y., et al., *Nitric Oxide-cGMP-PKG Pathway Acts on Orai1 to Inhibit the Hypertrophy of Human Embryonic Stem Cell-Derived Cardiomyocytes.* Stem Cells, 2015. **33**(10): p. 2973-84.
128. Dai, F., et al., *Overexpression of SARAF Ameliorates Pressure Overload-Induced Cardiac Hypertrophy Through Suppressing STIM1-Orai1 in Mice.* Cell Physiol Biochem, 2018. **47**(2): p. 817-826.
129. Bartoli, F., et al., *Orai1 Channel Inhibition Preserves Left Ventricular Systolic Function and Normal Ca(2+) Handling After Pressure Overload.* Circulation, 2020. **141**(3): p. 199-216.
130. Smani, T., et al., *Functional and physiopathological implications of TRP channels.* Biochim Biophys Acta, 2015. **1853**(8): p. 1772-82.
131. Bartoli, F. and J. Sabourin, *Cardiac Remodeling and Disease: Current Understanding of STIM1/Orai1-Mediated Store-Operated Ca(2+) Entry in Cardiac Function and Pathology.* Adv Exp Med Biol, 2017. **993**: p. 523-534.
132. Yue, Z., et al., *Role of TRP channels in the cardiovascular system.* Am J Physiol Heart Circ Physiol, 2015. **308**(3): p. H157-82.
133. Camacho Londono, J.E., et al., *A background Ca2+ entry pathway mediated by TRPC1/TRPC4 is critical for development of pathological cardiac remodelling.* Eur Heart J, 2015. **36**(33): p. 2257-66.
134. Kuwahara, K., et al., *TRPC6 fulfills a calcineurin signaling circuit during pathologic cardiac remodeling.* J Clin Invest, 2006. **116**(12): p. 3114-26.
135. Onohara, N., et al., *TRPC3 and TRPC6 are essential for angiotensin II-induced cardiac hypertrophy.* EMBO J, 2006. **25**(22): p. 5305-16.
136. Bush, E.W., et al., *Canonical transient receptor potential channels promote cardiomyocyte hypertrophy through activation of calcineurin signaling.* J Biol Chem,

2006. **281**(44): p. 33487-96.
137. Seo, K., et al., *Combined TRPC3 and TRPC6 blockade by selective small-molecule or genetic deletion inhibits pathological cardiac hypertrophy.* Proc Natl Acad Sci U S A, 2014. **111**(4): p. 1551-6.
138. Takahashi, S., et al., *Nitric oxide-cGMP-protein kinase G pathway negatively regulates vascular transient receptor potential channel TRPC6.* J Physiol, 2008. **586**(17): p. 4209-23.
139. Seth, M., et al., *TRPC1 channels are critical for hypertrophic signaling in the heart.* Circ Res, 2009. **105**(10): p. 1023-30.
140. Bartoli, F., et al., *Specific Upregulation of TRPC1 and TRPC5 Channels by Mineralocorticoid Pathway in Adult Rat Ventricular Cardiomyocytes.* Cells, 2019. **9**(1).
141. Niggli, E., *Ryanodine receptors: waking up from refractoriness.* Cardiovasc Res, 2011. **91**(4): p. 563-4.
142. Lakatta, E.G., et al., *The integration of spontaneous intracellular Ca2+ cycling and surface membrane ion channel activation entrains normal automaticity in cells of the heart's pacemaker.* Ann N Y Acad Sci, 2006. **1080**: p. 178-206.
143. Yaniv, Y., E.G. Lakatta, and V.A. Maltsev, *From two competing oscillators to one coupled-clock pacemaker cell system.* Front Physiol, 2015. **6**: p. 28.
144. Imtiaz, M.S., et al., *SR Ca2+ store refill--a key factor in cardiac pacemaking.* J Mol Cell Cardiol, 2010. **49**(3): p. 412-26.
145. Ju, Y.K., et al., *Store-operated Ca2+ influx and expression of TRPC genes in mouse sinoatrial node.* Circ Res, 2007. **100**(11): p. 1605-14.
146. Zhang, H., et al., *STIM1-Ca2+ signaling modulates automaticity of the mouse sinoatrial node.* Proc Natl Acad Sci U S A, 2015. **112**(41): p. E5618-27.
147. Liu, J., et al., *Store-operated calcium entry and the localization of STIM1 and Orai1 proteins in isolated mouse sinoatrial node cells.* Front Physiol, 2015. **6**: p. 69.
148. Nguyen, N., et al., *STIM1 participates in the contractile rhythmicity of HL-1 cells by moderating T-type Ca(2+) channel activity.* Biochim Biophys Acta, 2013. **1833**(6): p. 1294-303.
149. Cacheux, M., et al., *Cardiomyocyte-Specific STIM1 (Stromal Interaction Molecule 1) Depletion in the Adult Heart Promotes the Development of Arrhythmogenic Discordant Alternans.* Circ Arrhythm Electrophysiol, 2019. **12**(11): p. e007382.
150. Wang, P., et al., *Evidence that 2-aminoethoxydiphenyl borate provokes fibrillation in perfused rat hearts via voltage-independent calcium channels.* Eur J Pharmacol, 2012. **681**(1-3): p. 60-7.
151. Nattel, S., *Atrial electrophysiology and mechanisms of atrial fibrillation.* J Cardiovasc Pharmacol Ther, 2003. **8 Suppl 1**: p. S5-11.
152. Heijman, J., et al., *Calcium handling and atrial fibrillation.* Wien Med Wochenschr, 2012. **162**(13-14): p. 287-91.
153. Voigt, N., S. Nattel, and D. Dobrev, *Proarrhythmic atrial calcium cycling in the*

diseased heart. Adv Exp Med Biol, 2012. **740**: p. 1175-91.
154. Bootman, M.D. and K. Rietdorf, *Tissue Specificity: Store-Operated Ca(2+) Entry in Cardiac Myocytes.* Adv Exp Med Biol, 2017. **993**: p. 363-387.
155. Ju, Y.K., et al., *The involvement of TRPC3 channels in sinoatrial arrhythmias.* Front Physiol, 2015. **6**: p. 86.
156. Wen, H., et al., *Potential Arrhythmogenic Role of TRPC Channels and Store-Operated Calcium Entry Mechanism in Mouse Ventricular Myocytes.* Front Physiol, 2018. **9**: p. 1785.
157. Bonilla, I.M., et al., *Enhancement of Cardiac Store Operated Calcium Entry (SOCE) within Novel Intercalated Disk Microdomains in Arrhythmic Disease.* Sci Rep, 2019. **9**(1): p. 10179.
158. Prevention, C.f.D.C.a. *National Diabetes Statistics Report, 2017*. 2017; Available from: https://www.cdc.gov/diabetes/pdfs/data/statistics/national-diabetes-statistics-report.pdf.
159. Stamler, J., et al., *Diabetes, other risk factors, and 12-yr cardiovascular mortality for men screened in the Multiple Risk Factor Intervention Trial.* Diabetes Care, 1993. **16**(2): p. 434-44.
160. Huxley, R.R., et al., *Meta-analysis of cohort and case-control studies of type 2 diabetes mellitus and risk of atrial fibrillation.* Am J Cardiol, 2011. **108**(1): p. 56-62.
161. Sun, Y. and D. Hu, *The link between diabetes and atrial fibrillation: cause or correlation?* Journal of cardiovascular disease research, 2010. **1**(1): p. 10.
162. Zimering, M.B., *Diabetes Autoantibodies Mediate Neural-and Endothelial Cell-Inhibitory Effects Via 5-Hydroxytryptamine-2 Receptor Coupled to Phospholipase C/Inositol Triphosphate/Ca2+ Pathway.* Journal of endocrinology and diabetes, 2017. **4**(4).
163. Zimering, M.B. and Z. Pan, *Autoantibodies in type 2 diabetes induce stress fiber formation and apoptosis in endothelial cells.* The Journal of Clinical Endocrinology & Metabolism, 2009. **94**(6): p. 2171-2177.
164. Zimering, M.B. and Z. Pan, *Increased Neuronal Depolarization Evoked by Autoantibodies in Diabetic Obstructive Sleep Apnea: Role for Inflammatory Protease (S) in Generation of Neurotoxic Immunoglobulin Fragment.* Journal of endocrinology and diabetes, 2017. **4**(1).
165. Zimering, M.B., et al., *Anti-endothelial and anti-neuronal effects from auto-antibodies in subsets of adult diabetes having a cluster of microvascular complications.* Diabetes research and clinical practice, 2011. **93**(1): p. 95-105.
166. Qi, X.-Y., et al., *Atrial Fibrillation-Related Nuclear Calcium Remodeling and Transcriptional Signaling*. 2016, Am Heart Assoc.
167. Jian, L. and W. Ling-Peng, *GW27-e0977 The research of L type calcium channel in Turn SERCA 2a genetic model for acute atrial fibrillation atrial muscle cell.* Journal of the American College of Cardiology. **68**(16 Supplement): p. C35.
168. Harada, M., et al., *Atrial fibrillation activates AMP-dependent protein kinase and its*

regulation of cellular calcium handling: potential role in metabolic adaptation and prevention of progression. Journal of the American College of Cardiology, 2015. **66**(1): p. 47-58.
169. Heijman, J., et al., *Cellular and molecular electrophysiology of atrial fibrillation initiation, maintenance, and progression.* Circulation research, 2014. **114**(9): p. 1483-1499.
170. Nattel, S. and D. Dobrev, *Electrophysiological and molecular mechanisms of paroxysmal atrial fibrillation.* Nature Reviews Cardiology, 2016. **13**(10): p. 575.
171. Wang, Y., et al., *Suicide gene-mediated sequencing ablation revealed the potential therapeutic mechanism of induced pluripotent stem cell-derived cardiovascular cell patch post-myocardial infarction.* Antioxidants & redox signaling, 2014. **21**(16): p. 2177-2191.
172. Xia, M., et al., *Functional expression of L- and T-type Ca2+ channels in murine HL-1 cells.* J Mol Cell Cardiol, 2004. **36**(1): p. 111-9.
173. Sabourin, J., et al., *Ca(2+) handling remodeling and STIM1L/Orai1/TRPC1/TRPC4 upregulation in monocrotaline-induced right ventricular hypertrophy.* J Mol Cell Cardiol, 2018. **118**: p. 208-224.
174. Bootman, M.D., et al., *2-aminoethoxydiphenyl borate (2-APB) is a reliable blocker of store-operated Ca2+ entry but an inconsistent inhibitor of InsP3-induced Ca2+ release.* The FASEB Journal, 2002. **16**(10): p. 1145-1150.
175. Oka, T., et al., *Xestospongin C, a novel blocker of IP3 receptor, attenuates the increase in cytosolic calcium level and degranulation that is induced by antigen in RBL-2H3 mast cells.* British journal of pharmacology, 2002. **135**(8): p. 1959-1966.
176. Tjondrokoesoemo, A., et al., *Type 1 inositol (1, 4, 5)-trisphosphate receptor activates ryanodine receptor 1 to mediate calcium spark signaling in adult mammalian skeletal muscle.* Journal of Biological Chemistry, 2013. **288**(4): p. 2103-2109.
177. Leitner, M.G., et al., *Direct modulation of TRPM4 and TRPM3 channels by the phospholipase C inhibitor U73122.* Br J Pharmacol, 2016. **173**(16): p. 2555-69.
178. Lewandowicz, A.M., J. Vepsalainen, and J.T. Laitinen, *The 'allosteric modulator' SCH-202676 disrupts G protein-coupled receptor function via sulphydryl-sensitive mechanisms.* Br J Pharmacol, 2006. **147**(4): p. 422-9.
179. Berridge, M.J., *The inositol trisphosphate/calcium signaling pathway in health and disease.* Physiological reviews, 2016. **96**(4): p. 1261-1296.
180. Li, X., et al., *Endothelin-1–induced arrhythmogenic Ca2+ signaling is abolished in atrial myocytes of inositol-1, 4, 5-trisphosphate (IP3)–receptor type 2–deficient mice.* Circulation research, 2005. **96**(12): p. 1274-1281.
181. Yamada, J., et al., *Up-regulation of inositol 1, 4, 5 trisphosphate receptor expression in atrial tissue in patients with chronic atrial fibrillation.* Journal of the American College of Cardiology, 2001. **37**(4): p. 1111-1119.
182. Opel, A., et al., *Absence of the regulator of G-protein signalling, RGS4,*

predisposes to atrial fibrillation and is associated with abnormal calcium handling. Journal of Biological Chemistry, 2015: p. jbc. M115. 666719.
183. Tinker, A., et al., *The contribution of pathways initiated via the Gq\11 G-protein family to atrial fibrillation.* Pharmacological research, 2016. **105**: p. 54-61.
184. Mackenzie, L., et al., *The role of inositol 1, 4, 5-trisphosphate receptors in Ca2+ signalling and the generation of arrhythmias in rat atrial myocytes.* The Journal of Physiology, 2002. **541**(2): p. 395-409.
185. Kourliouros, A., et al., *Current concepts in the pathogenesis of atrial fibrillation.* American heart journal, 2009. **157**(2): p. 243-252.
186. MAIXENT, J.M., et al., *Antibodies against myosin in sera of patients with idiopathic paroxysmal atrial fibrillation.* Journal of cardiovascular electrophysiology, 1998. **9**(6): p. 612-617.
187. Baba, A., et al., *Autoantibodies: new upstream targets of paroxysmal atrial fibrillation in patients with congestive heart failure.* Journal of cardiology, 2002. **40**(5): p. 217-223.
188. Baba, A., et al., *Autoantibodies against M2-muscarinic acetylcholine receptors: new upstream targets in atrial fibrillation in patients with dilated cardiomyopathy.* European heart journal, 2004. **25**(13): p. 1108-1115.
189. Stavrakis, S., et al., *Activating autoantibodies to the beta-1 adrenergic and m2 muscarinic receptors facilitate atrial fibrillation in patients with Graves' hyperthyroidism.* Journal of the American College of Cardiology, 2009. **54**(14): p. 1309-1316.
190. Zimering, M.B., et al., *Plasma basic fibroblast growth factor is correlated with plasminogen activator inhibitor–1 concentration in adults from the Veterans Affairs Diabetes Trial.* Metabolism, 2008. **57**(11): p. 1563-1569.
191. Claycomb, W.C., et al., *HL-1 cells: a cardiac muscle cell line that contracts and retains phenotypic characteristics of the adult cardiomyocyte.* Proceedings of the National Academy of Sciences, 1998. **95**(6): p. 2979-2984.
192. Jansen, H.J. and R.A. Rose, *Isolation of Atrial Myocytes from Adult Mice.* J Vis Exp, 2019(149).
193. *WHO Model Lists of Essential Medicines*. 2019.
194. Li, M., et al., *Phosphoinositide 3-Kinase Gamma Inhibition Protects From Anthracycline Cardiotoxicity and Reduces Tumor Growth.* Circulation, 2018. **138**(7): p. 696-711.
195. Weiss, R.B., *The anthracyclines: will we ever find a better doxorubicin?* Semin Oncol, 1992. **19**(6): p. 670-86.
196. Zamorano, J.L., et al., *2016 ESC Position Paper on cancer treatments and cardiovascular toxicity developed under the auspices of the ESC Committee for Practice Guidelines: The Task Force for cancer treatments and cardiovascular toxicity of the European Society of Cardiology (ESC).* Eur Heart J, 2016. **37**(36): p. 2768-2801.

197. Caroni, P., F. Villani, and E. Carafoli, *The cardiotoxic antibiotic doxorubicin inhibits the Na+/Ca2+ exchange of dog heart sarcolemmal vesicles.* FEBS Lett, 1981. **130**(2): p. 184-6.
198. Arai, M., et al., *Sarcoplasmic reticulum genes are selectively down-regulated in cardiomyopathy produced by doxorubicin in rabbits.* J Mol Cell Cardiol, 1998. **30**(2): p. 243-54.
199. Touchberry, C.D., et al., *Store-operated calcium entry is present in HL-1 cardiomyocytes and contributes to resting calcium.* Biochem Biophys Res Commun, 2011. **416**(1-2): p. 45-50.
200. Ma, J. and Z. Pan, *Retrograde activation of store-operated calcium channel.* Cell Calcium, 2003. **33**(5-6): p. 375-84.
201. Ma, J. and Z. Pan, *Junctional membrane structure and store operated calcium entry in muscle cells.* Front Biosci, 2003. **8**: p. d242-55.
202. Kar, P. and A.B. Parekh, *Distinct spatial Ca2+ signatures selectively activate different NFAT transcription factor isoforms.* Mol Cell, 2015. **58**(2): p. 232-43.
203. Zhao, Z.H., et al., *SOX2-mediated inhibition of miR-223 contributes to STIM1 activation in phenylephrine-induced hypertrophic cardiomyocytes.* Mol Cell Biochem, 2018. **443**(1-2): p. 47-56.
204. Ross, G.R., et al., *Enhanced store-operated Ca(2+) influx and ORAI1 expression in ventricular fibroblasts from human failing heart.* Biol Open, 2017. **6**(3): p. 326-332.
205. Pu, W.T., Q. Ma, and S. Izumo, *NFAT transcription factors are critical survival factors that inhibit cardiomyocyte apoptosis during phenylephrine stimulation in vitro.* Circ Res, 2003. **92**(7): p. 725-31.
206. Tokudome, T., et al., *Calcineurin-nuclear factor of activated T cells pathway-dependent cardiac remodeling in mice deficient in guanylyl cyclase A, a receptor for atrial and brain natriuretic peptides.* Circulation, 2005. **111**(23): p. 3095-104.
207. Liang, F., S. Lu, and D.G. Gardner, *Endothelin-dependent and -independent components of strain-activated brain natriuretic peptide gene transcription require extracellular signal regulated kinase and p38 mitogen-activated protein kinase.* Hypertension, 2000. **35**(1 Pt 2): p. 188-92.
208. Suarez-Huerta, N., et al., *Actin depolymerization and polymerization are required during apoptosis in endothelial cells.* J Cell Physiol, 2000. **184**(2): p. 239-45.
209. Toldo, S., et al., *Comparative cardiac toxicity of anthracyclines in vitro and in vivo in the mouse.* PLoS One, 2013. **8**(3): p. e58421.
210. Luo, Y., et al., *Circulating IgGs in Type 2 Diabetes with Atrial Fibrillation Induce IP3-Mediated Calcium Elevation in Cardiomyocytes.* iScience, 2020. **23**(4): p. 101036.
211. Cui, C., et al., *Targeting Orai1-mediated store-operated calcium entry by RP4010 for anti-tumor activity in esophagus squamous cell carcinoma.* Cancer Lett, 2018. **432**: p. 169-179.

212. Choi, S., et al., *Selective inhibitory effects of zinc on cell proliferation in esophageal squamous cell carcinoma through Orai1.* FASEB J, 2018. **32**(1): p. 404-416.
213. Zhu, H., et al., *Elevated Orai1 expression mediates tumor-promoting intracellular Ca2+ oscillations in human esophageal squamous cell carcinoma.* Oncotarget, 2014. **5**(11): p. 3455-71.
214. Pan, Z. and J. Ma, *Open Sesame: treasure in store-operated calcium entry pathway for cancer therapy.* Sci China Life Sci, 2015. **58**(1): p. 48-53.
215. Cui, C., et al., *Targeting calcium signaling in cancer therapy.* Acta Pharm Sin B, 2017. **7**(1): p. 3-17.
216. Bolton, T.B., et al., *Smooth muscle cells and interstitial cells of blood vessels.* Cell Calcium, 2004. **35**(6): p. 643-57.
217. House, S.J., et al., *The non-excitable smooth muscle: calcium signaling and phenotypic switching during vascular disease.* Pflugers Arch, 2008. **456**(5): p. 769-85.
218. Lompre, A.M., et al., *STIM1 and Orai in cardiac hypertrophy and vascular proliferative diseases.* Front Biosci (Schol Ed), 2013. **5**: p. 766-73.
219. Gomez, D. and G.K. Owens, *Smooth muscle cell phenotypic switching in atherosclerosis.* Cardiovasc Res, 2012. **95**(2): p. 156-64.
220. Aird, W.C., *Spatial and temporal dynamics of the endothelium.* J Thromb Haemost, 2005. **3**(7): p. 1392-406.
221. Aird, W.C., *Phenotypic heterogeneity of the endothelium: I. Structure, function, and mechanisms.* Circ Res, 2007. **100**(2): p. 158-73.
222. Carmeliet, P. and R.K. Jain, *Molecular mechanisms and clinical applications of angiogenesis.* Nature, 2011. **473**(7347): p. 298-307.
223. Nelken, N.A., et al., *Thrombin receptor expression in normal and atherosclerotic human arteries.* J Clin Invest, 1992. **90**(4): p. 1614-21.
224. Hirano, K., *The roles of proteinase-activated receptors in the vascular physiology and pathophysiology.* Arterioscler Thromb Vasc Biol, 2007. **27**(1): p. 27-36.
225. Gonzalez-Cobos, J.C., et al., *Store-independent Orai1/3 channels activated by intracrine leukotriene C4: role in neointimal hyperplasia.* Circ Res, 2013. **112**(7): p. 1013-25.
226. Mignen, O., J.L. Thompson, and T.J. Shuttleworth, *Both Orai1 and Orai3 are essential components of the arachidonate-regulated Ca2+-selective (ARC) channels.* J Physiol, 2008. **586**(1): p. 185-95.
227. Mignen, O., J.L. Thompson, and T.J. Shuttleworth, *STIM1 regulates Ca2+ entry via arachidonate-regulated Ca2+-selective (ARC) channels without store depletion or translocation to the plasma membrane.* J Physiol, 2007. **579**(Pt 3): p. 703-15.
228. Abdullaev, I.F., et al., *Stim1 and Orai1 mediate CRAC currents and store-operated calcium entry important for endothelial cell proliferation.* Circ Res, 2008. **103**(11): p. 1289-99.
229. Simo-Cheyou, E.R., et al., *STIM-1 and ORAI-1 channel mediate angiotensin-II-*

induced expression of Egr-1 in vascular smooth muscle cells. J Cell Physiol, 2017. **232**(12): p. 3496-3509.
230. Guo, R.W., et al., *Stim1- and Orai1-mediated store-operated calcium entry is critical for angiotensin II-induced vascular smooth muscle cell proliferation.* Cardiovasc Res, 2012. **93**(2): p. 360-70.
231. Rodriguez-Moyano, M., et al., *Urotensin-II promotes vascular smooth muscle cell proliferation through store-operated calcium entry and EGFR transactivation.* Cardiovasc Res, 2013. **100**(2): p. 297-306.
232. Myllarniemi, M., et al., *Inhibition of platelet-derived growth factor receptor tyrosine kinase inhibits vascular smooth muscle cell migration and proliferation.* FASEB J, 1997. **11**(13): p. 1119-26.
233. Bisaillon, J.M., et al., *Essential role for STIM1/Orai1-mediated calcium influx in PDGF-induced smooth muscle migration.* Am J Physiol Cell Physiol, 2010. **298**(5): p. C993-1005.
234. Spinelli, A.M., et al., *Airway smooth muscle STIM1 and Orai1 are upregulated in asthmatic mice and mediate PDGF-activated SOCE, CRAC currents, proliferation, and migration.* Pflugers Arch, 2012. **464**(5): p. 481-92.
235. Mancarella, S., et al., *Targeted STIM deletion impairs calcium homeostasis, NFAT activation, and growth of smooth muscle.* FASEB J, 2013. **27**(3): p. 893-906.
236. Levitzki, A., *PDGF receptor kinase inhibitors for the treatment of restenosis.* Cardiovasc Res, 2005. **65**(3): p. 581-6.
237. Jandt, E., et al., *Stent-based release of a selective PDGF-receptor blocker from the bis-indolylmethanon class inhibits restenosis in the rabbit animal model.* Vascul Pharmacol, 2010. **52**(1-2): p. 55-62.
238. Makiyama, Y., et al., *Imatinib mesilate inhibits neointimal hyperplasia via growth inhibition of vascular smooth muscle cells in a rat model of balloon injury.* Tohoku J Exp Med, 2008. **215**(4): p. 299-306.
239. Trepakova, E.S., et al., *Properties of a native cation channel activated by Ca2+ store depletion in vascular smooth muscle cells.* J Biol Chem, 2001. **276**(11): p. 7782-90.
240. Smani, T., et al., *Role of Ca2+-independent phospholipase A2 and store-operated pathway in urocortin-induced vasodilatation of rat coronary artery.* Circ Res, 2007. **101**(11): p. 1194-203.
241. Hopson, K.P., et al., *S1P activates store-operated calcium entry via receptor- and non-receptor-mediated pathways in vascular smooth muscle cells.* Am J Physiol Cell Physiol, 2011. **300**(4): p. C919-26.
242. Zhang, W., et al., *Orai1-mediated I (CRAC) is essential for neointima formation after vascular injury.* Circ Res, 2011. **109**(5): p. 534-42.
243. Potier, M., et al., *Evidence for STIM1- and Orai1-dependent store-operated calcium influx through ICRAC in vascular smooth muscle cells: role in proliferation and migration.* FASEB J, 2009. **23**(8): p. 2425-37.

244. Berra-Romani, R., et al., *Ca2+ handling is altered when arterial myocytes progress from a contractile to a proliferative phenotype in culture.* Am J Physiol Cell Physiol, 2008. **295**(3): p. C779-90.
245. Taniguchi, H., et al., *Possible involvement of Ca2+ entry and its pharmacological characteristics responsible for endothelium-dependent, NO-mediated relaxation induced by thapsigargin in guinea-pig aorta.* J Pharm Pharmacol, 1999. **51**(7): p. 831-40.
246. Shaul, P.W., *Regulation of endothelial nitric oxide synthase: location, location, location.* Annu Rev Physiol, 2002. **64**: p. 749-74.
247. Hirano, K., M. Hirano, and A. Hanada, *Involvement of STIM1 in the proteinase-activated receptor 1-mediated Ca2+ influx in vascular endothelial cells.* J Cell Biochem, 2009. **108**(2): p. 499-507.
248. Boittin, F.X., et al., *Ca2+-independent PLA2 controls endothelial store-operated Ca2+ entry and vascular tone in intact aorta.* Am J Physiol Heart Circ Physiol, 2008. **295**(6): p. H2466-74.
249. Estrada, I.A., et al., *STIM1 restores coronary endothelial function in type 1 diabetic mice.* Circ Res, 2012. **111**(9): p. 1166-75.
250. Zhang, W. and M. Trebak, *Vascular balloon injury and intraluminal administration in rat carotid artery.* J Vis Exp, 2014(94).
251. Guo, R.W., et al., *An essential role for stromal interaction molecule 1 in neointima formation following arterial injury.* Cardiovasc Res, 2009. **81**(4): p. 660-8.
252. Jardin, I., et al., *Homers regulate calcium entry and aggregation in human platelets: a role for Homers in the association between STIM1 and Orai1.* Biochem J, 2012. **445**(1): p. 29-38.
253. Jia, S., et al., *Homer binds to Orai1 and TRPC channels in the neointima and regulates vascular smooth muscle cell migration and proliferation.* Sci Rep, 2017. **7**(1): p. 5075.
254. Garnier-Raveaud, S., et al., *Identification of membrane calcium channels essential for cytoplasmic and nuclear calcium elevations induced by vascular endothelial growth factor in human endothelial cells.* Growth Factors, 2001. **19**(1): p. 35-48.
255. Faehling, M., et al., *Essential role of calcium in vascular endothelial growth factor A-induced signaling: mechanism of the antiangiogenic effect of carboxyamidotriazole.* FASEB J, 2002. **16**(13): p. 1805-7.
256. Fasolato, C. and B. Nilius, *Store depletion triggers the calcium release-activated calcium current (ICRAC) in macrovascular endothelial cells: a comparison with Jurkat and embryonic kidney cell lines.* Pflugers Arch, 1998. **436**(1): p. 69-74.
257. Li, J., et al., *Orai1 and CRAC channel dependence of VEGF-activated Ca2+ entry and endothelial tube formation.* Circ Res, 2011. **108**(10): p. 1190-8.
258. Antigny, F., N. Girardin, and M. Frieden, *Transient receptor potential canonical channels are required for in vitro endothelial tube formation.* J Biol Chem, 2012. **287**(8): p. 5917-27.

259. Gandhirajan, R.K., et al., *Blockade of NOX2 and STIM1 signaling limits lipopolysaccharide-induced vascular inflammation.* J Clin Invest, 2013. **123**(2): p. 887-902.
260. Asahara, T., et al., *Isolation of putative progenitor endothelial cells for angiogenesis.* Science, 1997. **275**(5302): p. 964-7.
261. Sanchez-Hernandez, Y., et al., *Store-operated Ca(2+) entry is expressed in human endothelial progenitor cells.* Stem Cells Dev, 2010. **19**(12): p. 1967-81.
262. Shi, Y., et al., *Knockdown of stromal interaction molecule 1 attenuates hepatocyte growth factor-induced endothelial progenitor cell proliferation.* Exp Biol Med (Maywood), 2010. **235**(3): p. 317-25.
263. Kuang, C.Y., et al., *Silencing stromal interaction molecule 1 by RNA interference inhibits the proliferation and migration of endothelial progenitor cells.* Biochem Biophys Res Commun, 2010. **398**(2): p. 315-20.
264. Dragoni, S., et al., *Vascular endothelial growth factor stimulates endothelial colony forming cells proliferation and tubulogenesis by inducing oscillations in intracellular Ca2+ concentration.* Stem Cells, 2011. **29**(11): p. 1898-907.
265. Bao, P., et al., *The role of vascular endothelial growth factor in wound healing.* J Surg Res, 2009. **153**(2): p. 347-58.
266. Hanahan, D. and J. Folkman, *Patterns and emerging mechanisms of the angiogenic switch during tumorigenesis.* Cell, 1996. **86**(3): p. 353-64.
267. Sato, T.N., et al., *Distinct roles of the receptor tyrosine kinases Tie-1 and Tie-2 in blood vessel formation.* Nature, 1995. **376**(6535): p. 70-4.
268. Suri, C., et al., *Requisite role of angiopoietin-1, a ligand for the TIE2 receptor, during embryonic angiogenesis.* Cell, 1996. **87**(7): p. 1171-80.
269. Folkman, J. and P.A. D'Amore, *Blood vessel formation: what is its molecular basis?* Cell, 1996. **87**(7): p. 1153-5.
270. Jho, D., et al., *Angiopoietin-1 opposes VEGF-induced increase in endothelial permeability by inhibiting TRPC1-dependent Ca2 influx.* Circ Res, 2005. **96**(12): p. 1282-90.
271. Pardanaud, L., F. Yassine, and F. Dieterlen-Lievre, *Relationship between vasculogenesis, angiogenesis and haemopoiesis during avian ontogeny.* Development, 1989. **105**(3): p. 473-85.
272. Ribatti, D., B. Nico, and E. Crivellato, *Morphological and molecular aspects of physiological vascular morphogenesis.* Angiogenesis, 2009. **12**(2): p. 101-11.
273. Cines, D.B., et al., *Endothelial cells in physiology and in the pathophysiology of vascular disorders.* Blood, 1998. **91**(10): p. 3527-61.
274. Mead, L.E., et al., *Isolation and characterization of endothelial progenitor cells from human blood.* Curr Protoc Stem Cell Biol, 2008. **Chapter 2**: p. Unit 2C 1.
275. Wang, Q.C., et al., *TMCO1 Is an ER Ca(2+) Load-Activated Ca(2+) Channel.* Cell, 2016. **165**(6): p. 1454-1466.
276. Poteser, M., et al., *Identification of a rare subset of adipose tissue-resident*

progenitor cells, which express CD133 and TRPC3 as a VEGF-regulated Ca2+ entry channel. FEBS Lett, 2008. **582**(18): p. 2696-702.
277. Van Assche, T., et al., *Altered Ca2+ handling of smooth muscle cells in aorta of apolipoprotein E-deficient mice before development of atherosclerotic lesions.* Cell Calcium, 2007. **41**(3): p. 295-302.
278. Leung, F.P., et al., *Store-operated calcium entry in vascular smooth muscle.* Br J Pharmacol, 2008. **153**(5): p. 846-57.
279. Zhang, W. and M. Trebak, *STIM1 and Orai1: novel targets for vascular diseases?* Sci China Life Sci, 2011. **54**(8): p. 780-5.
280. Ruhle, B. and M. Trebak, *Emerging roles for native Orai Ca2+ channels in cardiovascular disease.* Curr Top Membr, 2013. **71**: p. 209-35.
281. Spinelli, A.M. and M. Trebak, *Orai channel-mediated Ca2+ signals in vascular and airway smooth muscle.* Am J Physiol Cell Physiol, 2016. **310**(6): p. C402-13.
282. Mazzucato, M., et al., *Sequential cytoplasmic calcium signals in a 2-stage platelet activation process induced by the glycoprotein Ibalpha mechanoreceptor.* Blood, 2002. **100**(8): p. 2793-800.
283. Rink, T.J. and S.O. Sage, *Calcium signaling in human platelets.* Annu Rev Physiol, 1990. **52**: p. 431-49.
284. Braun, A., et al., *Orai1 (CRACM1) is the platelet SOC channel and essential for pathological thrombus formation.* Blood, 2009. **113**(9): p. 2056-63.
285. Bergmeier, W., et al., *R93W mutation in Orai1 causes impaired calcium influx in platelets.* Blood, 2009. **113**(3): p. 675-8.
286. Grosse, J., et al., *An EF hand mutation in Stim1 causes premature platelet activation and bleeding in mice.* J Clin Invest, 2007. **117**(11): p. 3540-50.
287. Varga-Szabo, D., et al., *The calcium sensor STIM1 is an essential mediator of arterial thrombosis and ischemic brain infarction.* J Exp Med, 2008. **205**(7): p. 1583-91.
288. Gamage, T.H., et al., *STIM1 R304W causes muscle degeneration and impaired platelet activation in mice.* Cell Calcium, 2018. **76**: p. 87-100.
289. Ahmad, F., et al., *Relative contributions of stromal interaction molecule 1 and CalDAG-GEFI to calcium-dependent platelet activation and thrombosis.* J Thromb Haemost, 2011. **9**(10): p. 2077-86.
290. Gilio, K., et al., *Roles of platelet STIM1 and Orai1 in glycoprotein VI- and thrombin-dependent procoagulant activity and thrombus formation.* J Biol Chem, 2010. **285**(31): p. 23629-38.
291. McCarl, C.A., et al., *ORAI1 deficiency and lack of store-operated Ca2+ entry cause immunodeficiency, myopathy, and ectodermal dysplasia.* J Allergy Clin Immunol, 2009. **124**(6): p. 1311-1318 e7.
292. Picard, C., et al., *STIM1 mutation associated with a syndrome of immunodeficiency and autoimmunity.* N Engl J Med, 2009. **360**(19): p. 1971-80.
293. Elvers, M., et al., *Intracellular cyclophilin A is an important Ca(2+) regulator in*

platelets and critically involved in arterial thrombus formation. Blood, 2012. **120**(6): p. 1317-26.
294. Varga-Szabo, D., et al., *Store-operated Ca(2+) entry in platelets occurs independently of transient receptor potential (TRP) C1.* Pflugers Arch, 2008. **457**(2): p. 377-87.
295. Galan, C., et al., *STIM1, Orai1 and hTRPC1 are important for thrombin- and ADP-induced aggregation in human platelets.* Arch Biochem Biophys, 2009. **490**(2): p. 137-44.
296. Daemen, J., et al., *Early and late coronary stent thrombosis of sirolimus-eluting and paclitaxel-eluting stents in routine clinical practice: data from a large two-institutional cohort study.* Lancet, 2007. **369**(9562): p. 667-78.
297. Iakovou, I., et al., *Incidence, predictors, and outcome of thrombosis after successful implantation of drug-eluting stents.* JAMA, 2005. **293**(17): p. 2126-30.
298. Liang, S.J., et al., *Inhibition of Orai1 Store-Operated Calcium Channel Prevents Foam Cell Formation and Atherosclerosis.* Arterioscler Thromb Vasc Biol, 2016. **36**(4): p. 618-28.
299. Edwards, J.M., et al., *Exercise training decreases store-operated Ca2+entry associated with metabolic syndrome and coronary atherosclerosis.* Cardiovasc Res, 2010. **85**(3): p. 631-40.
300. Fang, M., et al., *miR-185 silencing promotes the progression of atherosclerosis via targeting stromal interaction molecule 1.* Cell Cycle, 2019. **18**(6-7): p. 682-695.
301. Gimbrone, M.A., Jr. and G. Garcia-Cardena, *Endothelial Cell Dysfunction and the Pathobiology of Atherosclerosis.* Circ Res, 2016. **118**(4): p. 620-36.
302. Wang, L.Y., et al., *Reduction of Store-Operated Ca(2+) Entry Correlates with Endothelial Progenitor Cell Dysfunction in Atherosclerotic Mice.* Stem Cells Dev, 2015. **24**(13): p. 1582-90.
303. Yang, J., et al., *Store-operated calcium entry-activated autophagy protects EPC proliferation via the CAMKK2-MTOR pathway in ox-LDL exposure.* Autophagy, 2017. **13**(1): p. 82-98.
304. Welt, F.G., et al., *Neutrophil, not macrophage, infiltration precedes neointimal thickening in balloon-injured arteries.* Arterioscler Thromb Vasc Biol, 2000. **20**(12): p. 2553-8.
305. Schaff, U.Y., et al., *Orai1 regulates intracellular calcium, arrest, and shape polarization during neutrophil recruitment in shear flow.* Blood, 2010. **115**(3): p. 657-66.
306. Wellman, G.C., et al., *Membrane depolarization, elevated Ca(2+) entry, and gene expression in cerebral arteries of hypertensive rats.* Am J Physiol Heart Circ Physiol, 2001. **281**(6): p. H2559-67.
307. Kitazono, T., et al., *Increased activity of calcium channels and Rho-associated kinase in the basilar artery during chronic hypertension in vivo.* J Hypertens, 2002. **20**(5): p. 879-84.

308. Goulopoulou, S. and R.C. Webb, *Symphony of vascular contraction: how smooth muscle cells lose harmony to signal increased vascular resistance in hypertension.* Hypertension, 2014. **63**(3): p. e33-9.
309. Kassan, M., et al., *Differential role for stromal interacting molecule 1 in the regulation of vascular function.* Pflugers Arch, 2015. **467**(6): p. 1195-202.
310. Kassan, M., et al., *Essential Role of Smooth Muscle STIM1 in Hypertension and Cardiovascular Dysfunction.* Arterioscler Thromb Vasc Biol, 2016. **36**(9): p. 1900-9.
311. Bendhack, L.M., R.V. Sharma, and R.C. Bhalla, *Altered signal transduction in vascular smooth muscle cells of spontaneously hypertensive rats.* Hypertension, 1992. **19**(2 Suppl): p. II142-8.
312. Bohr, D.F. and R.C. Webb, *Vascular smooth muscle membrane in hypertension.* Annu Rev Pharmacol Toxicol, 1988. **28**: p. 389-409.
313. Giachini, F.R., et al., *STIM1/Orai1 contributes to sex differences in vascular responses to calcium in spontaneously hypertensive rats.* Clin Sci (Lond), 2012. **122**(5): p. 215-26.
314. Giachini, F.R., et al., *Increased activation of stromal interaction molecule-1/Orai-1 in aorta from hypertensive rats: a novel insight into vascular dysfunction.* Hypertension, 2009. **53**(2): p. 409-16.
315. Tanwar, J., M. Trebak, and R.K. Motiani, *Cardiovascular and Hemostatic Disorders: Role of STIM and Orai Proteins in Vascular Disorders.* Adv Exp Med Biol, 2017. **993**: p. 425-452.
316. Trebak, M., et al., *Comparison of human TRPC3 channels in receptor-activated and store-operated modes. Differential sensitivity to channel blockers suggests fundamental differences in channel composition.* J Biol Chem, 2002. **277**(24): p. 21617-23.
317. Cortes, S.F., V.S. Lemos, and J.C. Stoclet, *Alterations in calcium stores in aortic myocytes from spontaneously hypertensive rats.* Hypertension, 1997. **29**(6): p. 1322-8.
318. Xu, Y.J., V. Elimban, and N.S. Dhalla, *Reduction of blood pressure by store-operated calcium channel blockers.* J Cell Mol Med, 2015. **19**(12): p. 2763-70.
319. Souza Bomfim, G.H., et al., *Functional Upregulation of STIM-1/Orai-1-Mediated Store-Operated Ca2+ Contributing to the Hypertension Development Elicited by Chronic EtOH Consumption.* Curr Vasc Pharmacol, 2017. **15**(3): p. 265-281.
320. Gillis, E.E. and J.C. Sullivan, *Sex Differences in Hypertension: Recent Advances.* Hypertension, 2016. **68**(6): p. 1322-1327.
321. Farber, H.W. and J. Loscalzo, *Pulmonary arterial hypertension.* N Engl J Med, 2004. **351**(16): p. 1655-65.
322. Ng, L.C., et al., *Orai1 interacts with STIM1 and mediates capacitative Ca2+ entry in mouse pulmonary arterial smooth muscle cells.* Am J Physiol Cell Physiol, 2010. **299**(5): p. C1079-90.

323. Fernandez, R.A., et al., *Upregulated expression of STIM2, TRPC6, and Orai2 contributes to the transition of pulmonary arterial smooth muscle cells from a contractile to proliferative phenotype.* Am J Physiol Cell Physiol, 2015. **308**(8): p. C581-93.
324. Song, M.Y., A. Makino, and J.X. Yuan, *STIM2 Contributes to Enhanced Store-operated Ca Entry in Pulmonary Artery Smooth Muscle Cells from Patients with Idiopathic Pulmonary Arterial Hypertension.* Pulm Circ, 2011. **1**(1): p. 84-94.
325. He, X., et al., *Hypoxia selectively upregulates cation channels and increases cytosolic [Ca(2+)] in pulmonary, but not coronary, arterial smooth muscle cells.* Am J Physiol Cell Physiol, 2018. **314**(4): p. C504-C517.
326. Wang, J., et al., *Orai1, 2, 3 and STIM1 promote store-operated calcium entry in pulmonary arterial smooth muscle cells.* Cell Death Discov, 2017. **3**: p. 17074.
327. Hou, X., et al., *Silencing of STIM1 attenuates hypoxia-induced PASMCs proliferation via inhibition of the SOC/Ca2+/NFAT pathway.* Respir Res, 2013. **14**: p. 2.

BIOGRAPHICAL INFORMATION

Xian Liu received her Bachelor of Science degree in Clinical Pharmacy from China Pharmaceutical University in 2014. Then she directly came to the United States and started Ph.D. program in Pharmacology and Toxicology in School of Pharmacy in University of Kansas. In the summer of 2017, she transferred to the Ph.D. program in Department of Kinesiology, College of Nursing and Health Innovation in University of Texas at Arlington, joining Dr. Zui Pan's Calcium Signaling research lab. Xian has successfully defended her dissertation on July 30, 2020 and is expecting to receive the Doctor of Philosophy degree in Kinesiology from University of Texas at Arlington (UTA). During the time at UTA, Xian firstly worked as a teaching assistant/course instructor teaching six undergraduate courses in Kinesiology including Introduction to Exercise Physiology, Biomechanics, Motor Control and Learning, Undergraduate Research Method, Fitness Assessment and Advanced Exercise Physiology. Then she continued working as a research assistant under the guidance of Dr. Zui Pan studying the calcium signaling in cardiomyocytes, specifically focusing on type 2 diabetes with atrial fibrillation and chemotherapy-induced cardiotoxicity. As a doctoral student, she has authored and co-authored 5 full peer-reviewed journal articles. Xian presented her studies in regional, national and international conferences, including one podium talk at joint Research Symposium between CONHI and School of Social Work at UTA. Based on Xian's achievement, her study was awarded College of Nursing and Health Innovation Center for Research and Scholarship Pilot Project Grant in 2019. In the future she hopes to

continue chasing her dream: providing safe and efficacious treatment for patients.